00109203

LX
t
30

THE
ASIATIC SOCIETY OF BOMBAY
TOWN HALL, BOMBAY-1.

Digitized with financial assistance from
Government of Maharashtra
on 13 March, 2020

PRB. 38. I(N)
1000

GOVERNMENT OF INDIA
RAILWAY DEPARTMENT
(CENTRAL STANDARDS OFFICE FOR RAILWAYS)

Track Stress Research

November 1935—November 1938

109203

PROGRESS REPORT, VOLUME I

by

W. E. GELSON and E. A. BLACKWOOD
INVESTIGATING OFFICERS

Calcutta
East Indian Railway Press
1939

Price Rs. 10 or 16s. (inclusive of Vol. II)

TRACK STRESS RESEARCH

REPORT ON WORK COMPLETED UP TO 30th NOVEMBER 1938

Introduction

The reporters were placed on special duty in the Central Standards Office during November 1935 with instructions to undertake a research into the permissible axle loads and speeds on various types of railway track existing in India, with the following terms of reference:—

(1) To verify or otherwise the speed allowance formula vide item D(4) of Technical Paper No. 245 for the increment of rail stress due to the passage of a wheel load on a rail at speed due to the elastic character of the support.

(2) To investigate the increment of stress over and above the static effect that may be expected to arise under normal conditions from defects in the track such as low points, rail joints or non-uniformity in the support offered by adjacent sleepers.

(3) To investigate the conditions of support at rail joints with a view to determining what reliance can be placed on the rail continuity effect of fishplates both new and worn, and the effect of closer sleeper spacing.

(4) To investigate the conditions of stability in the ballast of various types and designs of sleepers including recent designs of the Central Standards Office from the point of view of reducing maintenance and preserving a level track surface.

(5) To investigate the effects on rails and sleepers of the lateral forces on rails arising from the hunting movement of locomotives at speed both on straight track and on curves.

A Progress Report on the first year's work was submitted in December 1936, but this report supersedes it in all respects. By the summer of 1937 most of the programmed experiments covering the first four items were completed but there remained the important matter covered by Item (5), which was then taken in hand, and the greater part of the last sixteen months has been taken up with experiments to determine the inter-relation between vehicles and the track.

For purposes of this Report the various matters are grouped in the following sequence which seemed to be most convenient:—

		Page.
(1)	Working stresses in rails and fishplates ..	4
(2)	List of rail stress and deflection measurements ..	8
(3)	Static stresses and deflections in the solid rail ..	13
(4)	Dynamic deflections in the solid rail	20
(5)	Dynamic stresses in the solid rail	31
(6)	Fishplate stresses and joint deflections under static conditions	42
(7)	Dynamic stresses and deflections in fishplates for well-packed joints	48
(8)	Dynamic deflections and stresses in fishplates for low joints	48
(9)	Stability of sleepers in ballast under vertical and lateral loads	49
(10)	Description of the field testing equipment and its use in connexion with Items 3 to 9 ..	66
(11)	Experiments to determine the lateral strength and stiffness of permanent way and the lateral loads applied to it	70
(12)	Safe working loads and speeds	109
(13)	Summary of conclusions	111
(14)	Personnel	113

1. Working Stresses in Rails and Fishplates.

Existing materials only, including rail and fishplate steels which conform to the I. R. S. Specifications are considered in this chapter. Proposals for stronger fishplates to a new specification are given in the conclusions.

The selection of satisfactory working stresses for rail and fishplate steels is governed by the nature of the loading which is of a fluctuating or an alternating character. It is essential that the stresses shall be sufficiently low to prevent fracture during the whole of the working life of the material. It is also desirable that the loads shall not be large enough to produce permanent deformation of the rails.

Results of mechanical tests and chemical analyses on rail and fishplates steels carried out by the Metallurgical Inspector, Indian Stores Department, are given in Table 1.

TABLE 1.

Mark on fish-plate	Mark on rail	Railway	Rail	Site	Remarks	Test length (in inches)	Yield point (tons per sq. inch)	Ultimate stress (tons per sq. inch)	Elongation per cent.	Cross section at the fracture		Remarks from Test House	Chemical composition
										Reduced area	Reduction of area per cent.		
A	..	E. B. ..	75 F. F.	Muragachha.	Suspended joint wooden sleepers.	2·0	14·5	23·90	41	0·087	65	Silky grey fracture.	..
B	..	E. B. ..	75 F. F.	Do. ..	Do. ..	2·0	21·2	41·52	25	0·147	41	Dull grey fracture showing fine bright crystalline specks of the periphery of the fractured surface.	..
C	..	E. I. ..	75 D. H.	Colgong	Thicker type fishplate D. and O. plate sleepers.	2·0	15·5	25·86	35	0·115	54	Silky grey fracture showing a lamination almost at the centre of the fractured area.	..
D	..	E. I. ..	75 D. H.	Do. ..	Thinner type fishplate D. and O. plate sleepers.	2·0	13·8	22·80	16	0·196	22	Broke outside the middle of the test length showing an irregular silky grey fracture.	..
E	..	B. N. ..	85 F. F.	Khargpur	Existing fishplate on pot sleepers.	2·0	21·4	39·84	28	0·136	46	Dull grey fracture.	..
F	..	B. N. ..	85 F. F.	Do. ..	Repressed fishplate on pot sleepers.	2·0	21·6	39·60	29	0·119	52	Do. ..	..
G	..	E. I. ..	88½	Pradhankhanta.	Duplex sleepers	2·0	15·2	27·71	39	0·095	62	Half cup silky grey fracture.	..
H	..	E. I. ..	88½	Do. ..	D. & O. plates	2·0	15·6	25·92	41	0·088	65	Do. ..	..
J	..	E. I. ..	75 D. H.	Pakur ..	Do. ..	2·0	18·1	27·71	39	0·096	61	Do. ..	..
K	..	E. I. ..	90 R ..	Gomoh ..	Duplex and "G" type sleepers.	2·0	20·6	37·42	28	0·132	47	Dull grey fracture.	..
L	..	E. I. ..	90 BSS	Do. ..	Wooden sleepers.	2·0	16·1	37·78	36	0·099	60	Half cup silky grey fracture.	..
M	..	E. I. ..	90 BSS	Do. ..	90R type fishplate planed to suit 90 BSS rail wooden sleepers.	2·0	19·7	39·44	28	0·133	47	Dull grey fracture.	..
N	..	E. I. ..	90 BSS	Dehri-on-Sone.	90 BSS rails short L type fishplate CST9 and Duplex.	2·0	24·0	38·55	30	0·117	53	Do. ..	..
A	..	N. W.	75 F. F.	Macleod Ganj Road.	L type and wooden sleepers.	..	17·8	27·12	40	..	..	..	0·13C, 0·29Mn, 0·01Si, 0·097S, 0·050P.
B	..	N. W.	90 R ..	Phillaur ..	CST9 ..	..	18·9	36·92	31	..	..	..	0·29C, 0·72Mn, 0·02Si, 0·021S, 0·019P.
B	..	N. W.	90 R ..	Jullundur Cant.	Steel loose jaws	..	18·9	36·92	31	..	..	..	Ditto.
C	..	N. W.	73 B. H.	Hoshiarpur.	Wooden sleepers.	..	19·0	25·12	41	..	..	..	0·10C, 0·40Mn, 0·01Si, 0·107S, 0·151P.
D	..	N. W.	58½ F.F.	Kalabakra	Do. ..	..	14·0	28·00	36	..	..	..	0·24C, 0·63Mn, 0·04Si, 0·011S, 0.034P.
1	..	..	..	..	..	2·3	20·3	33·80	30	0·128	49	Half cup silky grey fracture.	0·28C, 0·69Mn, 0·07Si, 0·103S, 0·053P.
2	..	..	..	..	..	2.0	19·1	35·80	26	0·145	42	Half cup silky grey fracture with occasional fine crystalline specks.	0·33C, 0·66Mn, Nil Si, 0·034S, 0·091P.

Mark on fish-plate	Mark on rail	Railway	Rail	Site	Remarks	Test length (in inches)	Yield point (tons per sq. inch)	Ultimate stress (tons per sq. inch)	Elongation per cent.	Cross Section at the fracture		Remarks from Test House	Chemical Composition
										Reduced area	Reduction of area per cent.		
3	..	..	..	..	..	2·0	19·7	36·40	32	0·126	50	Half cup silky grey fracture.	0·42C, 0·71Mn, 0·06Si, 0·029S, 0·046P.
4	..	..	..	..	..	2·0	13·6	26·42	39	0·092	63	Do.	0·24C, 0·62Mn, 0·03Si, 0·027S, 0·026P.
5	..	..	..	..	..	1·5	15·9	25·63	43	0·040	68	Do.	0·10C, 0·43Mn, Nil Si, 0·070S, 0·064P.
1	..	..	..	..	..	2·0	20·56	39·42	28·1	..	..	..	·38C, ·77Mn, ·038S, ·035P.
2	..	..	..	..	..	2·0	18·84	38·48	29·5	..	..	..	·42C, ·74Mn, ·023S, ·023P.
3	..	..	..	..	..	2·0	20·68	40·68	28·1	..	..	..	·39C, ·80Mn, ·03S, ·029P.
79679	..	..	90 R	..	..	2·0	..	36·6	28·0	..	..	High Carbon steel.	·40C, ·05Si, ·66Mn, ·030S, ·064P.
79678	..	..	90 R	..	..	2·0	..	40·0	26·0	..	..	Do.	·42C, ·050Si, ·69Mn, ·031S, ·05P.
79689	..	..	90 R	..	..	2·0	..	38·0	26·0	..	..	Do.	·37C, ·044Si, ·76Mn, ·030S, ·03P.
79926	..	..	90 R	..	..	2·0	..	39·2	28·0	..	..	Do.	·41C, ·056Si, ·78Mn, ·027S, ·053P.
78712	..	..	90 R	..	..	2·0	..	40·6	27·0	..	..	Do.	·40C, ·103Si, ·72Mn, ·030S, ·05P.
79904	..	..	90 R	..	..	2·0	..	41·9	25·0	..	..	Do.	·41C, ·056Si, ·80Mn, ·026S, ·030P.
..	1	..	..	..	..	2·0	28·4	53·00	17·2	..	..	Ordinary Carbon.	·63C, ·80Mn, ·28 S, ·017P, ·00 Cr.
..	4	..	..	..	..	2·0	30·0	49·44	20·3	..	..	Med. Manganese.	·47C, 1·21Mn, ·032S, ·03P, ·00 Cr.
..	7	..	..	..	..	2·0	30·4	51·92	18·8	..	..	Chrome	·44C, ·72Mn, ·04S, ·03P, ·80 Cr.
..	1	..	60 lb.	..	..	2·0	..	54·7	15·5	..	..	Plain Carbon	·66C, ·06Si, ·88Mn, ·036S, ·029P, ·00 Cr.
..	2	..	60 lb.	..	..	2·0	..	52·8	17·0	..	..	Do.	·61C, ·056Si, ·85Mn, ·024S, ·039P, ·00 Cr.
..	3	..	60 lb.	..	..	2·0	..	44·7	20·0	..	..	Do.	·56C, ·005Si, ·66Mn, ·039S, ·043P, ·00 Cr.
..	4	..	60 lb.	..	..	2·0	..	53·2	20·0	..	..	Med. Manganese.	·50C, ·062Si, 1·43Mn, ·039S ·043P, ·00 Cr
..	5	..	60 lb.	..	..	2·0	..	52·4	18·7	..	..	Do.	·49C, ·051Si 1·25Mn, ·033S ·031P, ·00 Cr
..	6	..	60 lb.	..	..	2·0	..	46·2	25·0	..	..	Do.	·44C, ·44Si 1·20Mn, ·03S ·033P, ·00 Cr
..	7	..	60 lb.	..	..	2·0	..	52·6	21·8	..	..	Chrome	·47C, ·075Si ·80Mn, ·032S ·026P, ·91 Cr
..	8	..	60 lb.	..	..	2·0	..	53·4	19·5	..	..	Do.	·47C, ·053Si ·70Mn, ·035S ·042P, ·91 Cr
..	9	..	60 lb.	..	..	2·0	..	55·6	19·5	..	..	Do.	·45C, ·056Si ·84Mn, ·037S ·045P, ·94 Cr

In most cases sample fishplates were taken from the actual test milages and in other cases samples of new Tata rail and fishplate steels to I.R.S. Specifications were selected. No tests were made with rail steel from samples taken from the test milages.

These materials can be roughly fitted into three groups according to their ultimate tensile strengths, viz.,

(1) Fishplate steels to obsolete specifications of about 26·5 tons per square inch ultimate tensile strength.

(2) Fishplate steels similar to I.R.S. fishplate steel of about 40 tons per square inch ultimate tensile strength.

(3) Rail steels similar to I. R. S. rail steels of about 52 tons per square inch ultimate tensile strength.

In the case of the older tracks, the rails can probably be fitted into Group 2.

No experimental data is available for the fatigue strengths of Indian rail and fishplate steels. Many investigations have, however, been made on the subject of fatigue of metals generally and we may assume that the safe ranges of stress corresponding to given values of the mean stress for plain polished samples of the three groups of Indian rail and fishplate steels are covered by the "limiting range of stress diagram," Figure 1. It has been well established experimentally that the limiting range of stress for zero mean stress is about 0·45 multiplied by the value of the ultimate tensile strength for plain polished specimens (see "The Fatigue of Metals" by H. J. Gough, page 142, Figure 50).

Bairstow has shown, vide "The Fatigue of Metals" above quoted, page 124 that provided the superior limit of the repeated stress range is not greater than the limiting stress range for reversed stresses, no permanent deformation is produced.

Surface flaws and corrosion have been shown to have an adverse effect on the fatigue strength of metals, but their influence in the case of Indian rail and fishplate steels is unkown. In some experiments by Moore and Kommers, vide Proc. American Iron and Steel Institute, 1920, page 89, it has been shown that a test specimen having a rough turned finish has a fatigue range of only 81% of that for a similar specimen ground and polished.

In the case of fishplates stresses any over-stress results in permanent distortion, relief of stress and an increase in the joint sleeper reactions. There is comparatively little danger of fishplate-fracture.

If f is the maximum direct rail or fishplate bending moment stress, observed during the passage of a succession of wheel loads, then the maximum rail or fishplate bending moment stress due to reversal is not greater than $-0{\cdot}30\ f$ for normal conditions.

The criterion proposed in this Report for maximum rail and fishplate stress is, therefore, $f \geqslant 0{\cdot}45\ T$ where T is the ultimate tensile strength of the steel.

2. List of Rail Stress and Deflection Measurements.

A complete list of field experiments where rail stresses and deflections were recorded is given in Table 2.

TABLE 2.

Sleepers		Depth of ballast	Elastic modulus (average)	Weather	Railway	Section	Tests	Series	Appendix No.	Page No.	
Type	Date laid									Deflection	Stress
				100 B. H.	Track	on 2210 feet	Radius Curves.				
Wood N+3.	..	8" Stone	1056–1260	Dry	G. I. P.	BB–KYN Up line.	Solid Rail	580–588	I	I D 1	I S 46–47.
							Solid Rail bad spot.	589–595		..	I S 48.
							Low Joint	597–604	II	II D 1	II S 103–104.
							Do.	606–615	II	II D 2	II S 105–106.
							Solid Rail	616–621	I	I D 2	I S 49–50.
							Solid Rail low spot.	622–627		..	I S 51–25.
Wood N+3.	..	8" Stone	1007	Monsoon	G. I. P.	BB–KYN	Solid Rail	802–809	I	I D 3	I S 53–54.
							Do.	810–815	I	I D 4	I S 55–56.
							Low Joint	818–827	II	II D 3	II S 107–108.
							Do.	829–834	II	II D 4	II S 109–110.
				100 B.	H. Track on	Straight.					
C. I. Pot N+3.	..	12" Stone	2225	Dry	G. I. P.	PA–LNL Dn. line.	Packed Joint	631–638	II	II D 5	II S 111–112.
							Solid Rail	640–646	I	I DL 5 I D 6	I S 57–58.
							Low Joint	647–655	II	II D 6	II S 113–114.
C. I. Pot N+3.	..	12" Stone	1316–2436	Monsoon	G. I. P.	PA–LNL	Packed Joint	750–758	II	II D 7	II S 115–116.
							Solid Rail	761–769	I	I DL 6A–8 I D 9	I S 59–60.
							Low Joint	772–786	II	II D 8	II S 117–118.
							Solid Rail	786–798	I	I D 10	I S 61–62.
				90 R	Track on Str	aight.					
Deodar N+3.	1927	3" Stone	2160	Dry	N. W.	LDH–GZB	Solid Rail	10–20	I	I D 11	I S 63.
							Packed Joint	33–41	II	II D 9–12	II S 119.
							Low Joint	42–52	II	II D 13–16	II S 120.
							Packed Joint	53–63	II	II D 17–20	II S 121.
							Low Joint	64–75	II	II D 21–24	II S 122.
CST9 N+2.	..	6" Stone (Unsettled).	2730	Dry	N. W.	LHR–LDH Dn. line.	Solid Rail	83–94	I	I DL 12 I D 13–15	I S 64.
							Packed Joint	108–117	II	II D 25–28	II S 123.
							Low Joint	118–123	II	II D 29–32	II S 124.
							Packed Joint	124–129	II	II D 33–36	II S 125.
							Low Joint	134–141	II	II D 37–40	II S 126.
Steel loose jaw N+3.	..	6" Stone (Unsettled).	1810	Dry	N. W.	LHR–LDH Up line.	Solid Rail	148–155 162–163 169–170	I	I DL 16	I S 65.
							Packed Joint	156–161 164–168	II	..	II S 127.
							Low Joint	174–180	II	II D 41–42	II S 128.
							Packed Joint	181–187	II	II D 43–44	II S 129.
							Low Joint	188–193	II	II D 45–46	II S 130.
					Track	on 5730 ft. R	adius Curve.				
G. Type Plate N+1+D and N+2.	29–2–35	5" Stone	2545	Monsoon	E. I.	ASN–GMO Dn. line.	Packed Joint.*	355–360	II	II D 47–48	II S 131.
							Solid Rail	361–366	I	I DL 17–18 I D 19	I S 66.
							Low Joint*	367–374	II	II D 49–50	II S 132.
							Packed Joint.†	383–388	II	II D 51	II S 133.
							Low Joint†	389–394	II	II D 52	II S 134.

* Duplex Sleeper at Joint.

† "G" Type Sleeper at Joint.

Sleepers		Depth of ballast	Elastic modulus (average)	Weather	Railway	Section	Tests	Series	Appendix No.	Page No.	
Type	Date laid									Deflection	Stress
Steel with pressed lugs N+2.	..	9" Stone	1078	Dry	G. I. P.	KNW-ET Up line.	Solid Rail	520-525	I	I DL 20 I D 21	I S 67.
							Packed Joint	528-535	II	II D 53	II S 135.
							Solid Rail	538-540	I	..	I S 68.
							Low Joint	542-548	II	II D 54	II S 136.
				90 BSS Tr	ack on 5	730 ft. Radius	Curve				
Deodar	29-2-35	5" Stone		Monsoon	E. I.	ASN-GMO Dn. line.	Packed Joint.*	375-378	II	..	II S 137.
							Do.	379-381	II	..	II S 138.
					90 BSS	Track on Str	aight.				
CST/9 Duplex N+1+D	5-4-36	8" Stone	1732	Monsoon	E. I.	GYA-MGS	Solid Rail	497-501	I	I DL 22 I D 23	I S 69.
							Packed Joint	503-508	II	II D 55	II S 139.
							Low Joint	509-513	II	..	II S 140.
					88½ B.	H. Track on	Straight.				
D. and O. Plates N+1+D and N+2.	..	8" Stone	1690	Monsoon	E. I.	ASN-GMO	Packed Joint	316-320	II	II D 56-57	II S 141.
							Low Joint	322-330	II	II D 58-59	II S 142.
							Solid Rail	332-338	I	I DL 24-27 I D 28	I S 70.
							Packed Joint	339-344	II	II D 60-61	II S 143.
							Low Joint	345-348	II	II D 62-63	II S 144.
					85 F. F.	Track on St	raight				
Murray C. I. Pot N+3.	..	3" Stone	1680	Monsoon	B. N.	KGP-BPE	Packed Joint	395-401	II	II D 64-65	II S 145-146.
							Low Joint	403-408	II	II D 66-67	II S 147-148.
							Do.	411-414	II	II D 68	II S 149-150.
							Do.	415-418	II	II D 69	II S 151-152.
							Solid Rail	419-422	I	I DL 29 I D 30	I S 71.
					82 B. H.	Track on St	raight				
C. I. Pot N+2.	..	8"-10" Stone	2064	Dry	G. I. P.	KNW-ET Dn. line.	Solid Rail	550-559	I	I DL 31 I D 32	I S 72.
							Packed Joint	561-569	II	II D 70	II S 153.
							Low Joint	570-576	II	II D 71	II S 154-155.
					75 F. F.	(1892) Track	on Straight				
Deodar N+1.	1931	2" Stone and brick.	1685	Dry	N. W.	SMA-BT1	Solid Rail packed.	195-200	I	I DL 33	I S 73.
							Do.	201-206	I	..	I S 74.
							Do. Low Spot.	207-212	I	..	I S 75.
							Packed Joint	213-220	II	II D 72-75	II S 156.
							Low Joint	222-228	II	II D 76-81	II S 157.
							Rock of sleepers.	231-232	..	..	..

* L Type Fishplate.

Sleepers		Depth of ballast	Elastic modulus (average)	Weather	Railway	Section	Tests	Series	Appendix No.	Page No.	
Type	Date laid									Deflection	Stress
					75 F. F.	**(1904) Track**	**on Straight**				
Sal wood N+2.	1927	3" Stone over 6" bricks.	869	Monsoon	E. B.	LGL-KNJ	Packed Joint	425–431	II	II D 82	II S 158.
							Low Joint	433–438	II	II D 83	II S 159.
							Packed Joint (Supported).	441–446	II	II D 84	II S 160.
							Free Oscillation.				
							Solid Rail	448–453	I	I DL 34–35 I D 36	I S 76.
							Low Joint (Supported).	454–458	II	II D 85	II S 161.
					75 D. H.	**Track on St**	**raight**				
D. and O. Plate N+2.	..	11" Stone	4260	Monsoon	E. I.	SNT-BHW	Packed Joint	459–464	II	II D 86	II S 162.
							Solid Rail	466–470	I	I DL 37–38 I D 39	I S 77.
					75 D. H.	**Track on C**	**urve**				
D. and O. Plate N+2.	..	12" Stone	6150	Monsoon	E. I.	Sahibganj loop.	Low Joint	472–476	II	II D 87–88	II S 163
							Solid Rail near Joint.	477–481	I	..	I S 78
							Solid Rail between sleepers.	482–487	I	I DL 40 I D 41	I S 79.
							Solid Rail near sleepers.	488–490		..	I S 80.
							Low Joint	491–495		..	II S 164.
					73 B. H.	**Track on St**	**raight**				
Deodar	1923	2½" Stone	1112	Dry	N W	JUC-HSX	Solid Rail packed.	235–240	I	..	I S 81.
							Packed Joint	242–247	II	II D 89–92	II S 165.
							Solid Rail (packed).	248–251	I	I DL 42	I S 82.
							Solid Rail Low spot.	252–255		..	I S 83.
							Do.	256–259		..	I S 84.
							Packed Joint	260–263		..	II S 166.
							Low Joint	265–271	II	II D 93–96	II S 167.
					58½ F. F.	**Track on Stra**	**ight**				
Deodar N+1.	..	1½" Stone	1450	Dry	N. W.	JUC-MEX	Solid Rail	272–277	I	I DL 43	I S 85.
							Packed Joint	279–283	II	II D 97–98	II S 168.
							Low Joint	284–291	II	II D 99–100	II S 169.
					50 F. F.	**Track on St**	**raight**				
Wood N+1.	..	5" Stone	865	Dry	B. B. & C. I.	DLI-RE	Packed Joint	700–707	II	II D 101	II S 176.
							Solid Rail near sleeper.	709–714	I	I DL 44	I S 86.
							Solid Rail between sleepers.	715–721	I	I D 45	I S 87.
							Low Joint	723–728	II	II D 102	II S 171–172

Diagrams Figure 2 show the composition of the special test trains which were used on broad and metre gauge tracks respectively.

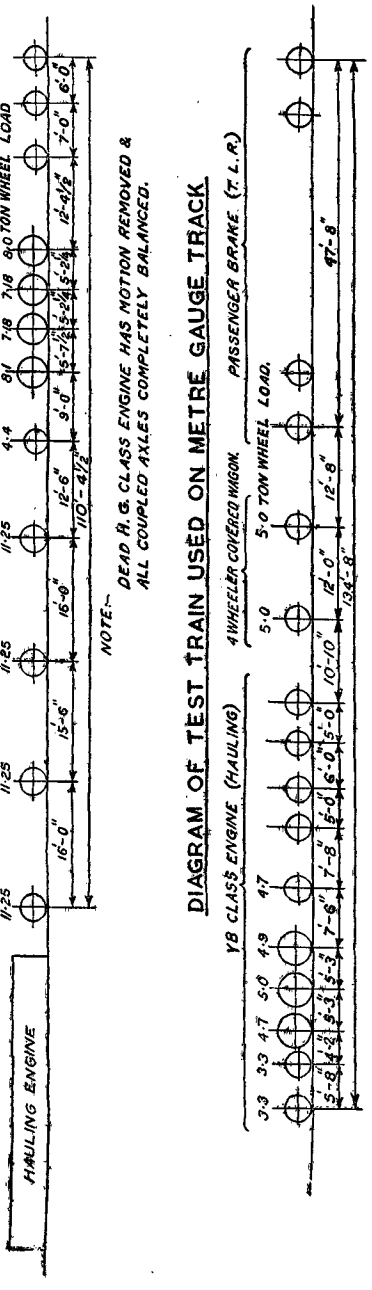

FIG. 2

3. Static Stresses and Deflections in the Solid Rail.

Under ideal track conditions for a concentrated vertical load P on a rail of infinite length in both directions, supported on a continuous elastic foundation which provides a vertical reaction μy per unit length, the depression of the rail at any point at a positive distance x from P is given by

$$y = \frac{P}{8\beta^3 EI} e^{-\beta x} (\cos \beta x + \sin \beta x) \qquad (1)$$

where $\beta = \sqrt[4]{\frac{\mu}{4EI}}$

E = the modulus of elasticity of rail steel.

I = the moment of inertia of one rail.

μ = vertical elastic modulus of the track, i.e., the number of force units per unit length of rail required to produce a uniform unit depression of the rail.

This is a solution of the equation :—

$$E I \frac{d^4y}{dx^4} + \mu y = 0 \qquad (2)$$

from (1) we get:

The bending moment $M = - EI \frac{d^2y}{dx^2}$

$$= - \frac{P}{4\beta} e^{-\beta x} (\sin \beta x - \cos \beta x) \qquad (3)$$

The maximum depression and maximum bending moment occur under P and are

$$\Delta = (y)_{x=0} = \frac{P}{8\beta^3 EI} = \frac{P\beta}{2\mu}$$

and $M = (M)_{x=0} = \frac{P}{4\beta}$

The distance to the point of contraflexure

$$X_1 = \frac{\pi}{4} \sqrt[4]{\frac{4EI}{\mu}}$$

y and M when plotted to a base of x are also influence lines for static deflection and bending moment respectively for the point on the rail $x=0$ and therefore the depression and bending moment for any combination of wheel loads can be determined by superposing curves from each wheel giving each its proper amplitude and phase relation. In order to facilitate such calculations, master diagrams and a system of tabulating the results have been published.*

The theory outlined above has been accepted as a basis of rail stress and deflection calculations for Indian Railways and it has been in general use since 1925.

* "The Report of the Bridge Sub-Committee on Track Stresses," Technical Paper No. 245, Government of India Central Publication Branch, Calcutta, 1925.

TABLE II A.

Calculated and Actual Stresses in Solid Rails under O. S. Wagon at Dead Slow Speeds.

Item No.	Series	Rail lb.	Sleepering	u	I	Actual Stresses		Calculated Stresses		Section Modulus	
						c	t	c	t	Zc	Zt
1*	761–769	100 B. H. Monsoon.	C. I. Pot N+3	b1316 a2436	38·6	15·4	14·5	b8·32 a7·46	9·57	14·0	12·7
2	640–646	100 B. H. dry.	C. I. Pot N+3	2225	39·2	4·7	8·3	7·5	8·35	14·0	12·7
3	802–809	100 B. H. Monsoon.	Wood N+3	1007	36·72	11·3	9·5	9·62	10·5	C13·25 U R V	12·1
4*	550–588	100 B. H. dry.	Wood N+3	b1056 a1260	36·8	5·4	6·0	b9·18 a8·9	10·55 10·3	E13·25	12·1
5	361–366	90 R ..	G Type N+1+D.	2545	38·45	8·0	6·4	7·9	6·9	13·05	14·38
6	520–525	90 R ..	Steel pressed jaws N+2.	1078	38·45	8·8	7·0	9·77	8·9	13·05	14·38
7	148–155	90 R ..	Steel loose jaws N+3.	1810	37·6	8·0	8·4	8·76	7·88	13·05	14·38
8	83–94	90 R ..	CST9 N+2	2730	38·45	9·2	7·0	7·75	7·04	13·05	14·38
9	10–20	90 R ..	Wood N+3 ..	2160	36·3	8·5	7·0	8·58	7·77	13·05	14·38
10	497–501	90 BSS ..	CST9 N+1+D.	1732	31·5	9·6	7·7	9·42	8·85	11·45	12·2
11	332–338	88½ B. H. ..	D. and O. N+1+D.	1690	31·0	10·4	10·4	8·89	11·3	12·35	9·85
12	419–422	85 F. F. ..	C. I. Pot N+3.	1680	28·5	9·8	8·9	9·56	9·74	11·35	11·1
13	550–559	82 B. H. ..	C. I. Pot N+2	2064	26·7	7·6	9·0	11·5	12·8	10·35	9·34
14	448–453	75 F. F. (1904).	Wood N+2 ..	869	19·68	13·0	13·6	14·0	14·8	8·17	8·13
15	201–206	75 F. F. (1892).	Wood N+1 ..	1685	23·8	12·5	10·8	10·68	10·78	9·64	9·54
16*	482–487	75 D. H. ..	D. & O. N+2	6150	22·0	12·2	11·8	8·4	8·8	8·56	8·28
17*	466–470	75 D. H. ..	D. & O. N+2	4260	20·7	11·4	6·9	9·8	9·5	7·9	8·13
18	235–240	73 B. H. ..	Wood N+2 ..	1112	22·1	10·2	11·5	12·05	14·05	9·16	7·84
19	272–277	58½ F. F. ..	Wood N+1 ..	1450	12·6	14·0	12·0	12·61	12·81	6·0	5·88
20*	715–731	50 F. F. ..	Wood N+1 ..	865	10·4	8·6	5·8	9·62	10·5	5·07	5·31

TABLE II B.

Calculated and actual stresses in solid rails under dead H. G. engine (2-8-0) at Dead Slow Speed.

Item No.	Series	Rail lb.	Sleepering	u	I	Actual Stresses		Calculated Stresses		Section Modulus	
						c	t	c	t	Zc	Zt
1*	761–769	100 B. H. Monsoon.	C. I. Pot N+3	b1316 a2436	38·6	13·2	10·6	4·83	5·32	14·0	12·7
2	640–646	100 B. H. dry.	C. I. Pot N+3	2225	38·6	2·7	4·8	4·40	4·85	14·0	12·7
3	802–809	100 B. H. Monsoon.	Wood N+3 ..	1007	36·72	7·0	6·2	5·68	5·81	13·25	12·1
4*	580–588	100 B. H. dry.	Wood N+3 ..	b1056 a1260	36·8	2·4	3·3	5·10	5·85	13·25	12·1
5	361–366	90 R ..	G type N+1+D.	2545	38·45	4·7	5·3	4·62	4·20	13·05	14·38
6	520–525	90 R ..	Steel pressed jaws N+2.	1078	38·45	5·0	4·3	5·34	4·85	13·05	14·38
7	148–155	90 R ..	Steel loose jaws N+3.	1810	37·6	5·4	5·8	4·96	4·50	13·05	14·38
8	83–94	90 R ..	CST/9 N+2	2730	38·45	6·2	5·8	4·53	4·12	13·05	14·38
9	10–20	90 R ..	Wood N+3 ..	2160	36·3	3·5	4·5	4·94	4·46	13·05	14·38
10	497–501	90 BSS ..	CST/9 N+2	1732	31·5	6·7	4·3	5·32	5·09	11·45	12·2
11	332–338	88½ B. H. ..	D. and O. N+1+D.	1690	31·0	5·4	6·0	5·04	6·31	12·35	9·85
12	419–422	85 F. F. ..	C. I. Pot N+3	1680	28·5	6·4	6·7	5·29	5·38	11·3	11·1
13	550–559	82 B. H. ..	C. I. Pot N+2	2064	26·7	4·7	6·1	5·65	6·26	10·35	9·34
14	448–453	75 F. F. (1904).	Wood N+2 ..	869	19·68	9·2	9·7	7·95	8·40	8·17	8·13
15	201–206	75 F. F. (1892).	Wood N+1 ..	1685	23·8	8·0	7·0	6·16	6·23	9·64	9·54
16*	482–487	75 D. H. ..	D. & O. N+2	6150	22·0	8·8	7·9	5·50	5·68	8·56	8·28
17*	466–470	75 D. H. ..	D. & O. N+2	4260	20·7	7·6	5·0	6·32	6·15	7·9	8·13
18	235–240	73 B. H. ..	Wood N+2 ..	1112	22·1	6·2	7·3	6·90	8·05	9·16	7·84
19	272–277	58½ F. F. ..	Wood N+1 ..	1450	12·6	..	..	..	..	6·0	5·88
20	715–721	50 F. F. ..	Wood N+1 ..	855	10·4	..	..	..	..	5·07	5·31

Tables II-A and II-B give the calculated maximum static bending stresses in the rail and the corresponding measured stresses under the O. S. wagon and Dead H. G. engine respectively.

The discrepancies are chiefly due to the following causes which modify the results to a greater or less extent:—

(1) Vehicle characteristics including imperfect springing.

(2) Contact stresses in rail head.

(3) Low and high spots in the track.

(4) Non-uniform contact pressure between rail and sleeper, chair or bearing plate.

(5) Eccentricity of contact between tyre and rail table.

(6) Cant of rails and coning of tyres.

(7) Relief in bending stress due to arching of rail supports.

(8) Modified value of elastic constant at points some distance from the wheel loads where reactions are negative.

It has not been possible to separate the actual effect of all the above factors in any given series of tests.

Cause 1.—Can result in serious discrepancies only in the case of locomotives having noncompensated springs where variations in wheel loads up to 40 per cent are common.

Cause 2.—The effect of the complex stresses near the contact zone in the head is normally to reduce the longitudinal compressive stresses near the point of contact as measured on the two inch telemeter gauge length. This is characterized by a sharp symmetrical dip in the stress record starting when the load is about three inches from the centre of the gauge length and rising to a maximum at the centre of the gauge length as indicated in diagram, Figure 3.

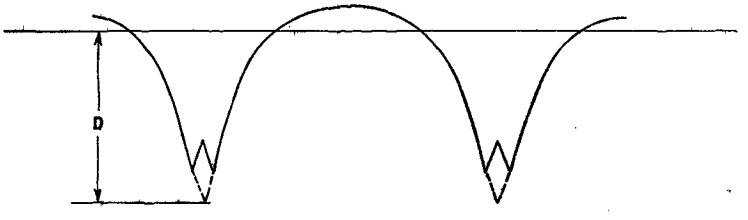

FIG. 3

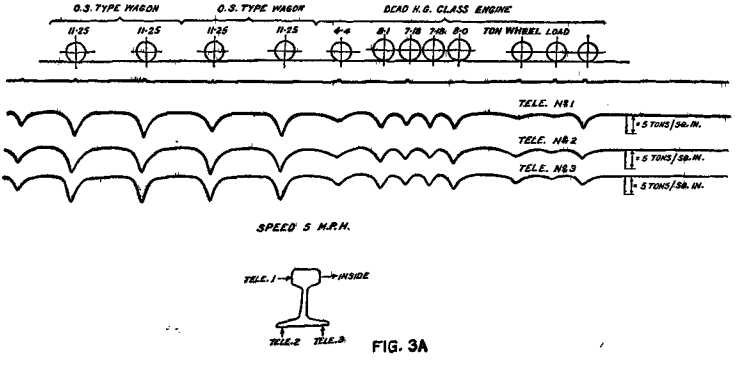

FIG. 3A

It should be specially noted that for purposes of plotting the graphs of rail bending stresses to a speed base, which appear later in this Report, and for estimating the position of the neutral axis of the rail section, local contact stresses have not been measured. The head stress has been deduced from the ordinate D given by the peak of the imaginary curve A B C which is drawn on the record by hand to correspond as nearly as possible with the shape of the peaks for tension stresses.

Cause 3.—Low and high spots are present in all tracks to a greater or less extent. Their effect is an important one directly dependent on maintenance of the track.

Cause 4.—In tests of flat footed rails the location of the telemeters was as in Fig. 4,

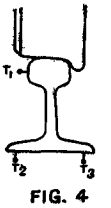

FIG. 4

and for Bull head rails as in Fig. 5,

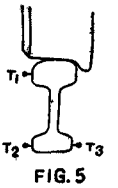

FIG. 5

or in certain cases as in Fig. 6.

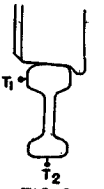

FIG. 6

As a general rule, considerable differences have been noted between the records from T_2 and T_3. Such differences may be considered to be a subject falling under Item 5 of the terms of reference. It has not, however, been determined to what exact extent the differences are due to speed or to track imperfections.

Cause 5.—Eccentricity of contact between the tyre and the rail table has important effects on fillet stresses which have been measured in the case of 90 R rails and the results are reported in a later chapter dealing with Item 5 of the terms of reference. It also has marked effects on the longitudinal head stresses, and results in an increase of compression at the side of the head remote from the eccentricity and a decrease at the other side. The practice mentioned in the preceding paragraph of taking D Fig. 3 to be the maximum compressive stress in the head is probably not far from the truth. Further research on this point is necessary.

Cause 6.—Cant and coning of tyres appear to effect some increase in secondary stresses in rails.

Cause 7.—For all tests, the rail depression under an O. S. type wagon has been used for calculating the elastic constant μ. The calculation can be made either from the average depression or from the deflection at the point immediately under the load. For normal well packed track there is little difference in the result whichever method is used. In using the average depression method the shaded area Fig. 7 only was taken and assumed to be produced by half the total rail load as there is sometimes doubt about the exact extent of the outer limbs of the curve.

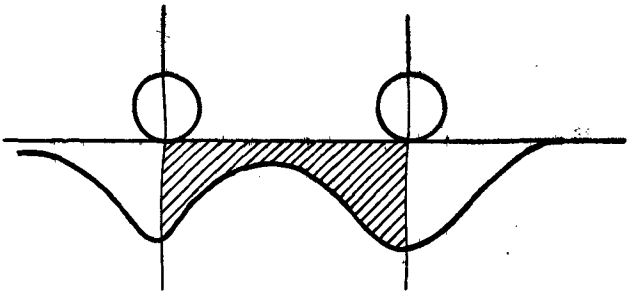

FIG. 7

Another method which has been used in America is to take depressions under two similar vehicles, one fully loaded and the other empty. A modified value of μ say μ_m can be obtained independent of any slack between the rail and the top of the ballast. The slack can be estimated, by assuming direct proportionality between load and deflection after the slack has been taken up. This method was tried but the values of μ_m so obtained when applied to rail stress calculation, yielded results much lower than the measured stresses.

Theoretically, μ is independent of the stiffness of the rail, and the true value of μ can only be obtained from depression of tracks loaded with a uniformly distributed load.

When the rail is stressed by a wheel load, there is longitudinal strain and extension of the rail foot extending from beneath the load up to the point of contraflexure, from which point there is shortening. Sleeper pressures are considerable for some distance beyond the point of contraflexure and where the sleepers and road offer resistance to the longitudinal strain in the rail, there will be a certain relief of stress in the latter.

Experiments were carried out on 90 lb BSS track on the North Western Railway at Ladhowal to investigate this effect; static stress measurements were made at two locations. At one of these, the bearing plates were removed and the rails were lifted to enable roller rocker bearing nests to be inserted between the rail foot and the sleeper.

The results are as follows:—

TABLE 3.

Extreme Fibre Stresses in the Rail Foot due to Vertical Bending; tons per square inch.

Wheel No.		1	2	3	4
With Rollers .. .. .. μ=1568 Calculated stress (Elastic Theory) .. = 9·38 tons per square inch.	1st Run ..	9·27	9·1	9·14	9·1
	2nd Run ..	9·32	9·45	9·40	9·4
	Mean ..	9·295	9·275	9·27	9·25
Normal Track .. .. .. μ=1360 Calculated Stress (Elastic Theory) .. = 9·08 tons per square inch.	1st Run ..	7·25	6·95	7·33	7·24
	2nd Run ..	6·62	6·95	6·89	6·61
	Mean	6·935	6·95	7·11	6·925

For the 90 lb. BSS rails tested,

$I = 32{\cdot}3$ inches^4.

$A = 8{\cdot}8$ square inch.

See Figure 8.

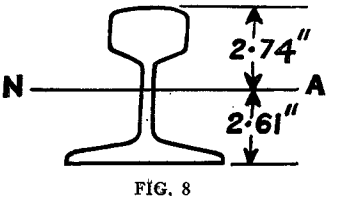

FIG. 8

The calculated stress in the rail foot = 9·08 tons per square inch. The corresponding mean recorded stress is 6·98 tons per square inch.

If P is the horizontal relief force, then

$$\frac{P}{8{\cdot}8} + \frac{P \times 2{\cdot}61^2}{32{\cdot}3} = 9{\cdot}08 - 6{\cdot}98$$

$$P = 6{\cdot}48 \text{ tons.}$$

The calculated extreme fibre stress in the head

$$= \frac{9{\cdot}08 \times 2{\cdot}74}{2{\cdot}61} = 9{\cdot}55 \text{ tons per sq. in.}$$

$$\text{increase} = \frac{P}{A} = \frac{6{\cdot}48}{8{\cdot}8} = 0{\cdot}74 \text{ tons per sq. in.}$$

Decrease due to bending moment

$$= \frac{6{\cdot}48 \times 2{\cdot}61 \times 2{\cdot}74}{32{\cdot}3} = 1{\cdot}43 \text{ tons per sq. in.}$$

Net relief of stress in the head

= 0·69 tons per square inch.

= 7·0%

Net relief in foot = 23%.

Whereas causes 1 to 6 tend to increase maximum and decrease minimum bending stresses, cause 7 always tends to reduce these stresses. It is considered that the arching effect is the chief reason for the actual stresses due to isolated concentrated loads falling short of those calculated.

Cause 8.—This is only appreciable when considering reversal stresses, especially under wagon axles and bogie stock.

Results of stress measurements in the solid rail at slow speeds.

Tables IIA and B give actual and calculated static rail stresses for all test sites under the O. S. wagon and Dead H. G. engine. Those items which are marked with an asterisk are considered to be abnormal cases, i.e., in the case of Item 1, the black cotton sub-soil was known to be seriously overloaded and underpinning was about to be commenced ; in the case of Items 4, 16, 17 and 20, there is some uncertainty regarding the correct value of μ to be taken in the calculations.

In the following table, the ratios

$$R = \frac{a}{c} = \frac{\text{Average value of the actual maximum static tensile stresses at the centre of the rail base due to all causes}}{\text{Calculated maximum static tensile stress at the centre of the rail base due to bending moment}},$$

$$A = \frac{\text{Maximum recorded values of static tensile stress in rail base}}{a}$$

R, A and A × R are given in table 4 for various vehicles at all test sites except those marked with an asterisk in tables 2A and 2B.

TABLE 4.

Vehicle	R	A	A×R
Metre gauge wagon 10 ton axle	0·85	1·57	1·33
Metre gauge YB class engine coupled axles	1·00	1·95	1·95
Broad gauge O. S. wagon 22½ T axles	0·905	1·65	1·49
2-8-0 N. W. R. H. G. engine 16 T axles	1·08	2·2	2·38
4-6-0 G. I. P. D/5 class engine coupled axles	1·00	1·73	1·73
4-6-2 G. I. P. metrovic electric passenger 20 T driving axles	1·00	1·84	1·84

The largest variation occurs in the case of the 2-8-0 N. W. R., H. G. engine. It is probable that this is due to the type and condition of the compensating gear used on this engine.

4. Dynamic Deflections in the Solid Rail.

Curves showing the variation of maximum solid rail deflection with speed for all tests where these deflections were measured form Appendix I D, Vol. 2. The mean of the maxima of the left and of the right hand rails in each test run is, in most instances, also plotted. Tests have been grouped in series. Each series comprises all tests, usually made at a range of speeds at one particular spot in the track which were made on the same day and therefore as far as possible under identical track conditions.

100 LB.B.H.
SOLID RAIL DEFLECTION

Speed increment as percentage of deflection at dead slow speed

Curve A for series 761-766
-do- B -do- 802-807

HAULING ENGINE 4-6-2 ELECTRIC PASSENGER.

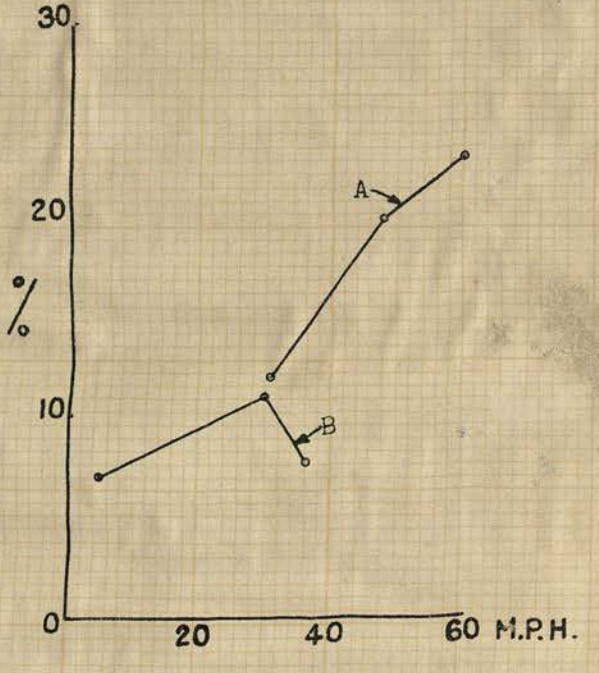

FIG. 8A

100 LB.B.H. GIP.

SOLID RAIL DEFLECTION

STRAIGHT AND CURVED TRACKS

SPEED INCREMENT AS PERCENTAGE OF DEFLECTION AT DEAD SLOW SPEED

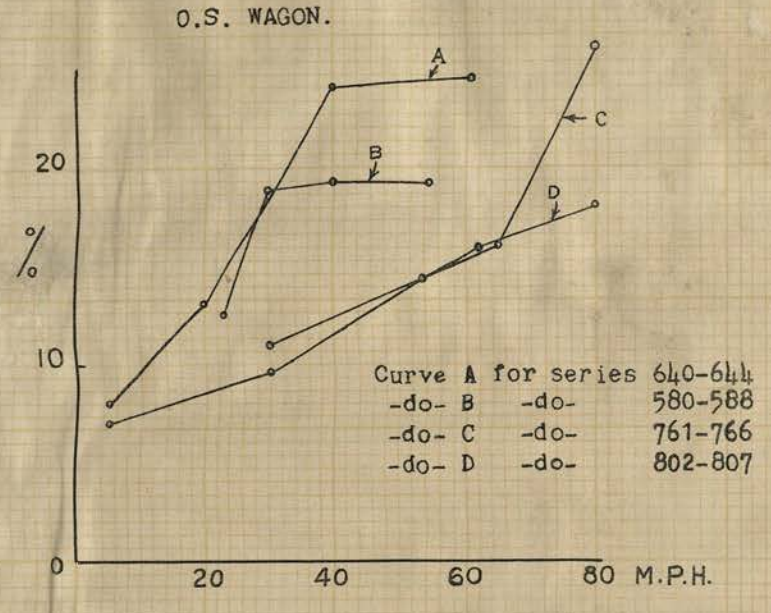

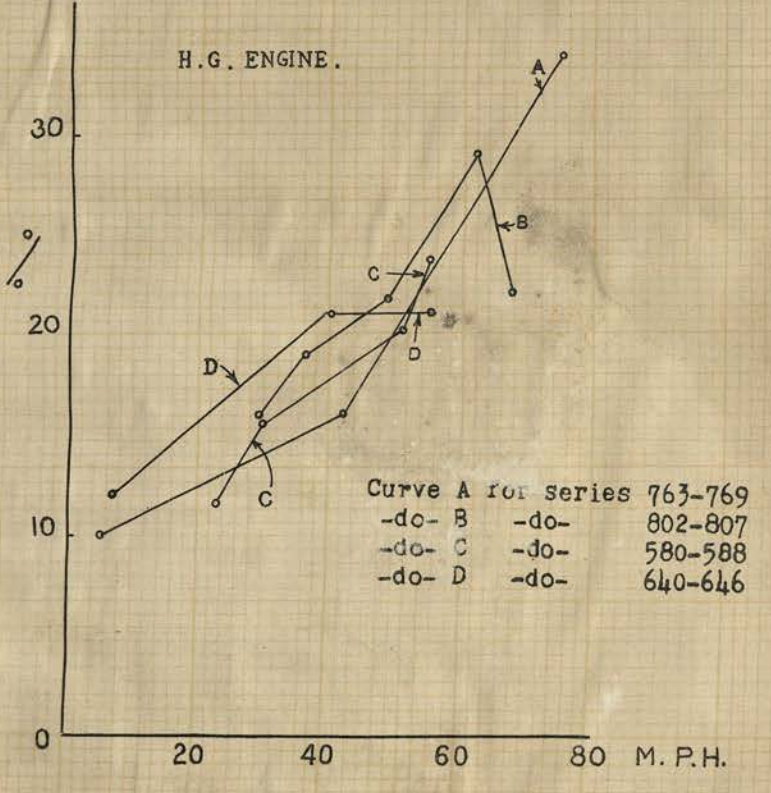

FIG.9

100 LB.B.H. GIP.

SOLID RAIL DEFLECTION

Speed increment as percentage of deflection at dead slow speed

Curve A for series 616-621 Trailer
-do- B -do- 616-621 Motor Coach
-do- C -do- 810-815 Trailer
-do- D -do- 810-815 Motor Coach

MULTIPLE UNIT SUBURBAN STOCK

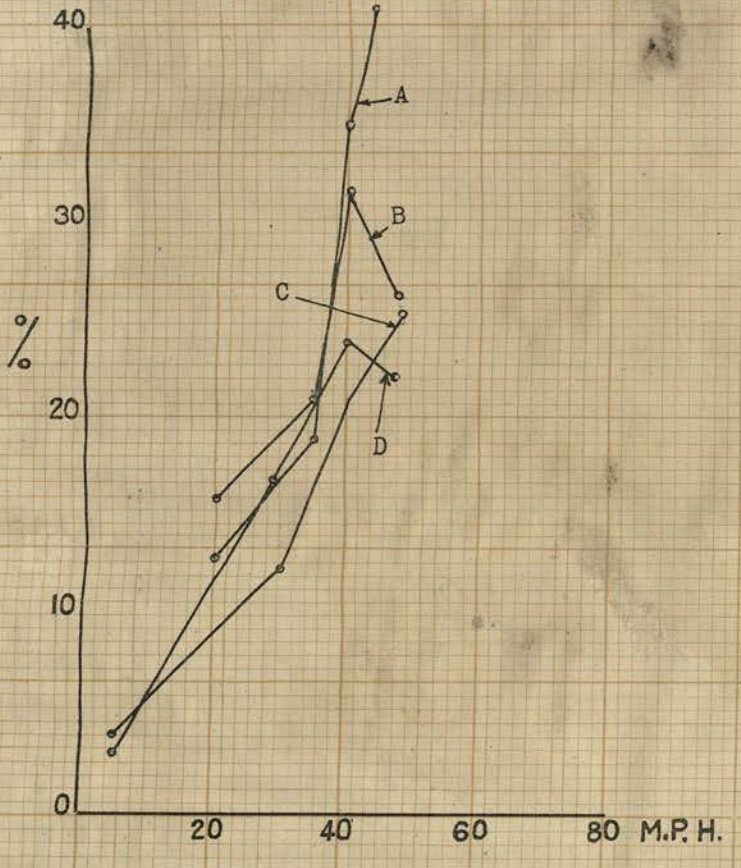

FIG.10

90 R.

SOLID RAIL DEFLECTION

STRAIGHT TRACK

SPEED INCREMENT AS PERCENTAGE OF DEFLECTION AT DEAD SLOW SPEED

O.S. WAGON.

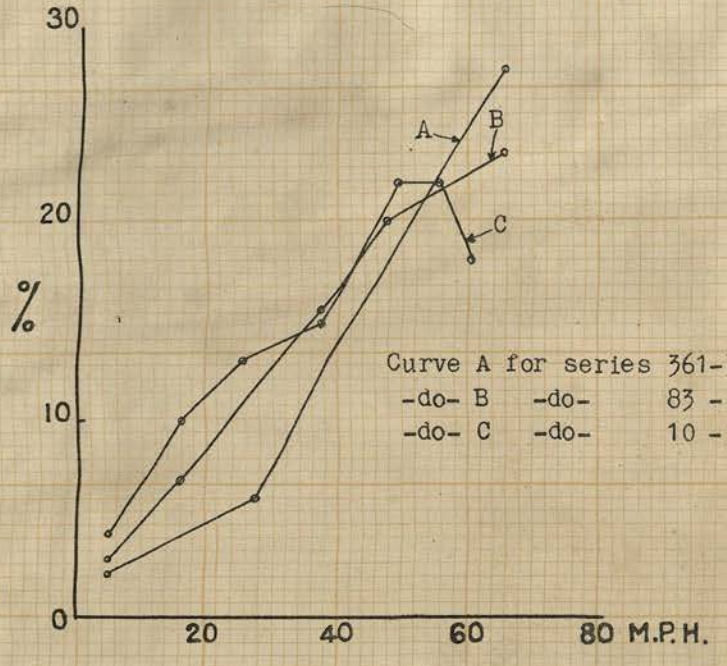

Curve A for series 361-366
-do- B -do- 83 - 92
-do- C -do- 10 - 20

DEAD H.G. ENGINE.

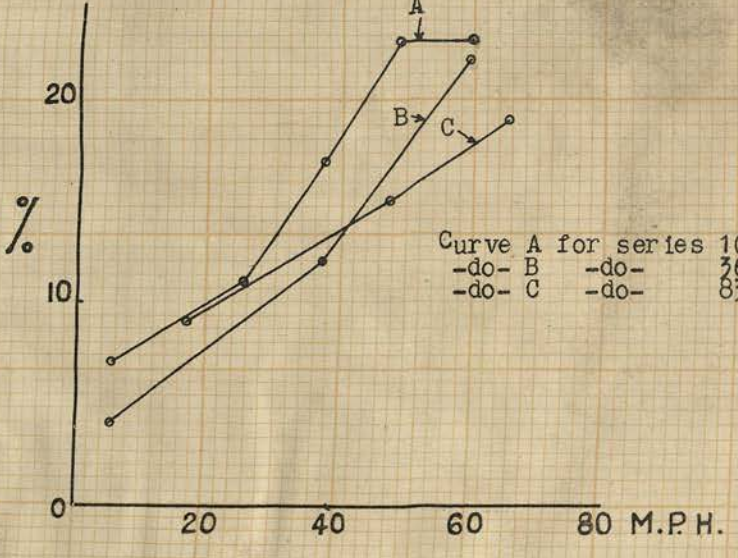

Curve A for series 10 - 20
-do- B -do- 361-366
-do- C -do- 83 - 92

FIG. 11

85 LB.F.F. BNR.
SOLID RAIL DEFLECTION

Speed increment as percentage of deflection at dead slow speed

Curve A for O.S. Wagon.
-do- B for H.G. Engine.

SERIES 419-422

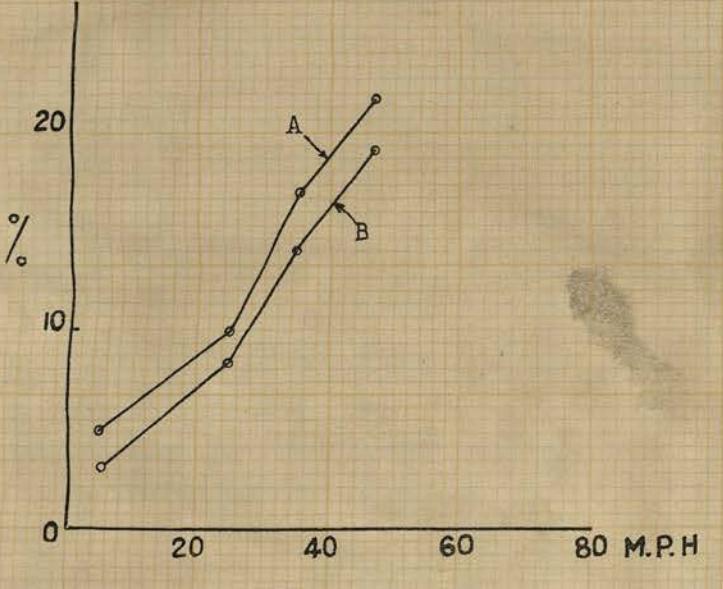

FIG. 12

75 LB.F.F. NWR & EBR.
SOLID RAIL DEFLECTION

Speed increment as percentage of deflection at dead slow speed

Curve A for series 448-453 O.S.Wagon.
-do- B -do- 448-453 H.G.Engine.
-do- C -do- 201-206 O.S.Wagon.
-do- D -do- 201-206 H.G.Engine.

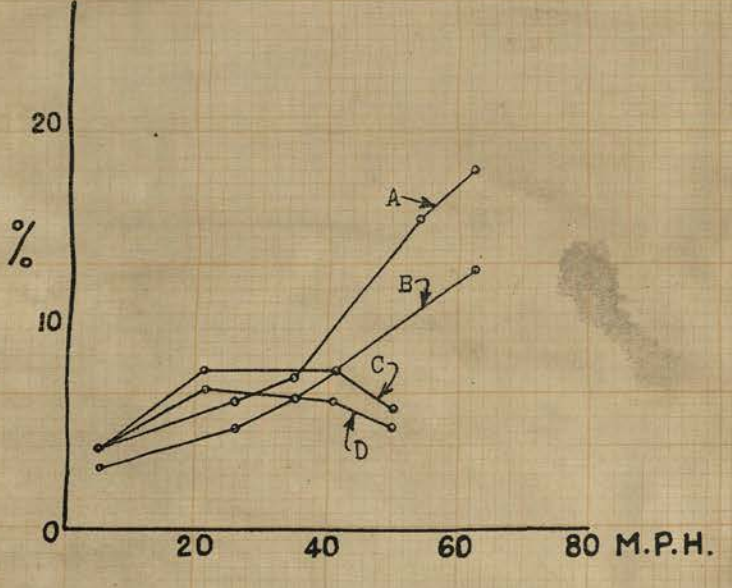

FIG.13

*† Curves Figures 8 A to 13 show the increment in deflection to a speed base expressed as a percentage of the average of the dead slow maxima under all wheels of the same type running in the test train. It will be seen that except in the case of the multiple unit G. I. P. suburban stock on 100 lb B. H., curved track, all contingencies are covered by the straight line

$$T=\left[10+0{\cdot}37V\right] \begin{matrix}\text{for deflection and sleeper}\\ \text{pressure speed increments}\end{matrix}$$

where T is the percentage increment due to speed, and V is the speed in miles per hour.

The abnormally large deflections recorded under the multiple unit electric suburban stock on the 2640 feet radius curve may be due to rolling of the superstructures and is probably characteristic of the type of vehicle. Very few experiments with bogie stock have been included in the programme of tests.

Mathematical Analysis of the Effect of Speed on Rail Deflection and Sleeper Pressures.

Under good track conditions, the deflection of the rail immediately under a moving wheel load is constant. The extent to which the deflexion varies from the static value will depend upon the effective mass of the rails, fastenings, sleepers and formation which participate in the vertical movement. It will also depend upon friction forces which oppose the movement. If, therefore, we call m the effective mass of the track per unit length, N the damping factor, and v the velocity of a concentrated load P and y the deflexion at any point, the partial differential equation for calculation of y neglecting shearing strains is

$$EI\frac{\partial^4 y}{\partial x^4}+m\frac{\partial^2 y}{\partial t^2}+N\frac{\partial y}{\partial t}+uy=\frac{2p}{l}\left[\sin\frac{\pi x}{l}\sin\frac{\pi vt}{l}+\sin\frac{2\pi x}{l}\sin\frac{2\pi vt}{l}+\sin\frac{3\pi x}{l}\sin\frac{3\pi vt}{l}+\text{etc.}\right]\ldots.(4)$$

where $l\geq\frac{4\pi}{\beta}$

$$\beta=\sqrt[4]{\frac{\mu}{4EI}}$$

E = modulus of elasticity of rail steel.

I = moment of Inertia of one rail.

μ = vertical elastic modulus of the track, i.e., the number of force units per unit length of rail required to produce a uniform unit depression of the rail.

The damping is taken to be of the fluid friction type proportional to velocity

The particular integral of (4) gives the elastic curve of the rail after any free oscillations have been damped out, i.e.,

$$y=\frac{P}{l}\left[\frac{\left\{EI\left(\frac{\pi}{l}\right)^4-\left(2\pi n\right)^2 m+u\right\}\cos\left(\frac{\pi x}{l}-2\pi nt\right)-2\pi n\,N\sin\left(\frac{\pi x}{l}-2\pi nt\right)}{\left\{EI\left(\frac{\pi}{l}\right)^4-4\pi^2n^2m+u\right\}^2+4\pi^2n^2N^2}\right.$$

$$-\frac{\left\{EI\left(\frac{\pi}{l}\right)^4-4\pi^2n^2m+u\right\}\cos\left(\frac{\pi x}{l}+2\pi nt\right)-2\pi n\,N\sin\left(\frac{\pi x}{l}+2\pi nt\right)}{\left\{EI\left(\frac{\pi}{l}\right)^4-4\pi^2n^2m+u\right\}^2+4\pi^2n^2N^2}$$

$$+\frac{\left\{EI\left(\frac{2\pi}{l}\right)^4-(4\pi n)^2m+u\right\}\cos\left(\frac{2\pi x}{l}-4\pi nt\right)-4\pi n\,N\sin\left(\frac{2\pi x}{l}-4\pi nt\right)}{\left\{EI\left(\frac{2\pi}{l}\right)^4-(4\pi n)^2m+u\right\}^2+(4\pi n)^2N^2}$$

$$\left.+\text{etc.}\right]\ldots\ldots\ldots\ldots\ldots\ldots\ldots\ldots(5).$$

where $n=\frac{v}{2l}$

* In these and in many other curves which appear later in this report, the lines connecting plotted points are not actual curves but are intended to connect up or trace all points in a series.

† As there is always some variation in wheel loads which are nominally equal all percentage increments are greater than zero even at dead slow speed in Figs. 8A to 13 and in corresponding curves for stresses.

Owing to the slow convergence of the series on the right hand side of the equation its evaluation in particular cases involves cosiderable labour.

m is determined by comparing depression time diagrams of wheel loads moving at high speeds with those obtained at very low speeds.

N can be estimated by comparing the shape of the deflexion diagrams at speed with those at dead slow speed.

Certain important cases have been evaluated:

Elastic lines are plotted in Fig. 14, for an isolated wheel load of 20,000 lb travelling at 60 miles per hour on 90 lb R track continuously and uniformly supported:—

$E = 30 \times 10^6$ lb. per square inch.

$I = 38{\cdot}45$ ins.^{4}

$u = 1700$ lb in^2

$l = 504$ inches.

$v = 1056$ inches per second (60 miles per hour).

The elastic lines are plotted for six combinations of m and N as indicated on Fig. 14 from which it will be seen that the effect of N is to make the curve unsymmetrical about the y axis and the effect of m is to increase the maximum depression and to squeeze in both limbs of the curve towards the y axis.

Maximum positive and maximum reversal deflexions have been evaluated for the following conditions:—

TABLE 5.

Rail	Elastic constant μ	m lb mass per inch	N	Speed range
90 R	700	0·387	3·92	0-70 miles per hour.
	1700	0·387	3·92	0-70 miles per hour.
	2700	0·387	3·92	0-70 miles per hour.
75 R	700	0·25	3·92	0-70 miles per hour.
		0·50	3·92	0-70 miles per hour.
	1700	0·25	3·92	0-70 miles per hour.
		0·50	3·92	0-70 miles per hour.
	2700	0·25	3·92	0-70 miles per hour.
		0·50	3·92	0-70 miles per hour.
50 R	500	0·15	3·92	0-60 miles per hour.
		0·30	3·92	0-60 miles per hour.
	900	0·15	3·92	0-60 miles per hour.
		0·30	3·92	0-60 miles per hour.
	1300	0·15	3·92	0-60 miles per hour.
		0·30	3·92	0-60 miles per hour.

A formula has been obtained to enable the theoretical speed deflection increment under good track conditions to be evaluated:

LIBRARY
OF THE
BOMBAY
BRANCH
OF THE
ROYAL ASIATIC SOCIETY

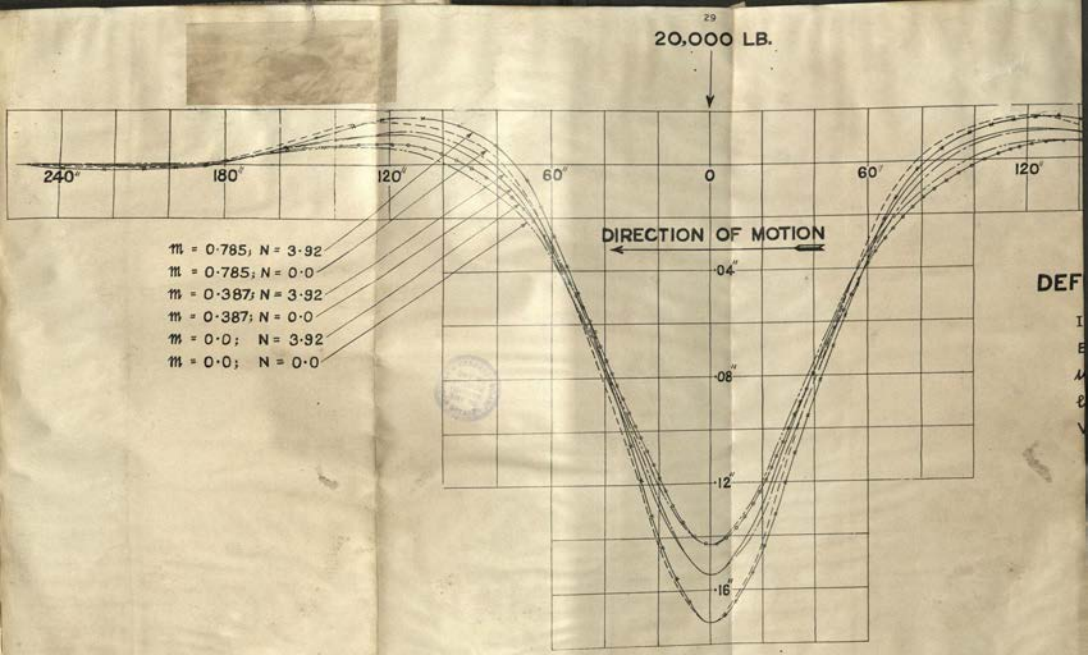
20,000 LB.
240"
180"
120"
60"
0
60"
120"
DIRECTION OF MOTION
·04"
·08"
·12"
·16"
m = 0·785; N = 3·92
m = 0·785; N = 0·0
m = 0·387; N = 3·92
m = 0·387; N = 0·0
m = 0·0; N = 3·92
m = 0·0; N = 0·0

FIG. 14

$$\Psi = S\left[\frac{69500\,m^2}{u\,I}\right]^{\frac{1}{4}}$$

WHERE S = SPEED IN MILES PER HOUR
u = ELASTIC MODULUS
I = MOMENT OF INERTIA OF ONE RAIL
m = EQUIVALENT MASS OF THE TRACK PER INCH RUN

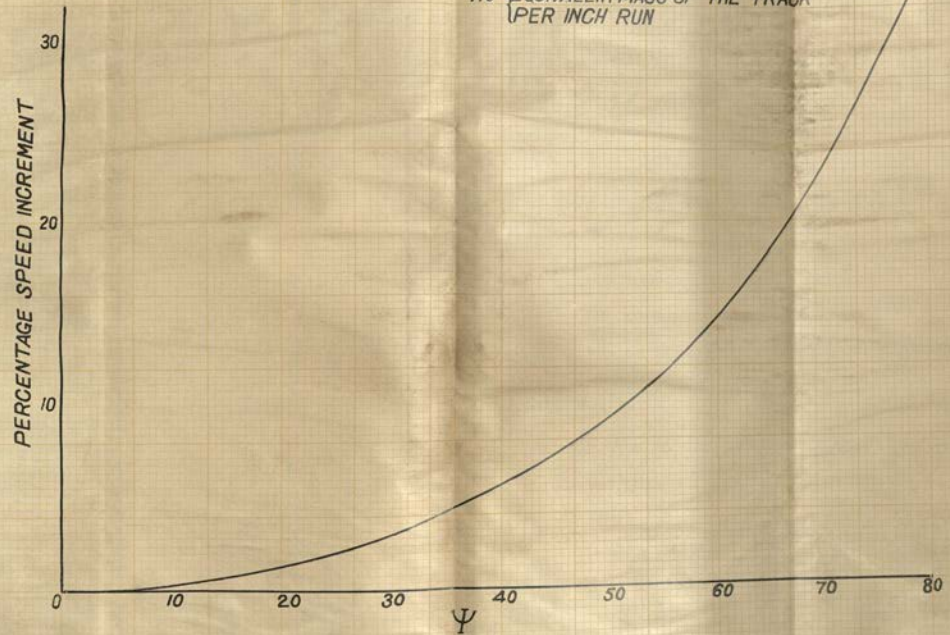

FIG. 15

Curve Fig. 15 shows the relation between the speed increment and a certain function ψ given by the relation

$$\psi = S\left[\frac{69500m^2}{uI}\right]^{\frac{1}{4}}$$

where S is the speed in miles per hour.

u is the elastic track constant in lb. per in^2

I is the moment of inertia of one rail in ins.^{4} units.

m is the equivalent mass of the track in lb. mass per inch run.

The speed increment is given by the ordinate to the curve Fig. 15 by iserting the appropriate value for ψ.

$m = 0{\cdot}39$ appears to be a suitable value for the broad gauge tracks but the experiments in the case of metre gauge have hardly been sufficiently numerous to enable a value to be assessed.

In a number of cases among the results in Appendix ID volume 2, there is fair agreement between actual and theoretical deflexion speed increments.

$N = 3{\cdot}92$ has been found to express the damping effect on 90 R tracks to a reasonable degree of accuracy. The damping appears to be partly of the fluid friction and partly of the solid friction type. N is in the nature of a small correction.

5. Dynamic Stresses in the Solid Rail.

Curves of maximum positive and reversal stresses at the centre of the rail base* and at the top of the head plotted to a speed base are given as Appendix IS, volume 2.

Curves Figures 16 to 22 (pages 32 to 39) show for 100 lb. B. H., 90 R, 85 F. F., 82 lb B. H. and 75 F. F., broad gauge tracks and 50 lb F. F., metre gauge tracks the increment in longitudinal rail stress in the rail head and foot due to all causes plotted against speed as a percentage above the average of the maximum direct stresses in the solid rail.

It has been ascertained that all contingencies will be covered for longitudinal direct and bending stresses due to all causes including speed, hammer blow and steam effects by the provision of a factor which when multiplied by the calculated static bending stress will give the actual maximum static rail stress

For Broad gauge ..	.. 22½T wagon axles at 16′—0″ centre on tracks 88½ lb. and heavier.	(1·24+0·007V).
For Broad gauge ..	.. 22½T wagon axles at 16′—0″ centre on tracks below 88½ lb.	(1·3+0·014V).
For Broad gauge ..	.. 4-6-0 D/5 type G. I. P. passenger locomotive 17·5T axles. 82 lb and heavier.	(1·8+0·012V).
For Broad gauge ..	.. 4-6-2 type G. I. P. electric passenger locomotive 20·0T axles. 100 lb and heavier.	(1·9+0·012V).
For Metre gauge ..	.. 10T wagon axles at 12′—0″ centres. 50 lb and heavier.	(1·5+0·014V).
For Metre gauge ..	.. YB class pacific locomotive .. 50 lb and heavier.	(2·0+0·019V).

where V is the speed in miles per hour.

* i.e. the average of the maxima recorded by the two telemeters attached to the base in cases where more than one telemeter was used at a particular section of the rail.

100 LB.B.H. GIP.

SOLID RAIL STRESS

STRAIGHT & CURVED TRACKS

SPEED INCREMENT AS PERCENTAGE OF MEAN STRESS AT SLOW SPEED

Curve A	for series	640-646	Dry	
-do- B	-do-	802-809	Monsoon	Curved Track
-do- C	-do-	761-766	-do-	
-do- D	-do-	616-621	Dry	-do-
-do- E	-do-	580-588	Dry	-do-

O.S. WAGON.

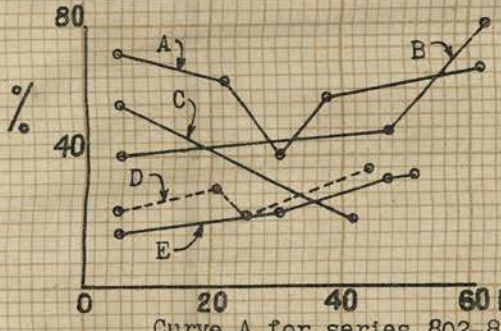

Curve A	for series	802-809	Curved Track	
-do- B	-do-	640-646		
-do- C	-do-	761-766		
-do- D	-do-	580-588	do-	

DEAD H.G. ENGINE.

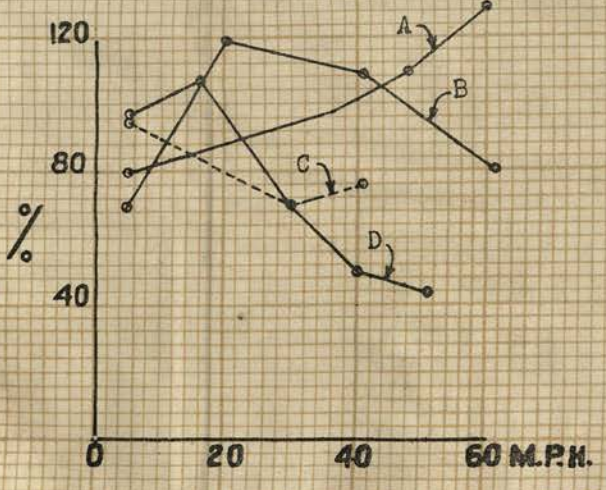

FIG. 16

100 LB.B.H. GIP.

SOLID RAIL STRESS

STRAIGHT & CURVED TRACKS

SPEED INCREMENT AS PERCENTAGE OF MEAN STRESS AT SLOW SPEED

Curve A for series		640-644	
-do- B	-do-	761-766	
-do- C	-do-	802-809	Curved Track
-do- D	-do-	580-588	-do-

HAULING ENGINE 4-6-2 ELECTRIC PASSENGER.

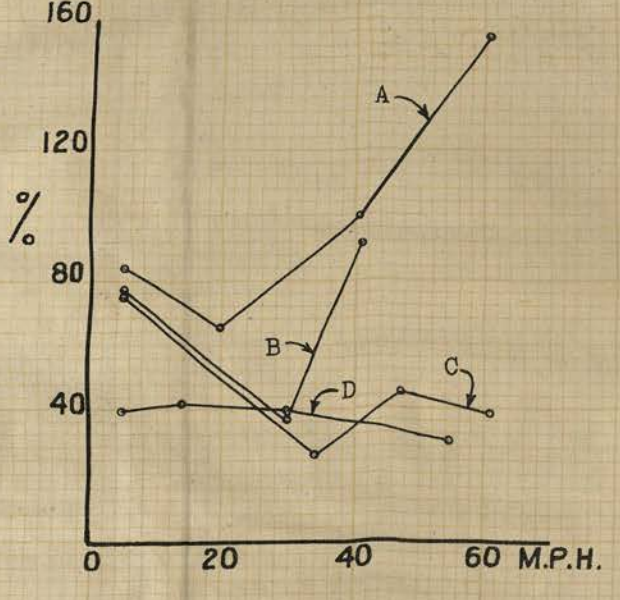

FIG. 16A

90R
SOLID RAIL STRESS
STRAIGHT TRACK

SPEED INCREMENT AS PERCENTAGE OF MEAN STRESS AT DEAD SLOW SPEED

O S WAGON

SLEEPER SPACING 30-31 INCHES.

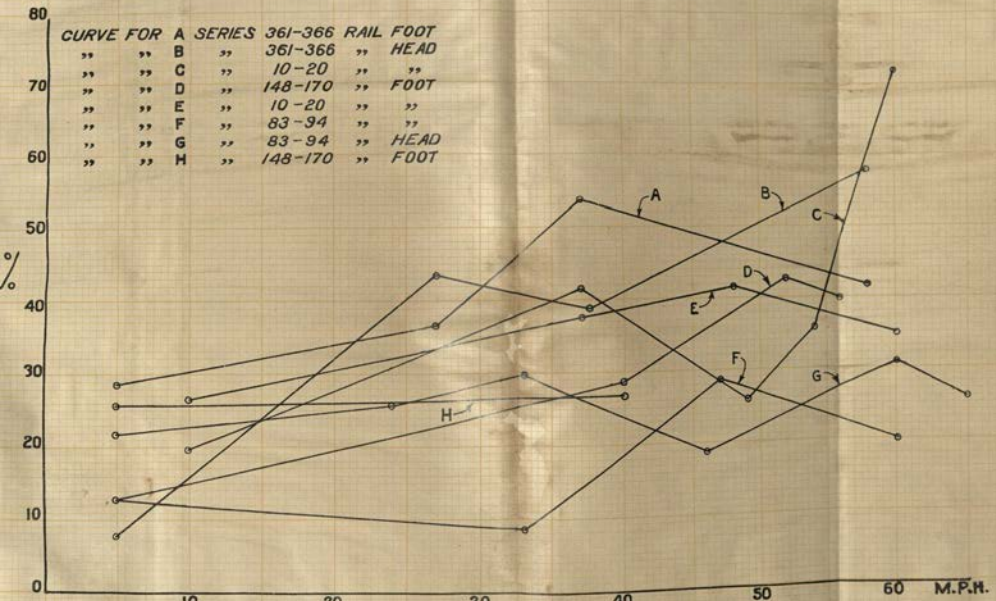

FIG. 17

90R

SOLID RAIL STRESS
STRAIGHT TRACK

SPEED INCREMENT AS PERCENTAGE OF MEAN STRESS AT DEAD SLOW SPEED

DEAD H G ENGINE

CURVE FOR A SERIES 361-366 RAIL FOOT
" " B " 361-366 " HEAD
" " C " 10-20 " FOOT
" " D " 148-170 " "
" " E " 10-20 " "
" " F " 538-541 " "
" " G " 83-94 " "
" " H " 83-94 " HEAD

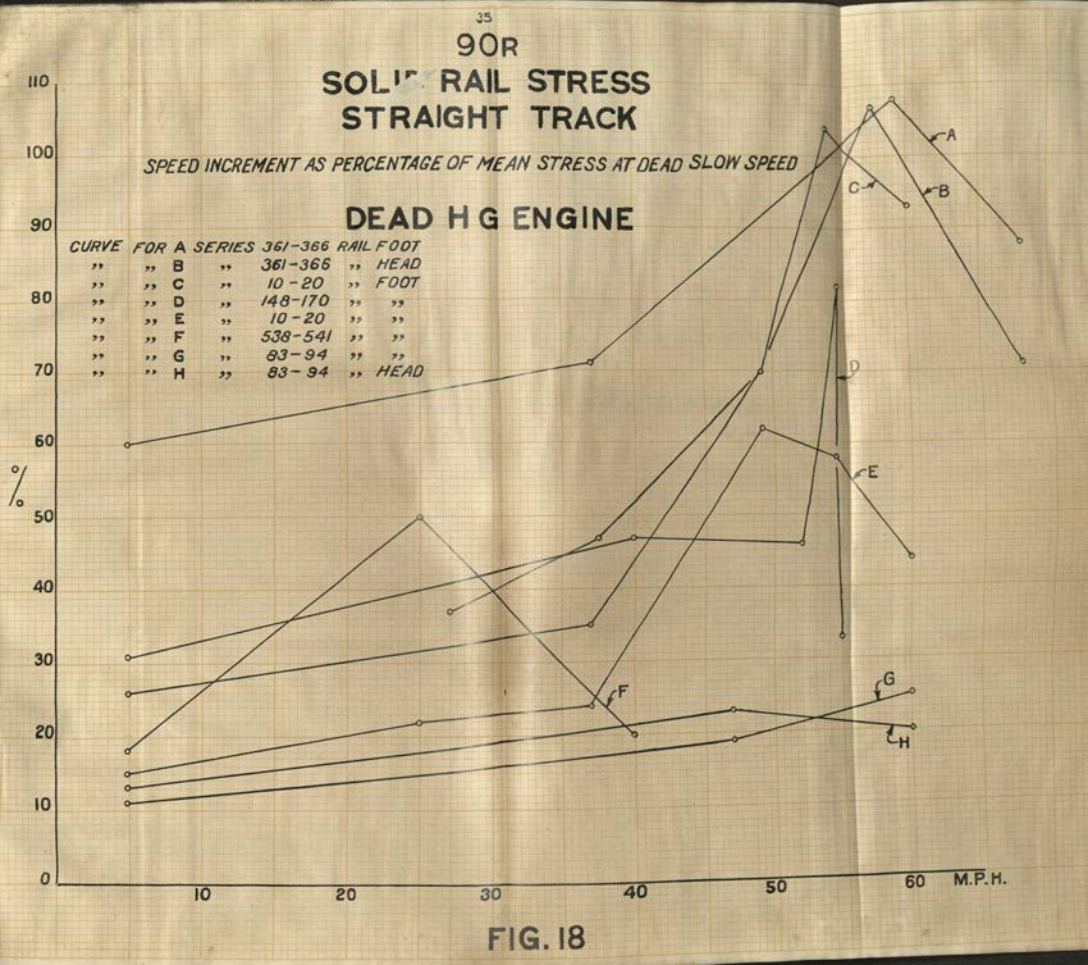

FIG. 18

90 R & 82 LB.B.H. GIP.
SOLID RAIL STRESS

SPEED INCREMENT AS PERCENTAGE OF MEAN STRESS AT SLOW SPEED

Curve A for series 520-525
-do- B -do- 538-541
-do- C -do- 551-559

4-6-0 D/5 CLASS HAULING ENGINE.

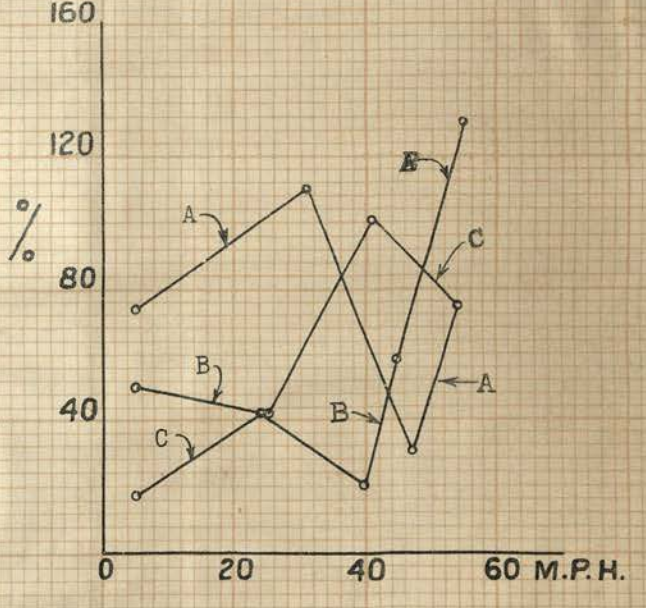

FIG.19

85 LB.F.F. BNR.

SOLID RAIL STRESS

SPEED INCREMENT AS PERCENTAGE OF MEAN STRESS AT SLOW SPEED

Curve A for O.S. Wagon 19.5 tons/sq.in.max.
-do- B for H.G. Engine.

SERIES 419-420

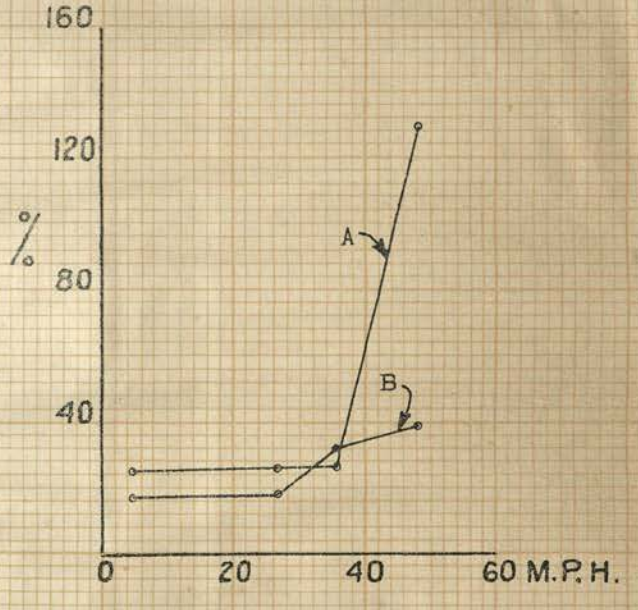

FIG. 20

75 LB.F.F. NWR & EBR.

SOLID RAIL STRESS

SPEED INCREMENT AS PERCENTAGE OF MEAN STRESS AT SLOW SPEED

Curve A	for series	201-206	(37")	O.S.Wagon
-do- B	-do-	449-453	(32")	-do-
-do- C	-do-	449-453	(32")	H.G. Engine
-do- D	-do-	201-206	(37")	-do-

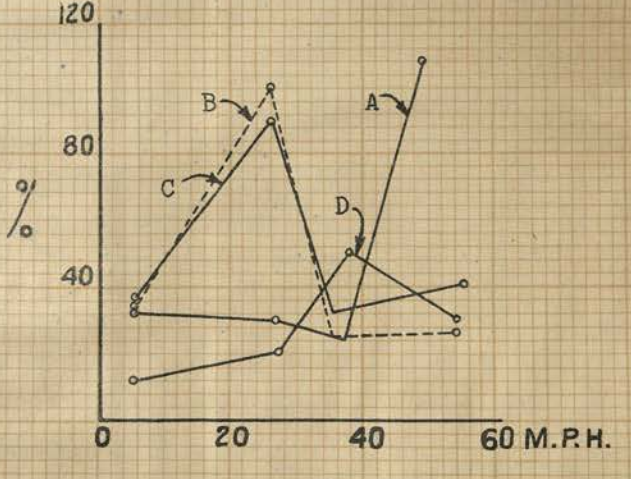

FIG. 21

50 LB.F.F. METRE GAUGE B.B. & C.I.

SOLID RAIL STRESS

SPEED INCREMENT AS PERCENTAGE OF MEAN STRESS AT SLOW SPEED

Curve A for YB engine coupled wheels leading and trailing

driving stress 6.4 tons/sq.in.) near sleeper
driving stress 5.4 -do-) Series 709-714

Curve B for YB engine coupled wheels leading and trailing

Series 715-721 driving stress 4.75 tons/sq.in.) between
driving stress 4.2 -do-) sleepers

Curve C for 10 ton axle of wagon stress 5.4 tons per sq.in.) between sleepers
Series 715-721

Curve D for 10 ton axle of wagon stress 8.1 tons per sq.in)near sleeper
Series 709-714

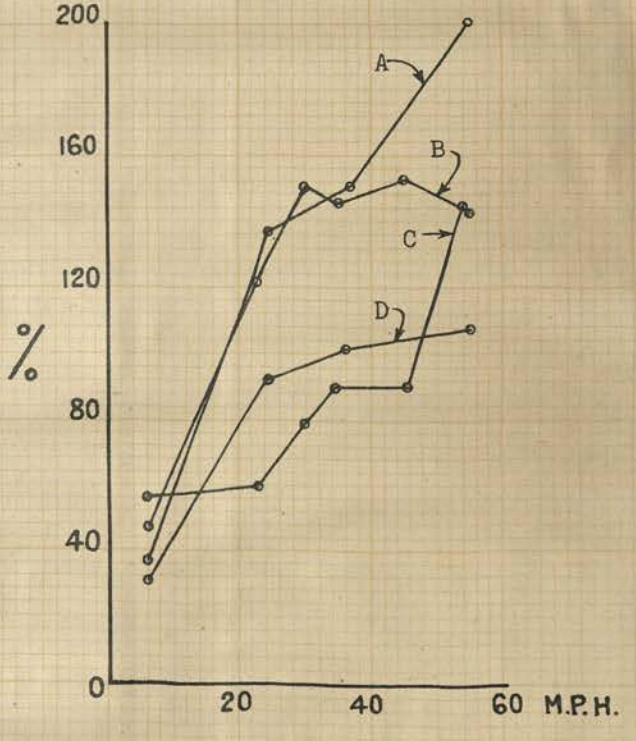

FIG. 22

Longitudinal Rail Stresses at Speed Obtained by Analysis.

Differentiating (5) we get

$$M = -EI\frac{d^2y}{dx^2}$$

$$= -EI\frac{\pi^2P}{l^3}\Bigg[\frac{-A_1\cos\left(\frac{\pi x}{l}-2\pi nt\right)+2\pi n\,N\sin\left(\frac{\pi x}{l}-2\pi nt\right)+A_1\cos\left(\frac{\pi x}{l}+2\pi nt\right)+2\pi n\,N\sin\left(\frac{\pi x}{l}+2\pi nt\right)}{A_1^2+N^2(2\pi n)^2}$$

$$+\frac{2^2\left\{-A_2\cos\left(\frac{2\pi x}{l}-4\pi nt\right)+4\pi n\,N\sin\left(\frac{2\pi x}{l}-4\pi nt\right)\right\}+2^2\left\{A_2\cos\left(\frac{2\pi x}{l}+4\pi nt\right)+4\pi n\,N\sin\left(\frac{2\pi x}{l}+4\pi nt\right)\right\}}{A_2^2+N^2(4\pi n)^2}$$

$$+\ \&c.\Bigg]$$

where $A_1 = EI\left(\frac{\pi}{l}\right)^4 - m\frac{\pi^2v^2}{l^2}+\mu,$

$$A_n = EI\left(\frac{n\pi}{l}\right)^4 - m\left(\frac{n\pi v}{l}\right)^2+\mu. \qquad (6)$$

The following cases have been evaluated from Equation 6.

TABLE 6.

Rail	Elastic constant μ	m	N	Speed Range
90 R	700	0·387	3·92	0-70 miles per hour.
	1700	0·387	3·92	0-70 miles per hour.
	2700	0·387	3·92	0-70 miles per hour.
75 R	700	0·25	3·92	0-70 miles per hour.
	1700	0·25	3·92	0-70 miles per hour.
	2700	0·25	3·92	0-70 miles per hour
50 R	500	0·15	0·0	0-60 miles per hour.
	900	0·15	0·0	0-60 miles per hour.

As in the case of deflexions, a formula has been constructed to enable the speed stress increments for good track conditions based on Equation 6 to be evaluated.

The curve Figure 23 shows the relation between the speed increment and a function which is given by

$$X = S\left[\frac{180000m^2}{\mu I}\right]^{\frac{1}{6}}$$

The speed increment is given by the ordinate to the curve Figure 23 by inserting the appropriate value for X

$$X = S\left[\frac{180000\,m^2}{4I}\right]^{\frac{1}{6}}$$

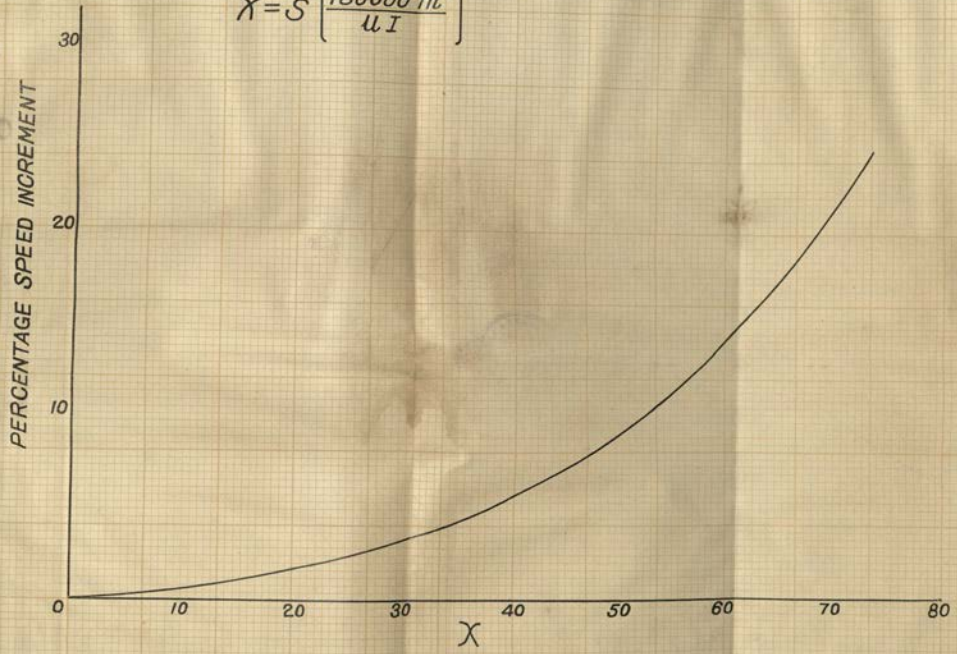

FIG. 23

109203

While good agreement has frequently been observed between the actual recorded deflections at speed and those calculated by the elastic theory given above, the position is not so satisfactory in the case of rail stresses. Satisfactory agreement has been observed only when the rails and fastenings have been in first class condition. Defects due to non-uniform sleeper packing are undoubtedly important causes of discrepancies. An analogous case exists in railway bridges where live load stresses due to all causes often increase with the speed of the load at a greater rate than the deflections, due to high frequency resonances and other causes. In the case of rails, the frequencies of sleeper re-actions may control stress-speed effects to a certain extent.

In the tests of 50 lb F. F. metre gauge track where rail bending moment stresses were recorded close to a sleeper and also midway between sleepers, there was considerable divergence in the results probably on account of the very wide sleeper spacing for a comparatively small rail. Further investigation appears to be required to ascertain whether in such cases, by increasing the number of sleepers, a more uniform rail-stress distribution and less dynamic stress increments can be secured.

Curved Tracks.

The results for curved tracks are included in the Graphs Figures 16 to 22 and in no case is the recorded stress so large as to affect the covering formulæ in last paragraph on page 31.

The fact that rail vehicles tend to run with less lateral oscillation on curves may be the reason for this but since comparatively few curved tracks were examined, this cannot be put forward as a definite explanation.

6. Fishplate Stresses and Joint Deflections under Static Conditions.

For a perfect rail-joint, the depression under a moving wheel load would be constant and equal to the solid rail deflection. This condition would be very approximately attained if

(a) The sleeper spacing were uniform throughout and the stiffness of a pair of fishplates equalled that of the rail

or

(b) The sleeper spacing were uniform throughout and the effective length of the fishplates were negligibly small.

In practice the difficulties in designing fishplates of strength comparable with that of the solid rail are very great especially in the case of flat footed rails, and in order to compensate for lack of stiffness in the fishplates, it is customary to bring the joint sleepers in to a closer spacing than the intermediate sleepers and in some cases their bearing area is also increased. It is possible by these means to arrange that the maximum joint deflection shall be equal to or less than the solid rail deflection at slow speeds, but local increase in supporting power cannot entirely compensate for lack of stiffness in the connexion and the deflection of the wheel when passing over the joint is not constant.

Calculation of Rail Joint Deflections and Fishplate Stresses.

Timoshenko has shown* that the deflexion curve for a long beam supported on a continuous elastic foundation and carrying a downward vertical load P′ combined with a sagging bending moment at one end is given by

$$y = \frac{e^{-\beta x}}{2\beta^3 EI}\left[P' \cos \beta x - \beta M_o (\cos \beta x - \sin \beta x)\right]$$

The deflection at the end where P′ and M_o are acting

$$= \delta = (y)_{x=0} = \frac{P' - \beta M_o}{2\beta^3 EI}$$

In the case of a rail joint, M_o is applied to the rail by the fishplate, and can be readily determined experimentally.

When the wheel load has reached the joint, P′ may be taken equal to W or half the wheel load minus the effect of the upward re-action due to any **additional** sleeper bearing area near the rail end in question.

If for example the moment of inertia of the fishplates is very small compared to that of the rail, M_o will approach zero and if there is no additional sleepering at or near the joint, then provided the fishplates can take the shearing forces involved, when an isolated load 2W is at or close to the joint, the maximum deflexion is $\frac{2W\beta}{\mu}$ which is exactly twice the maximum deflexion of the solid rail under 2W at points sufficiently far removed from the joint to be unaffected by the discontinuity.

The stiffness of an intermediate sleeper is

$$\rho = \mu S \text{ lb. per inch deflection}$$

where S is the intermediate sleeper spacing in inches.

In order to ensure that under an isolated wheel load 2W, the maximum deflexion δ at the joint shall be equal to the maximum solid rail deflection Δ_1, we assume that there is additional bearing area 2 ε at or near the joint expressed as a fraction of the effective area of one intermediate sleeper.

Let M_o = the bending moment in the fishplates

and $P' = W - \rho \Delta_1 \varepsilon = W - R$ say

$$\text{then } \delta = (y)_{x=o} = \frac{P' - \beta M_o}{2\beta^3 EI}$$

* " Applied Elasticity " by Timoshenko and Lessells, page 140, Constable London 1928.

* Calculation of M_o.

Assume R acts at a distance a from the rail end and that l is the effective length of the fish-plates. The strain energy in one pair of fish-plates, moment of inertia I_p per pair

$$= \frac{M_o^2 l}{2EI_p}$$

and in the rails

$$= 2\int_0^{\frac{2\pi}{\beta}} \frac{M^2\,dx}{2EI}$$

$$= \frac{1}{\beta^2 EI}\left[\frac{P'^2}{8\beta} - \frac{(M_o - Ra)P'}{2} + \tfrac{3}{4}\beta(M_o - Ra)^2\right]$$

and on the ballast and formation.

$$= \mu \int_0^{\frac{2\pi}{\beta}} y^2\,dx$$

$$= \frac{1}{\beta^2 EI}\left[\frac{3}{8}\frac{P'^2}{\beta} - \frac{(M_o - Ra)P'}{2} + \frac{\beta(M_o - Ra)^2}{4}\right]$$

The total strain energy

$$U = \frac{1}{\beta^2 EI}\left[\frac{P'^2}{2\beta} - M_o P' + Ra\,P' + \beta M_o^2 - 2\beta Ra\,M_o + \beta R^2 a^2\right] + \frac{M_o^2 l}{2EI_p}$$

$$\frac{dU}{dM_o} = \frac{1}{\beta^2 EI}\left[-P' + 2\beta M_o - 2\beta Ra\right] + \frac{M_o l}{EI_p} = 0$$

$$M_o = \frac{I_p}{2I_p + \beta l I}\left(\frac{P'}{\beta} + 2Ra\right)$$

Specimen joint deflexion and fish-plate bending stress calculations are given below:—

Method (a).

2W = 25200 lb. ($22\frac{1}{2}$ T axle)

Rail 90 R I = 38·45 ins.^{4}

Fish-plates 90 R I_p = 10·8 ins.^{4} per pair.
Zt = 5·97 ins.^{3} „ „
l = 10 ins.

μ = 1000 lb per in^2.

β = 0·0216.

a = 7·0 ins.

Intermediate sleeper spacing .. .. = $30\frac{1}{2}$ inches centres.

Distance, centre to centre between joint sleepers .. 14 inches.

Distance, centre to centre between shoulder and adjacent joint sleepers .. .. 26 inches.

Distance, centre to centre between shoulder sleepers 66 inches.

---

* An exact solution has not been developed here as it has been ascertained that the two approximate methods given are sufficiently accurate for all practical purposes.

The method of estimating 2 ε is conveniently shown graphically see Figure 24.

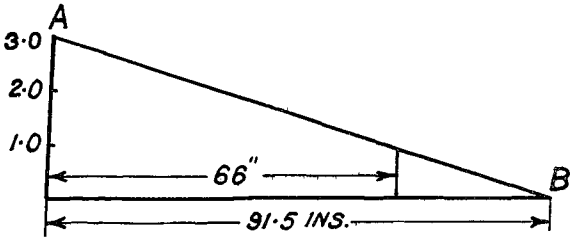

FIG. 24

If the distance, centre to centre of shoulder sleepers were 91·5 inches, then 2 ε would be zero; if this distance could be made zero, then 2 ε would be 3·0. Thus two points A and B when joined give 2 ε for various arrangements of joint sleepering.

In the example chosen,

$$2\ \varepsilon = \frac{91{\cdot}55 - 66}{91{\cdot}55} \times 3{\cdot}0 = 0{\cdot}835$$

$$\delta = \frac{W - \beta M_o - \rho\delta\ \varepsilon}{2\beta^3 EI}$$

$$= \frac{W - \beta M_o}{2\beta^3 EI + \rho\ \varepsilon}$$

First assume that $M_o = 12 \times 2240 \times Z_e$ inch lb

$$\text{then}\quad \delta = \frac{12600 - 3460}{(2\times 0{\cdot}0216^3 \times 30\times 10^6 \times 38{\cdot}45)+12720} = 0{\cdot}255 \text{ ins.}$$

$$\text{giving } P' = 12600 - 30500 \times 0{\cdot}255 \times \frac{0{\cdot}835}{2} = 9350 \text{ lbs.}$$

$$M_o = \frac{10{\cdot}8}{21{\cdot}6 + 0{\cdot}0216 \times 38{\cdot}45}\left(\frac{9350}{0{\cdot}0216} + 3250 \times 2 \times 7\right)$$

$$= 173000 \text{ inch lbs.}$$

$$\text{Fishplate Bending Stress} = \frac{173000}{5{\cdot}97 \times 2240} = 12{\cdot}9 \text{ tons per sq. in.}$$

The deflection is then re-calculated using a larger value of the fish-plate bending stress, say 12·5 tons per sq. inch and this deflection is used for final calculation of M_o.

Method (b).

Using again the above example, it can be shown that

$$M_o = \frac{I_p}{\beta^2 I l}\left\{ W - 2\beta M_o - \frac{(W - \beta M_o)\ \rho\ \alpha\ \varepsilon}{2\beta^3 EI + \rho\ \alpha\ \varepsilon}\right\}$$

where α is the influence factor determined from the master diagram (Technical Paper No. 245).

α for 7″ from load = 0·74

$$\therefore M_o = \frac{10{\cdot}8\times10^4}{4{\cdot}7\times10\times38{\cdot}45}$$

$$\left\{5{\cdot}625 - 0{\cdot}0432M_o - \frac{(5{\cdot}625 - 0{\cdot}0216M_o)\ 1000\times30{\cdot}5\times0{\cdot}74\times0{\cdot}417}{2\times13{\cdot}5\times30\times38{\cdot}45 + 30{\cdot}5\times1000\times0{\cdot}74\times0{\cdot}417}\right\}$$

= 164000 lb. ins.

$$\text{Fish-plate bending stress} = \frac{164000}{5{\cdot}97\times2240}$$

= 12·4 tons per sq. in.

Method (b) is preferable when an accurately drawn master bending moment influence line diagram is available.

Most of the experimentally determined fish-plate stresses at low speeds under the O. S. wagon and the H. G. engine have been analysed in accordance with the theory given above and the results are summarized in Table 7.

TABLE 7.

Tests Nos.	Rail	Jt. sleeper spacing	μ	Effective length of fish-plate ins.		Dead slow stress due to B. M. tons/sq. in.		Over all maximum recorded tons/sq. in.		Longitudinal direct stress as a % of B. M. stress (maximum of each series)		State of joint	Remarks
				O. S. Wagon	H. G. Engine	O. S. Wagon	H. G. Engine	O. S. Wagon	H. G. Engine	O. S. Wagon	H. G. Engine		
33-41	90 R ..	22″ crs.	2160	—	4·2	3·6	8·1	6·5	10·0	..	25%	..	
42-52	,, ..	22″ ,, ..	2160	..	..	21·1	13·0	28·5	15·1	17%	17%	$\frac{1}{16}$″ low.	
53-63	,, ..	14″ ,, ..	2160	16·2	—4·2	9·0	13·0	12·5	14·5	28%	8%	..	
64-75	,, ..	14″ ,, ..	2160	..	..	11·5	..	15·5	..	34%	..	$\frac{1}{32}$″ low.	
108-117	,, ..	14″ ,, ..	2730	19·2	38·5	6·7	2·5	9·2	4·7	19%	34%	$\frac{1}{16}$″ high.	
118-123	90 R *a* ..	14″ ,,	2730	6·8	6·3	9·6	5·9	14·5	9·0	21%	27%	..	
124-129	,, *a* ..	22″ ,, ..	2730	10·0	11·8	9·4	5·1	15·5	9·0	27%	10%	..	
134-141	90 R ..	22″ ,, ..	2730	..	..	20·9	17·5	27·0	19·6	19%	12%	$\frac{1}{16}$″ low.	
156-168	,, ..	14″ ,, ..	1810	9·0	..	10·7	..	12·5	..	17%	..	..	
174-180	,, ..	14″ ,, ..	1810	..	..	10·2	..	14·0	..	8%	..	..	
181-187	,, ..	22″ ,, ..	1810	17·6	..	8·6	..	13·5	..	8%	..	..	
188-193	,, ..	22″ ,, ..	1810	..	..	9·0	..	14·0	..	36%	..	$\frac{1}{32}$″ low.	
355-360	,, ..	Duplex	2545	16·9	11·7	8·2	..	5·5	..	5%	5%	..	
367-374	,, ..	,, ..	2545	..	..	18·9	9·1	26·5	10·0	22%	..	$\frac{3}{32}$″ low.	
383-388	,, ..	25″ crs.	2545	25·0	36·0	7·1	3·5	10·1	4·2	10%	10%	..	
389-394	,, ..	25″ ,, ..	2545	..	..	19·5	9·1	22·5	17·5	20%	41%	$\frac{3}{32}$″ low.	
528-535	,, ..	18″ ,, ..	..	..	..	6·2	4·5	9·0	6·5	20%	35%	..	
542-548	,, ..	18″ ,, ..	..	..	..	12·9	9·5	18·6	12·9	44%	36%	$\frac{3}{32}$″ low.	
597-604	100 lb. B. H.	20″ crs. *b*	1260 1056	22·6	19·5	8·6	5·1	13·2	10·1	40%	30%	..	
829-834	,,	20″ ,, *b*	1007	7·4	—3·0	12·8	9·8	18·0	11·7	19%	8%	..	
631-638	,, ..	20″ ,, ..	2225	25·2	18·7	6·8	4·5	9·0	6·4	32%	20%	..	
647-655	,, ..	20″ ,, ..	2225	..	..	13·2	10·0	16·3	13·4	19%	10%	$\frac{3}{32}$″ low.	
750-758	,, ..	20″ ,, ..	1316	8·4	—2·0	11·3	8·6	15·5	11·6	23%	25%	..	
772-786	,, ...		1316	..	..	23·5	13·0	30·4	23·5	16%	10%	$\frac{1}{16}$″ low.	
339-344	88½ lb. B. H.	25″ crs.	1630	6·5	8·5	13·5	7·1	17·6	9.6	23%	35%	..	
345-348	,, ..	25″ ,, ..	1690	..	..	28·5	..	31·4	..	10%	..	$\frac{1}{16}$″ low.	
316-320	,, ..	..	..	..	..	1·5	1·7	5·8	4·0	..	..	..	

Note.—(*a*) These joints are evenly packed and represent almost perfect conditions.
(*b*) These joints are low in service. The remaining low joints were artificially lowered.

TABLE 7.

Tests Nos.	Rail	Jt. sleeper spacing	μ	Effective length of fish-plate ins. O. S. Wagon	Effective length of fish-plate ins. H. G. Engine	Dead slow stress due to B. M. tons/sq. in. O. S. Wagon	Dead slow stress due to B. M. tons/sq. in. H. G. Engine	Over all maximum recorded tons/sq. ip. O. S. Wagon	Over all maximum recorded tons/sq. ip. H. G. Engine	Longitudinal direct stress as a % of B. M. stress (maximum of each series) O. S. Wagon	Longitudinal direct stress as a % of B. M. stress (maximum of each series) H. G. Engine	State of joint	Remarks.
322-330	82½ lb. B. H.	..	..	..	..	6·3	1·2	10·5	1·4	67%	..	..	
395-401	85 lb. ..	30" crs.	..	..	..	10·8	9·1	14·4	10·2	10%	10%	..	
403-408	„ ..	30" „ ..	..	..	..	14·6	9·6	25·0	10·2	5%	5%	$\frac{3}{16}$" low.	
561-569	82 lb. B. H.	20" crs.	..	..	..	5·5	7·1	8·6	9·6	13%	12%	..	
570-576	„ ..	20" „ ..	..	..	..	9·9	7·4	11·8	9·6	20%	20%	$\frac{1}{8}$" low.	
425-431	75 lb. F. F. 1904.	24" crs.	869	13·6	12·3	17·9	9·8	19·5	11·6	15%	22%	..	
433-438	„ ..	..	869	..	..	29·0	18·4	31·0	21·5	7%	17%	$\frac{3}{16}$" low.	
459-464	75 lb. D. H.	28" crs.	..	..	..	5·0	5·0	12·5	7·2	31%	25%	..	
472-476	„ ..	28" „	..	..	..	16·0	12·0	21·4	14·2	..	..	..	
700-707	50 lb. F. F.	26" crs.	865	3.3	..	10·7	..	14·4	..	15%	..	..	M. G. 10 ton axles 12 ft. crs.
723-728	„ ..	26" „ ..	865	..	..	23·0	..	31·0	..	26%	..	¼" low.	Ditto.

Wide variations appear in the recorded stresses due largely to differences in the joint sleeper packing and to the presence or otherwise of wear at the fishing faces. It is doubtful whether the low joints which were obtained artificially represent conditions of sufficiently frequent occurrence to justify special notice being taken of the severe stresses set up. In almost every case of the older and lighter rails below 90 lb. (26·5 ton fish-plates) and with joints which nominally were packed, fish-plate stresses were above the limit at which noticeable permanent deformation is to be expected after a number of 22½ ton axle loads have passed over. Failure of the fish-plates to act in bending has led to the joint supports being packed much harder than the others.

Usually in measuring fish-plate stresses, one telemeter was located near the top of the plate at the centre, the second near the neutral axis at the centre and the third at or near to the bottom immediately below the other two, all telemeters being on the outer fish-plate. In a few tests, however, simultaneous records were taken on the tension flanges of a pair of fish-plates and it was found that the maximum stresses differed sometimes by as much as 33 per cent showing that in compiling Table 7, the resisting moment of the fish-plates may in some cases have been underestimated. In any future rail joint investigation, a larger number of telemeters (at least five) should be used.

Duplex Joint Sleepers.

Calculations, confirmed by static stress measurements by means of Huggenberger Strain Gauges, show that a reduction in fish-plate bending stress of 10 per cent may be effected by changing from the sleepering arrangement given in the example of fish-plate stress, page 44 to the Duplex type of joint at the foot of sleepers. In critical cases, this reduction is most beneficial.

Conditions of Support at Rail Joints.

Graphs Figure 25 show the theoretical paths of a 20000 lb. wheel load passing over a joint in 90 R track at dead slow speed for the following conditions.

TABLE 8.

Curve No.	Elastic Constant	Solid Rail Depression	Depression at Joint
1	1300	·1775"	·1775"
2	1300	·1775"	·1598"
3	1820	·1385"	·1385"
4	1820	·1385"	·1246"
5	2300	·1160"	·1160"
6	2300	·1160"	·1043"

The sudden change in stiffness of the rail due to the fish-plates results in a departure from the ideal condition of constant deflection. These graphs have been prepared to demonstrate that any extra support which may be provided at the joint cannot entirely compensate for the rail discontinuity.

7. Dynamic Stresses and Deflections in Fish-plates for Well Packed Joints.

Curves giving maximum longitudinal fish-plate stress to a speed base for all tests with packed joints are given in the first part of Appendix II-S, Volume 2, and corresponding curves for maximum recorded deflexion at and near the joint for packed joints are given in the first part of Appendix II-D, Volume 2.

In the case of fish-plate stresses, for the O.S. wagon, the dead H.G. engine and the 10 T axle meter gauge wagon, the speed increments have been deduced from curves in the first part of Appendix II-S and plotted in Figures 26 to 37 as a percentage of the bending moment stress at slow speed with joints packed. It is assumed that the longitudinal direct stresses which are included in Table 7 are not likely to increase with speed.

It is considered that an allowance of fifty per cent added to the bending moment stress at all service speeds would cover satisfactorily dynamic effects in the fish-plates for the packed joint condition.

8. Dynamic Deflections and Stresses in Fish-plates for Low Joints.

Curves giving maximum joint deflexions and longitudinal bending stress in the fish-plates to a speed base for low joints are given in the second parts of Appendix II-D and II-S respectively of Volume II.

The speed increments for fish-plate bending moment stress as a percentage of the corresponding stress with packed joint at slow speed are given for most of the tests in Figures 26 to 37. It will be noticed that the tendency for this increment to increase with speed is very small. The critical speeds at which appreciable dynamic augments are to be expected for such low joints as have been examined are usually in the range 0-20 miles per hour.

In making an impact allowance for fish-plate design some allowance should be made for lowness at the joint and it is considered that the fish-plates should be capable of withstanding twice the static load calculated for the packed joint condition without permanent deformation.

The position of the sleepers at the joint for I. R. S. tracks for various numbers of sleepers per rail are given in the tables below. This information has been derived by calculation using the methods given on pages 44 to 46.

TABLE 8A.

FOR H TYPE DUPLEX JOINT SLEEPERS

Rail	Elastic constant μ	Sleepers	Distance from centre line of shoulder sleeper to centre line of joint (Dimension A)
90R ..	900 to 2,700	N+4+D	30 Inches.
		N+3+D	31½ ,,
		N+2+D	33 ,,
		N+1+D	35 ,,
75R ..	600 to 1,400	N+4+D	30 ,,
		N+3+D	30½ ,,
		N+2+D	33 ,,
		N+1+D	35½ ,,
60R ..	500 to 1,000	N+4+D	28 ,,
		N+3+D	29 ,,
		N+2+D	31½ ,,
		N+1+D	33½ ,,
50R ..	400 to 900	N+4+D	27½ ,,
		N+3+D	29 ,,
		N+2+D	32 ,,
		N+1+D	34 ,,

TABLE 8B.

FOR STEEL, CST 9 AND TIMBER SLEEPERS THROUGHOUT

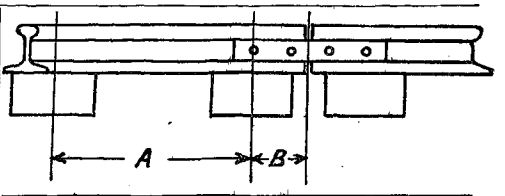

Rail	Elastic constant μ	Sleepers	Dimension A	Dimension B
90R ..	900 to 2,700	N+4	27½ Inches.	7 Inches.
		N+3	29½ ,,	7 ,,
		N+2	32 ,,	7 ,,
		N+1	36 ,,	7 ,,
75R ..	600 to 1,400	N+4	27½ ,,	7 ,,
		N+3	29½ ,,	7 ,,
		N+2	32 ,,	7 ,,
		N+1	36 ,,	7 ,,
60R ..	500 to 1,000	N+4	26 ,,	6½ ,,
		N+3	28½ ,,	6½ ,,
		N+2	31½ ,,	6½ ,,
		N+1	34½ ,,	6½ ,,
50R ..	400 to 900	N+4	27 ,,	6½ ,,
		N+3	29 ,,	6½ ,,
		N+2	31½ ,,	6½ ,,
		N+1	34½ ,,	6½ ,,

Provision has been made for sleeper bearing area at the joint to produce a maximum deflection there equal to the maximum solid rail deflection under a given wheel load for static conditions. It has been found that large variations in the elastic constant of the track have little effect on the value for the required bearing area of sleepers at the joint. It is pointed out that the above spacings apply only to track material conforming to current standard designs throughout and they might not be suitable in cases where non-standard short or poorly fitting fish-plates were installed.

9. Stability of Sleepers in Ballast under Vertical and Lateral Loads.

Nine experiments have been made to record the "rock" of the rail and that of the sleeper under it due to the passage of a wagon loaded to 22½ tons per axle. Optical deflectometers as shown on Drawing Figure 38, page 64 were used for the work which was carried out on three types of 90 R track, one 88½ B.H., one 85 F.F., and one 75 F.F. The results of these tests are given in Table 9 and it will be seen that the worst result was obtained from the 85 lb. F.F. rails on Murray cast iron pot sleepers. This is not surprising in view of the long rail seat provided which is considered to be an objectionable feature of this design of pot sleeper.

TABLE 9.

Track	Site	Railway	Rock of rail in minutes	Sleeper Rock ×100÷ rail rock	Bed	Ballast	Remarks
90 R ..	Phillaur ..	N.W. R.	9·0	50%	Sandy clay	1" new stone	Trailing side joint sleeper.
CST/9 ..	Do. ..	Do. ..	7·5	60%	Do. ..	6" deep unsettled new stone.	Landing side joint sleeper.
90 R steel loose jaws.	Jullundur Cant.	Do. ..	11·0	43%	Do. ..	Do. ..	Do.
75 F. F. Deodar.	Macleod Ganj Road.	Do. ..	18·0	50%	Do. ..	2" stone and brick mixed 2" deep.	Solid Rail.
85 F. F. Murray 1896 C. I. pots.	Khargpur	B. N. R.	9·0	85%	Alluvial clay.	Rounded, a mixture of hard and soft stone.	Do.
88½ B. H. D. & O.	Pradhan-khanta.	E. I. R.	Total rock of Duplex sleepers. Left rail .. 3' Right rail 6'		Sandy clay	1½" stone, 8" deep.	Instrument attached at the centre of Duplex sleeper. Rail:—Landing side of joint.
90 R G type	Gomoh ..	Do. ..	Total rock of Duplex sleepers. Left rail .. 7·6 Right rail 3·0	..	Soft clay	1½" stone 5" deep on 12" of consolidated mud, mixed with ballast.	Do.

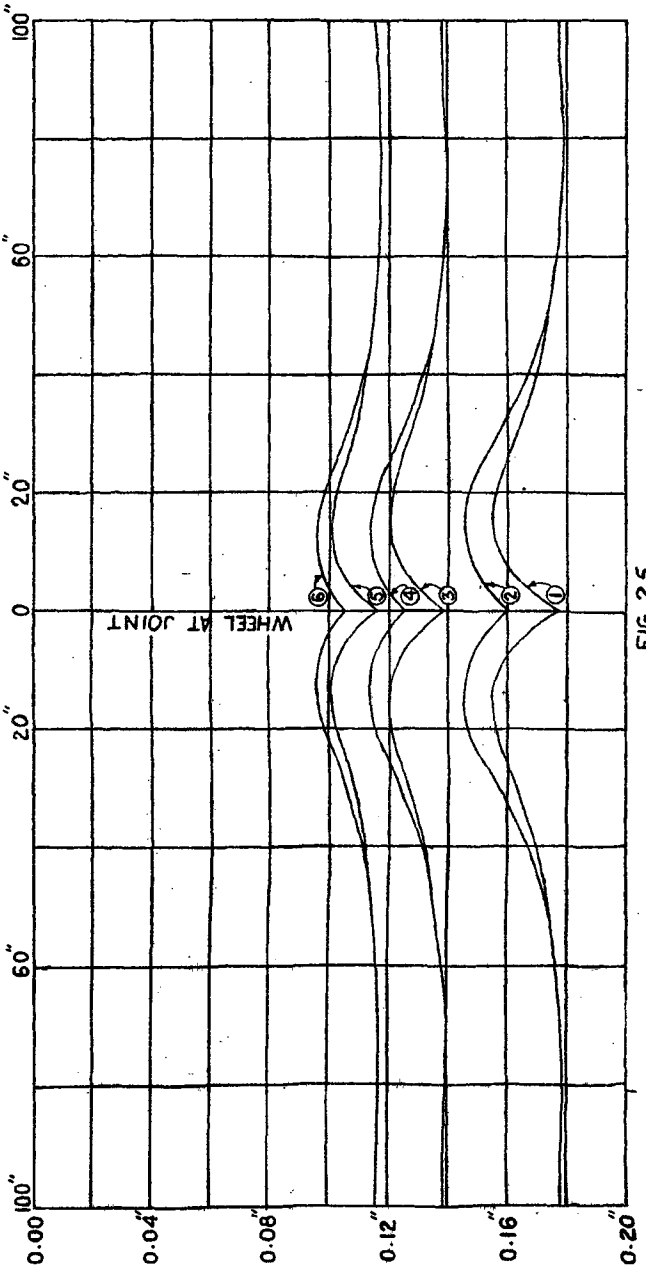
WHEEL AT JOINT
100"
60"
20"
0
20"
60"
100"
0.00"
0.04"
0.08"
0.12"
0.16"
0.20"
1
2
3
4
5
6

FIG. 25.

100 LB. B.H.
PACKED JOINT
FISHPLATE BENDING MOMENT STRESS

SPEED INCREMENT AS PERCENTAGE OF BENDING MOMENT STRESS AT SLOW SPEED WITH JOINT PACKED.

Curve A for series 631-638 (23") crs. jnt. slprs.
-do- B -do- 750-758 (26") -do-

O.S. WAGON.

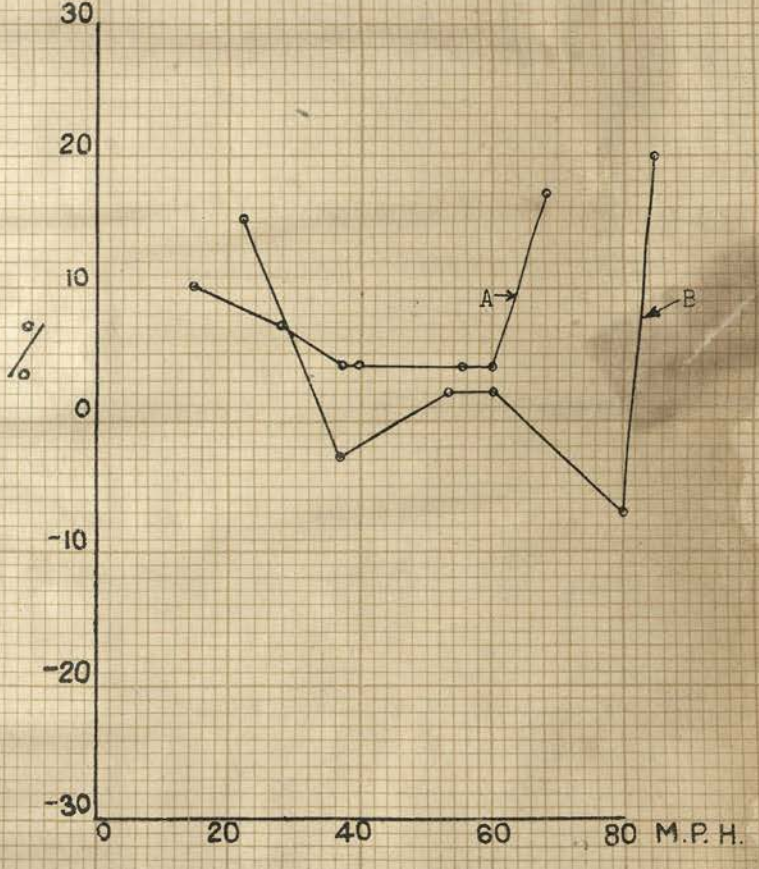

FIG.26

100 LB.B.H.

PACKED JOINT

FISHPLATE BENDING MOMENT STRESS

SPEED INCREMENT AS PERCENTAGE OF BENDING MOMENT STRESS AT SLOW SPEED WITH JOINT PACKED

Curve A for series 631-638 (22") crs. jnt. slprs.
-do- B -do- 750-758 (26") -do-

DEAD H.G. ENGINE

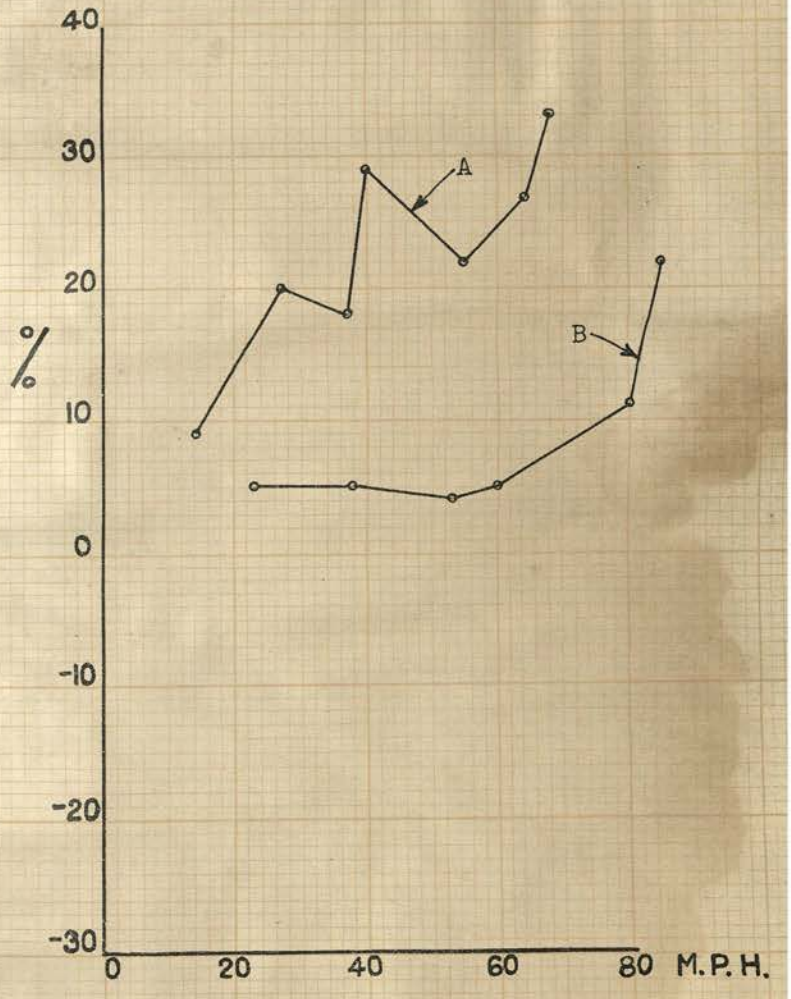

FIG. 27

90 R

PACKED JOINT

FISHPLATE BENDING MOMENT STRESS

SPEED INCREMENT AS PERCENTAGE OF BENDING MOMENT STRESS AT SLOW SPEED WITH JOINT PACKED.

Curve A for series 528-535 (18") crs. jnt. slprs.

-do- B	-do-	124-129 (22")	-do-
-do- C	-do-	181-187 (22")	-do-
-do- D	-do-	108-117 (14")	-do-
-do- E	-do-	33 - 41 (23")	-do-
-do- F	-do-	53 - 63 (14")	-do-
-do- G	-do-	156-168 (14")	-do-

O.S. WAGON.

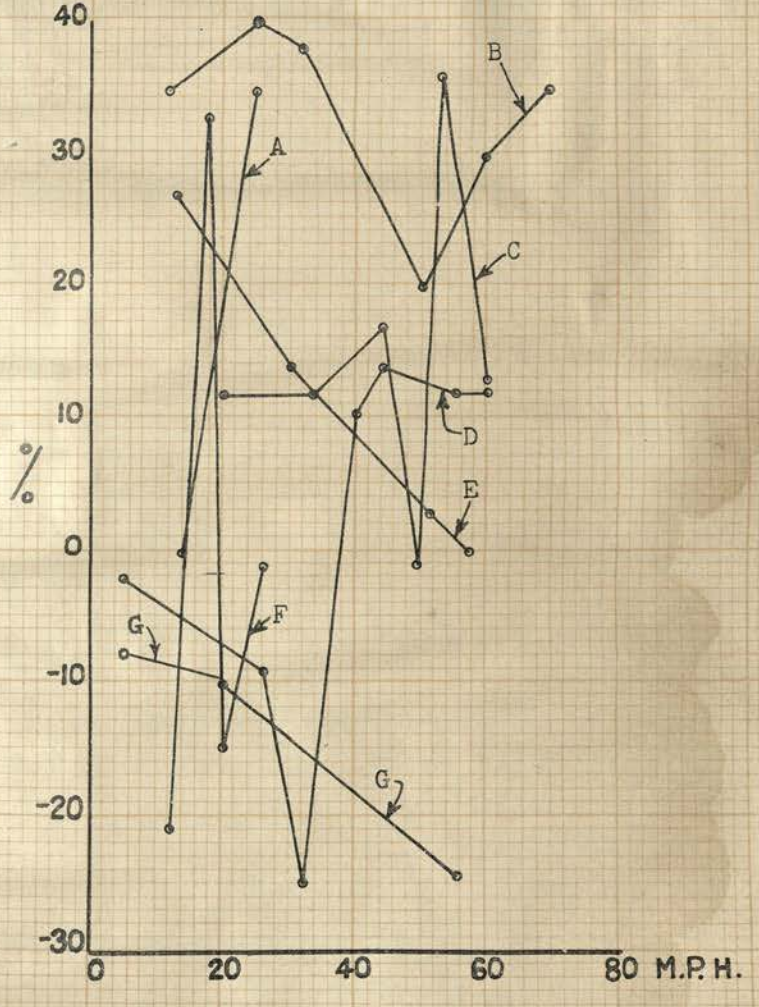

FIG.28

90 R.

PACKED JOINT

FISHPLATE BENDING MOMENT STRESS

SPEED INCREMENT AS PERCENTAGE OF BENDING MOMENT STRESS AT SLOW SPEED WITH JOINT PACKED.

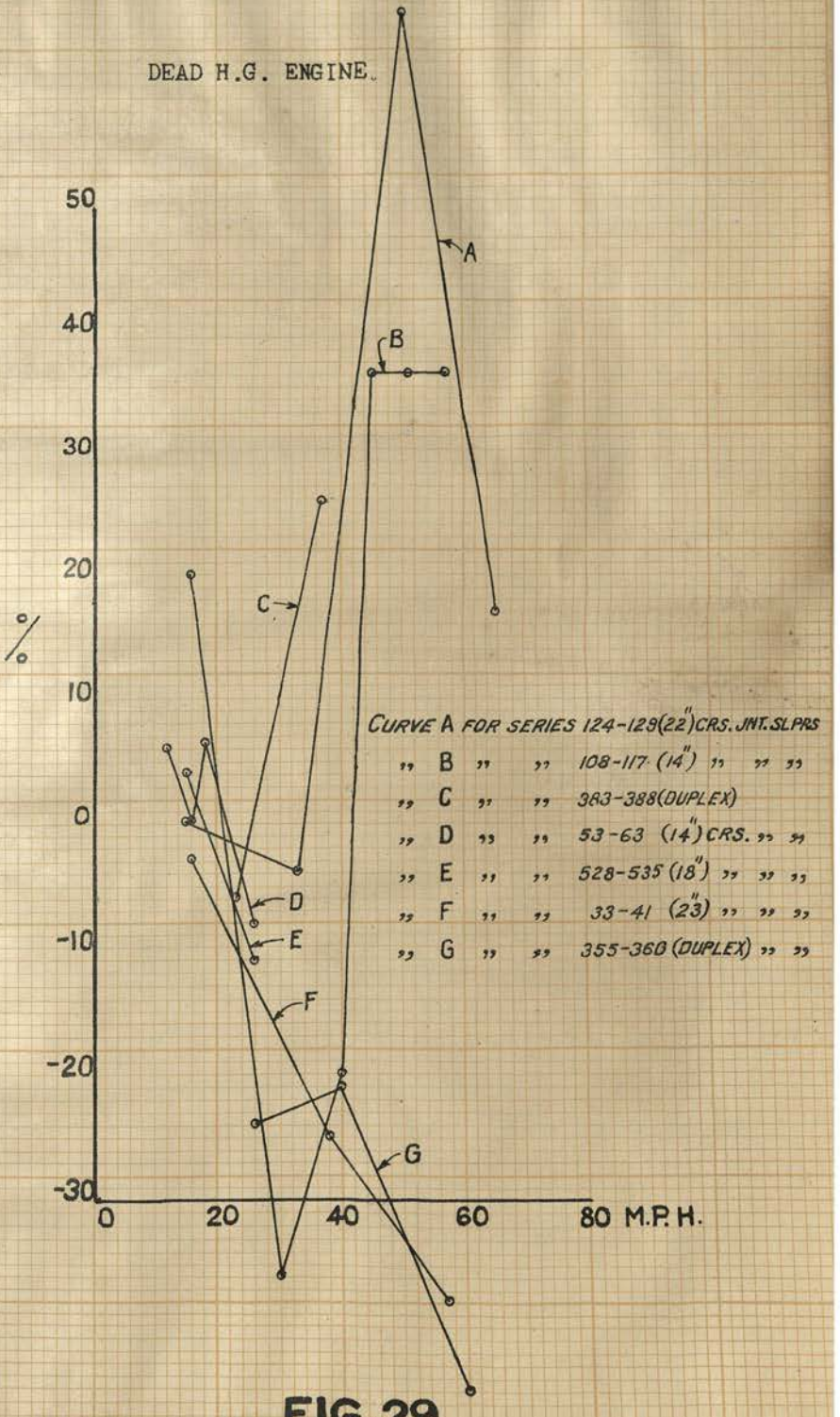

FIG. 29

88½ LB.B.H.,85 LB.F.F.,82 LB.B.H.,75 LB.F.F.,75 LB.D.H.,
73 LB.B.H.,58½ LB.F.F. & 50 LB.F.F.

PACKED JOINTS

FISHPLATE BENDING MOMENT STRESS

SPEED INCREMENT AS PERCENTAGE OF BENDING MOMENT STRESS AT SLOW SPEED WITH JOINTS PACKED.

Curve A for series	459-464	Rail 75 D.H.	(28")	crs.	Jnt.slprs.
-do- B -do-	700-707	-do- 50*F.F.	(25")		-do-
-do- C -do-	279-283	-do- 58½*F.F.			
-do- D -do-	561-569	-do- 82 B.H.	(20")		-do-
-do- E -do-	339-344	-do- 88½*F.F.	(21½")		-do-
-do- F -do-	425-431	-do- 75 F.F.	(24")		-do-
-do- G -do-	395-601	-do- 85 F.F.	(30")		-do-
-do- H -do-	242-247	-do- 73 B.H.	(28")		-do-
-do- J -do-	213-220	-do- 75 F.F.	(13")		-do-

O.S.WAGON.

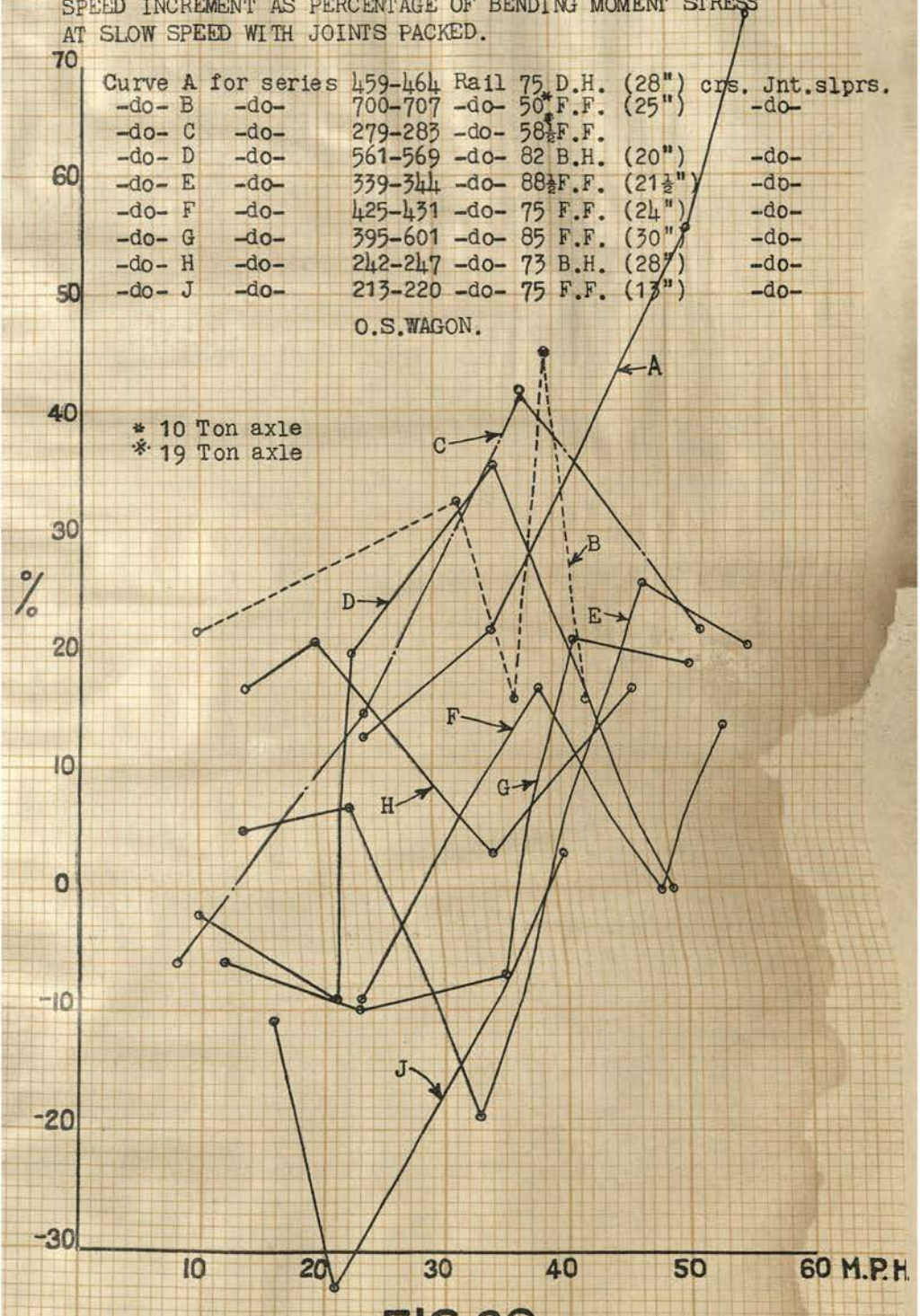

FIG.30

88½LB.B.H., 88½LB.F.F., 82LB.B.H., 75LB.F.F., 75LB.D.H., 73LB.B.H & 50 LB.F.F

PACKED JOINTS

FISHPLATE BENDING MOMENT STRESS

SPEED INCREMENT AS PERCENTAGE OF BENDING MOMENT STRESS AT SLOW SPEED WITH JOINTS PACKED.

CURVE A FOR SERIES 700-707 ※50LB.F.F. (25")CRS. JNT. SLPRS
" B " " 242-247 73LB.B.H.(28") " " "
" C " " 459-464 75LB.D.H.(28") " " "

DEAD H.G. ENGINE.

※YB CLASS METRE GAUGE ENGINE.

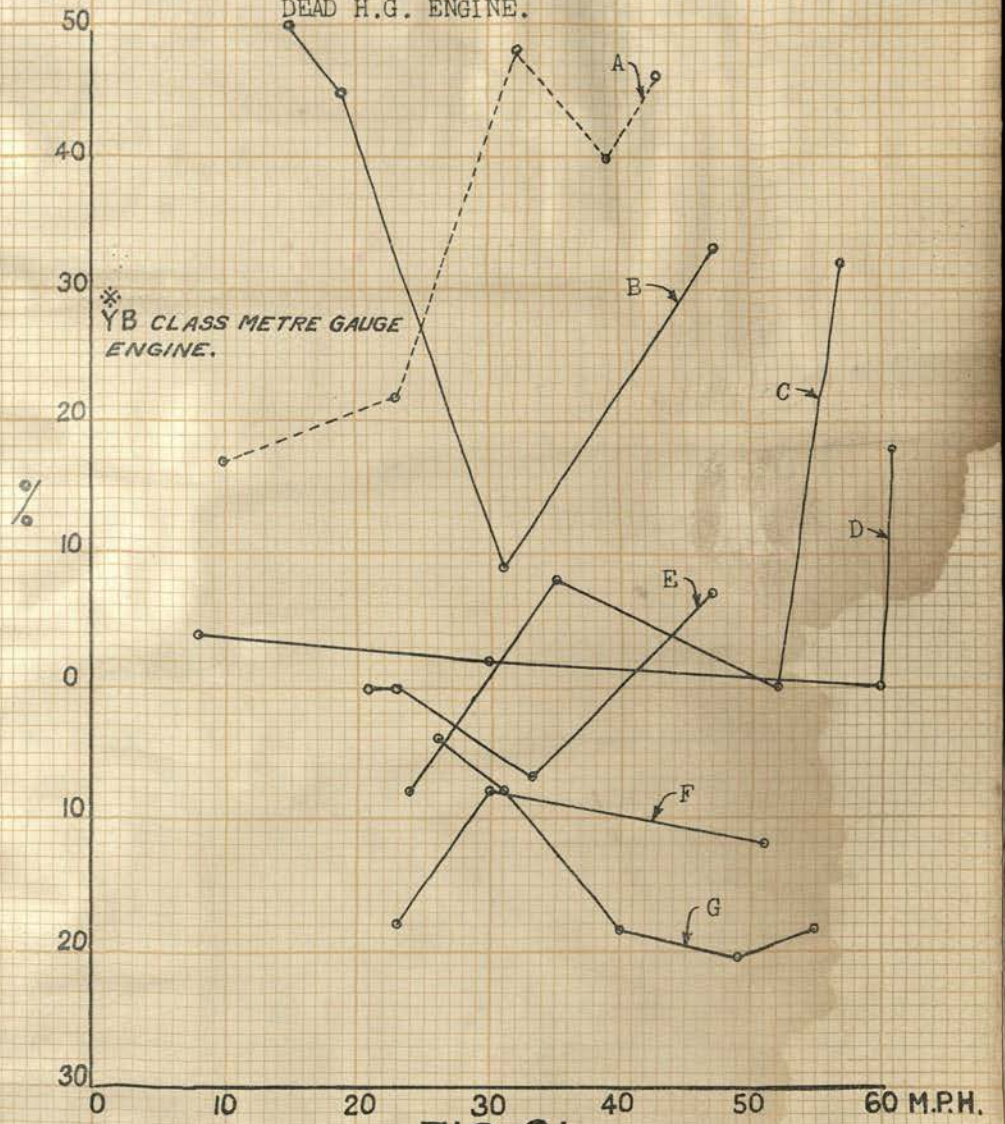

FIG. 31

CURVE D FOR SERIES 441-446 75LB.F.F. SUPPORTED
" E " " 339-344 88½LB.B.H.(25")CRS. JNT. SLPRS
" F " " 395-401 85LB F.F (23") " " "
" G " " 425-431 75LB F.F.(24") " " "

100 LB. B.H. LOW JOINT

FISHPLATE BENDING MOMENT STRESS

SPEED INCREMENT AS PERCENTAGE OF BENDING MOMENT STRESS AT SLOW SPEED WITH JOINT PACKED.

Curve A for Series 647-655 (23") crs. jnt. slprs.
-do- B -do- 772-786 (26") -do-

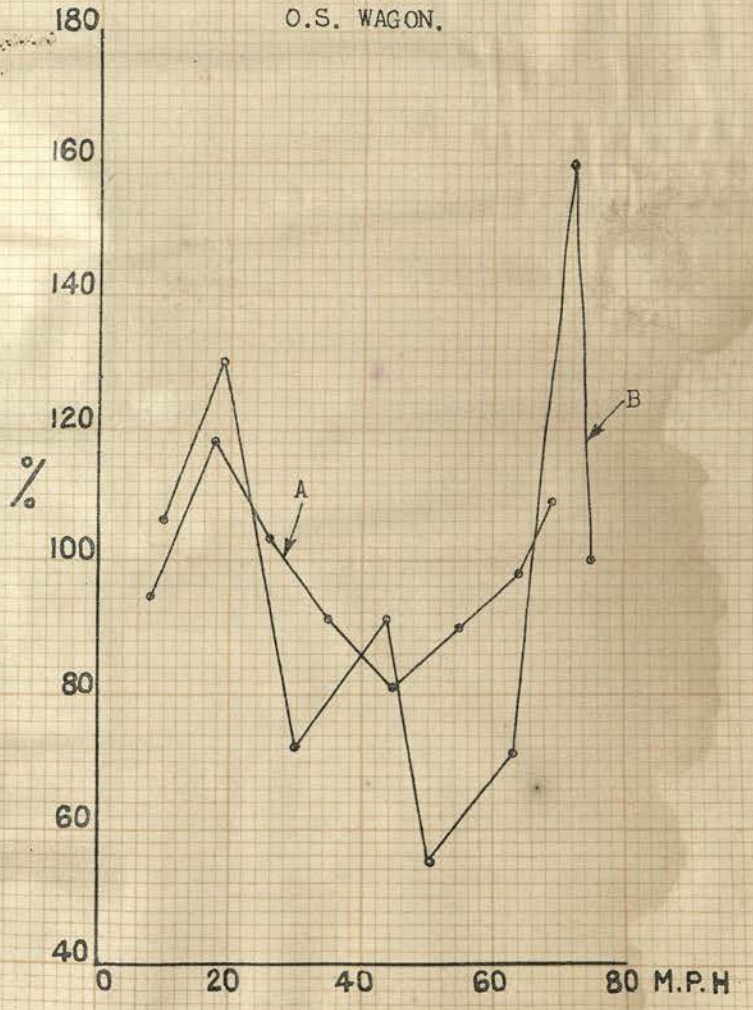

FIG.32

100 LB.B.H. LOW JOINT

FISHPLATE BENDING MOMENT STRESS

SPEED INCREMENT AS PERCENTAGE OF BENDING MOMENT STRESS AT SLOW SPEED WITH JOINT PACKED.

curve A for series 647-655 (24") crs. jnt. slprs.
-do- B -do- 772-786 (26") -do-

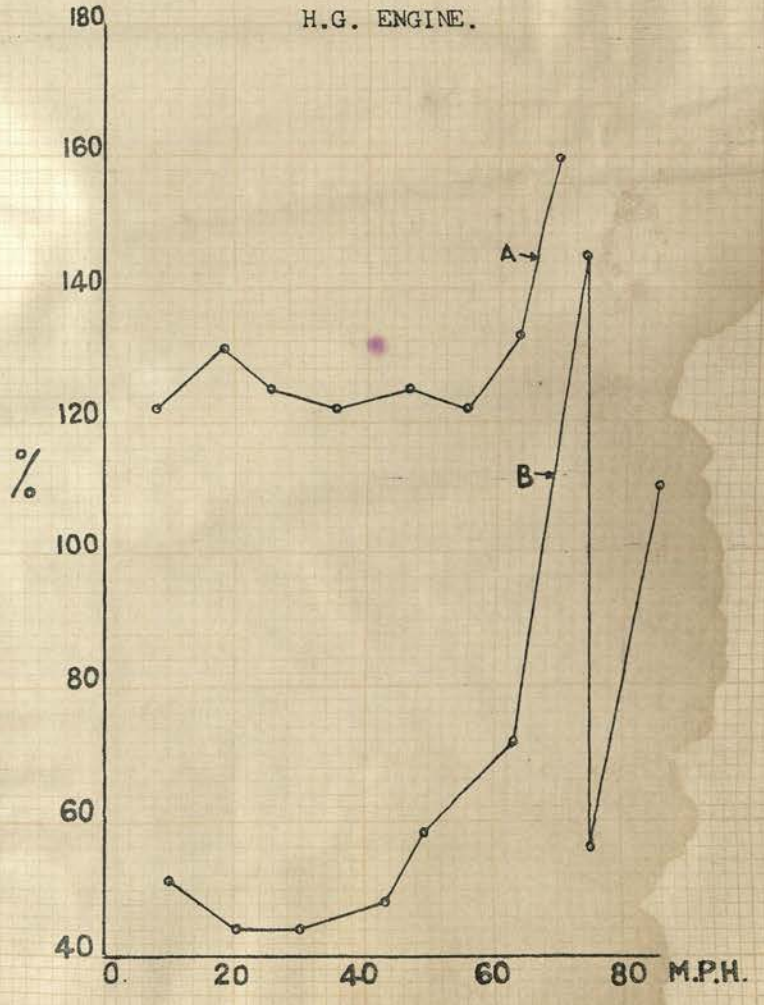

FIG. 33

90 R LOW JOINT

FISHPLATE BENDING MOMENT STRESS

SPEED INCREMENT AS PERCENTAGE OF BENDING MOMENT STRESS AT SLOW SPEED WITH JOINT PACKED.

Curve A	for series	134-141 (22")	crs. jnt. slprs.
-do- B	-do-	542-548 (18")	-do-
-do- C	-do-	118-123 (14")	-do-
-do- D	-do-	64 - 74 (14")	-do-
-do- E	-do-	174-180 (14")	-do-

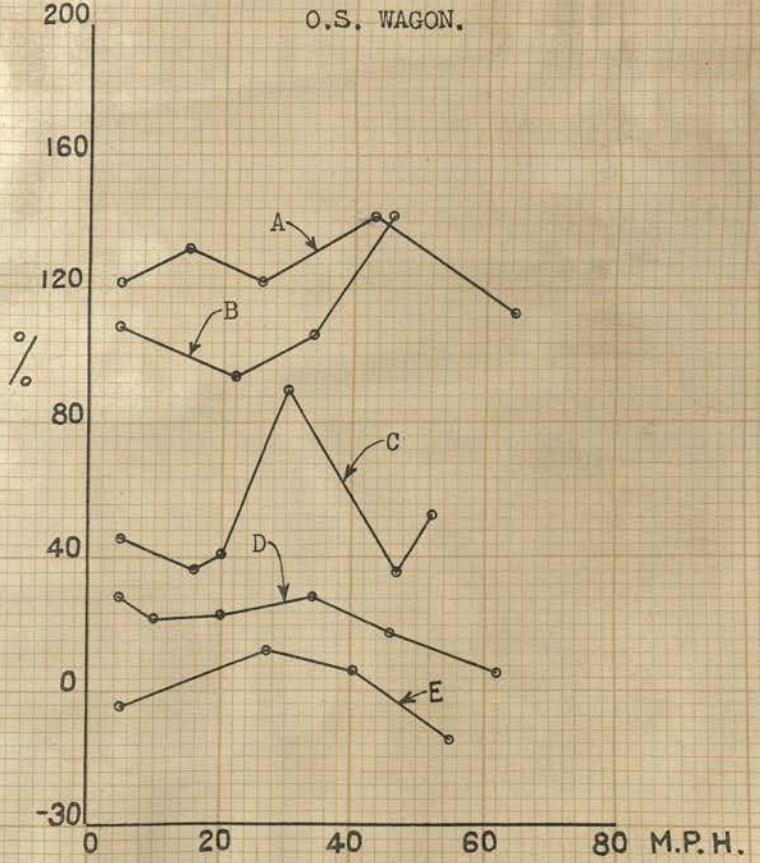

FIG. 34

90 R LOW JOINT
FISHPLATE BENDING MOMENT STRESS

SPEED INCREMENT AS PERCENTAGE OF BENDING MOMENT STRESS AT SLOW SPEED WITH JOINT PACKED.

Curve A for Series		389-394	
-do- B	-do-	134-141 (22")	crs. jnt. slprs.
-do- C	-do-	118-123 (14")	-do-
-do- D	-do-	367-374	
-do- E	-do-	542-548 (18")	-do-
-do- F	-do-	42 - 52 (14")	-do-

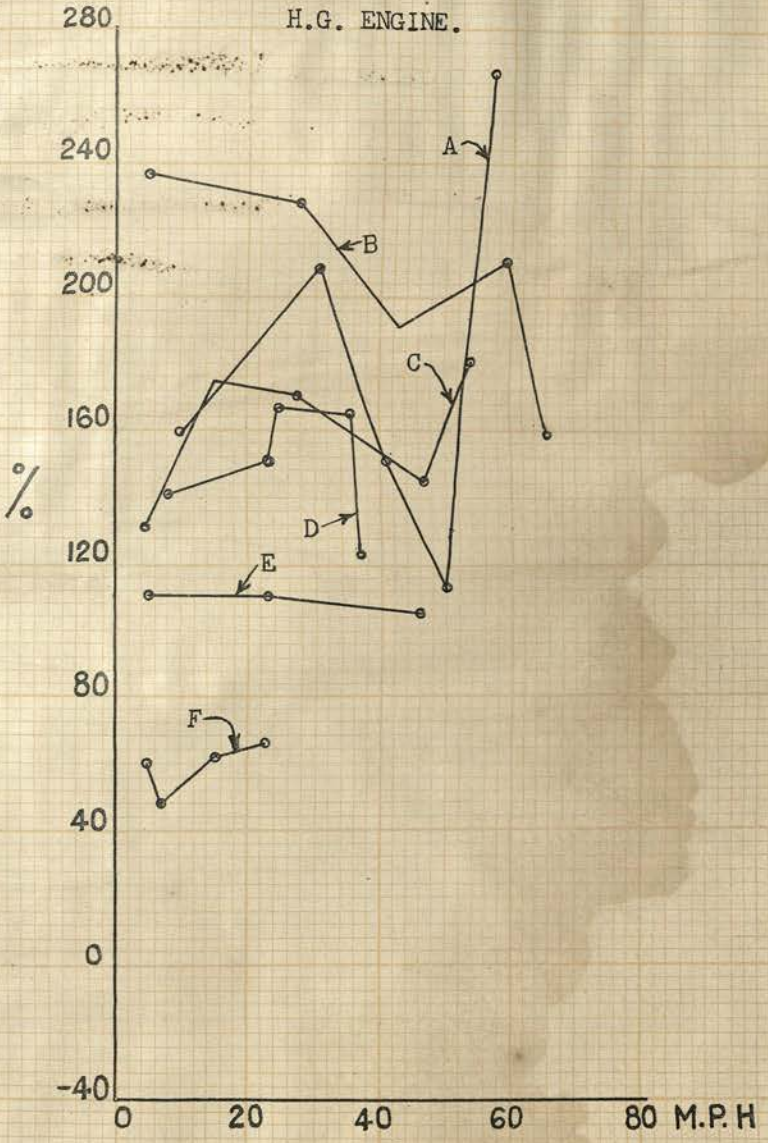

FIG. 35

85 LB.F.F., 82 LB.B.H.,75 LB.F.F.,75 LB D.H.,73LB.B.H.&50 LB.F.F.

LOW JOINTS

FISHPLATE BENDING MOMENT STRESS

SPEED INCREMENT AS PERCENTAGE OF BENDING MOMENT STRESS AT SLOW SPEED WITH JOINT PACKED.

Curve A	for Series	433-438	Rail	75 F.F.	(24") crs.	jnt. slprs.
-do- B	-do-	472-476	-do-	75 D.H.	(28")	-do-
-do- C	-do-	403-408	-do-	85 F.F.	(30")	-do-
-do- D	-do-	415-418	-do-	85 F.F.	(30")	-do-
-do- E	-do-	265-271	-do-	73 B.H.	(28")	-do-
-do- F	-do-	454-458	-do-	75 F.F.	Supported Joint	
-do- G	-do-	411-414	-do-	85 F.F.	(30") crs.	jnt. slprs.
-do- H	-do-	723-738	-do-	50 F.F.		
-do- J	-do-	284-291	-do-	58½F.F.	(14")	-do-
-do- K	-do-	570-576	-do-	82 B.H.	(20")	-do-

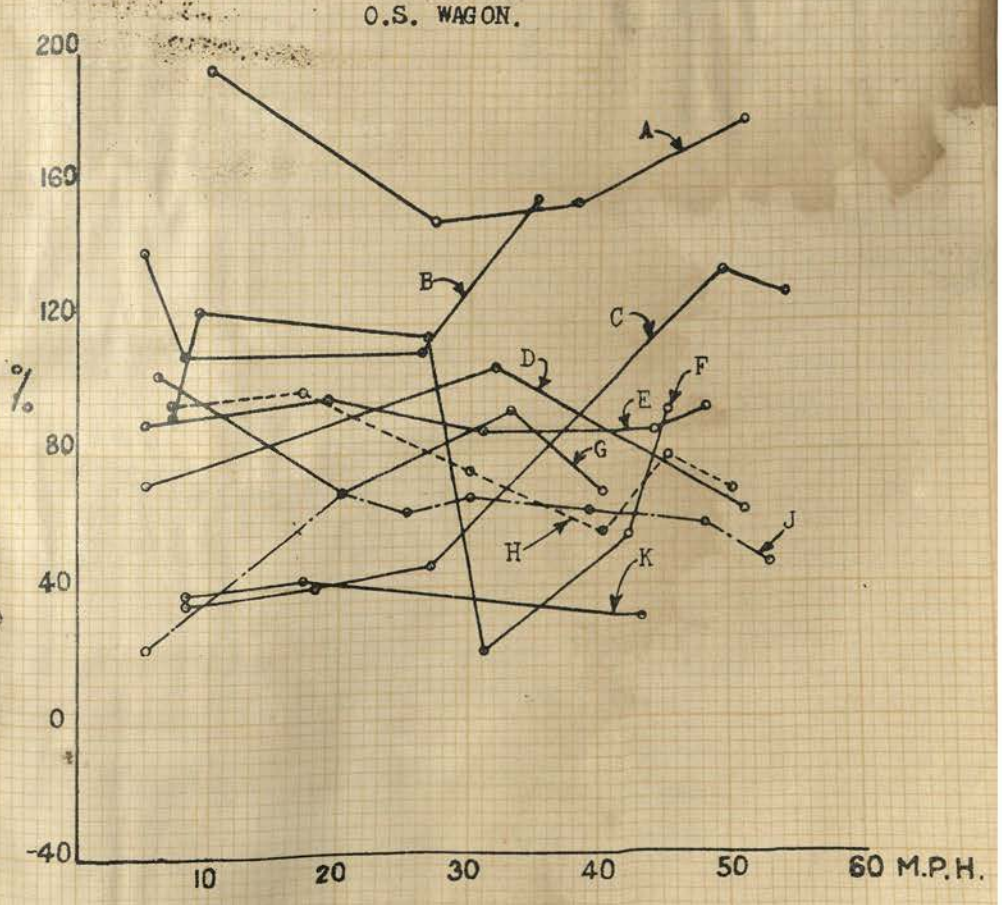

FIG. 36

85 LB.F.F.,82 LB.B.H.,75 LB.F.F.,75 LB.D.H.,73 LB.B.H.&50 LB.F.F.
LOW JOINTS

FISHPLATE BENDING MOMENT STRESS

SPEED INCREMENT AS PERCENTAGE OF BENDING MOMENT STRESS
AT SLOW SPEED WITH JOINT PACKED.

Curve A	for series	265-271	Rail	73 B.H.	(28")	crs. jnt. slprs.
-do- B	-do-	433-438	-do-	75 F.F.	(24")	-do-
-do- C	-do-	723-728	-do-	50 F.F.	(26")	-do-
-do- D	-do-	472-476	-do-	75 D.H.	(28")	-do-
-do- E	-do-	454-458	-do-	75 F.F.		
-do- F	-do-	415-418	-do-	85 F.F.		
-do- G	-do-	411-414	-do-	85 F.F.	(30")	crs. jnt. slprs.
-do- H	-do-	570-576	-do-	82 B.H.	(20")	-do-
-do- J	-do-	403-408	-do-	85 F.F.	(30")	-do-

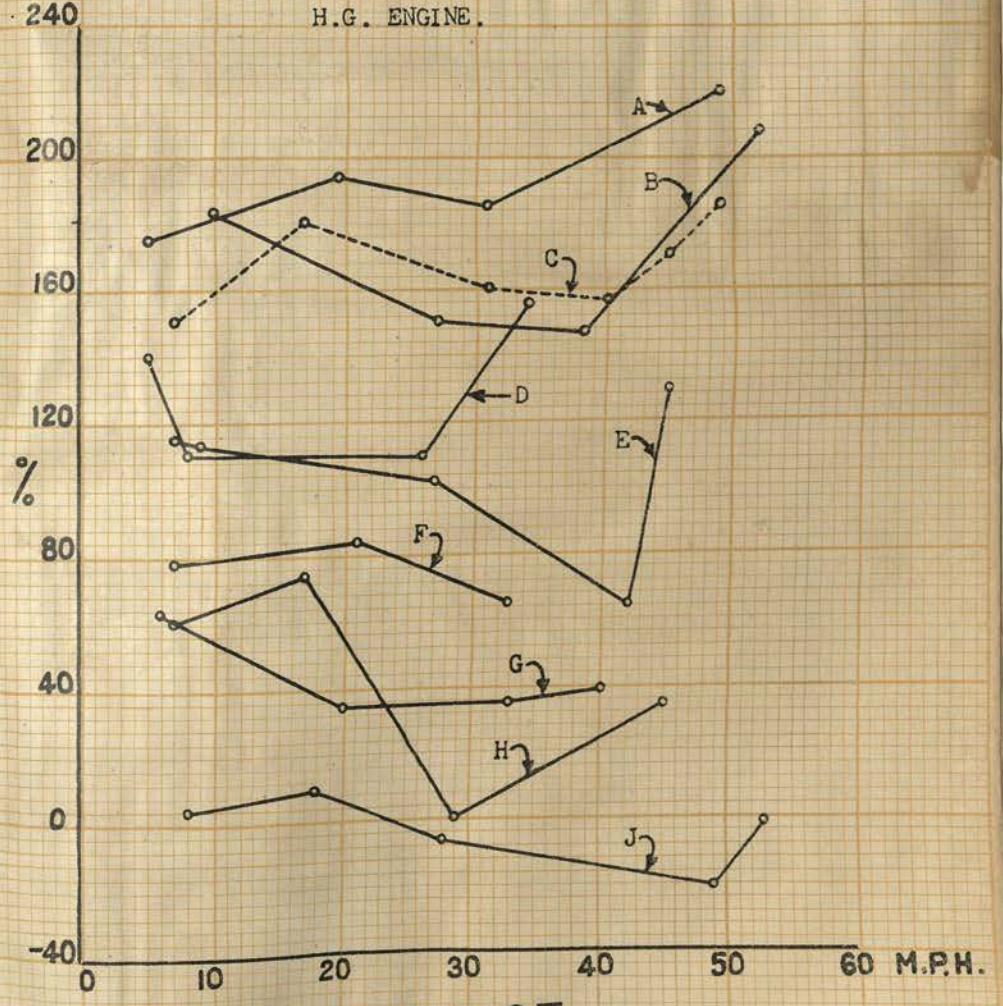

FIG. 37

Effect of Shape of Sleeper on Load Bearing Capacity.

Experiments were made in this connexion with two types of suitably stiffened steel plates having flat rectangular bases of equal bearing area. In one type the dimensions of the base were 7″×16″ and in the other 10″×11¼″. Both types were placed in turn under a rail in 2′—6″ gauge track (after the ordinary sleeper had been removed) and the deflexion under a slowly moving load was carefully measured in each case.

There was on the average no noticeable difference in the deflection for the two types of plate which proves that the vertical stiffness of a sleeper with a flat base is directly proportional to the area of its base irrespective of the shape of the base. These experiments did not include tests up to the point of failure.

The question of lateral stability of sleepers is considered under Item 11 (or 5 of the terms of reference), but it may be mentioned here that the lateral strength of the track at a joint laid with the earliest type of Duplex joint sleeper showed a slight falling off in the neighbourhood of the joint. In the current designs of Duplex sleepers, the lateral stability has been considerably augmented.

Pressure distribution in the ballast under the various types of sleepers has not yet been investigated on account of the lack of suitable experimental apparatus and the limited time available.

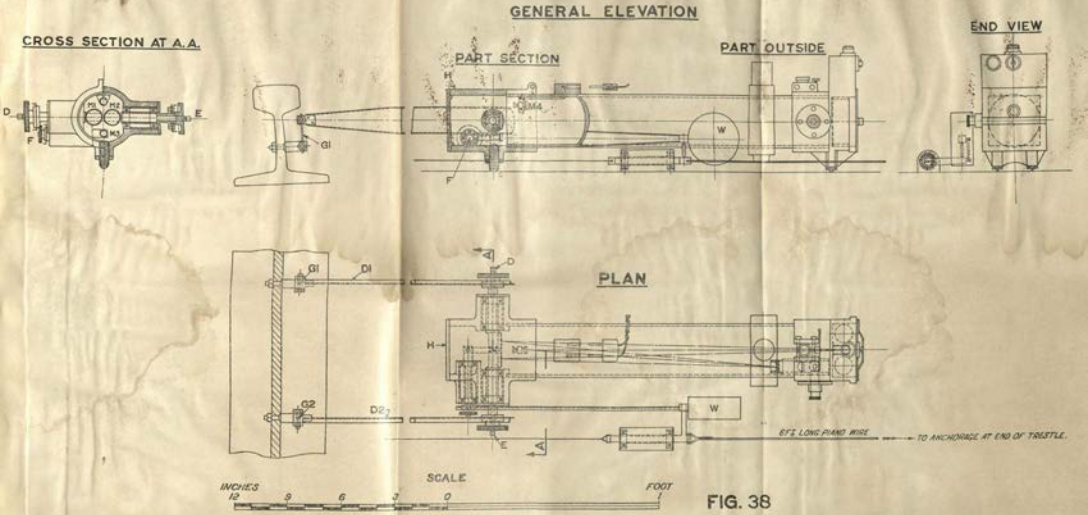
GENERAL ELEVATION
CROSS SECTION AT A.A.
PART SECTION
PART OUTSIDE
END VIEW
PLAN
SCALE
INCHES
FOOT
TO ANCHORAGE AT END OF TRESTLE.

FIG. 38

PLATFORM SUPPORTS FOR DEFLECTOMETERS

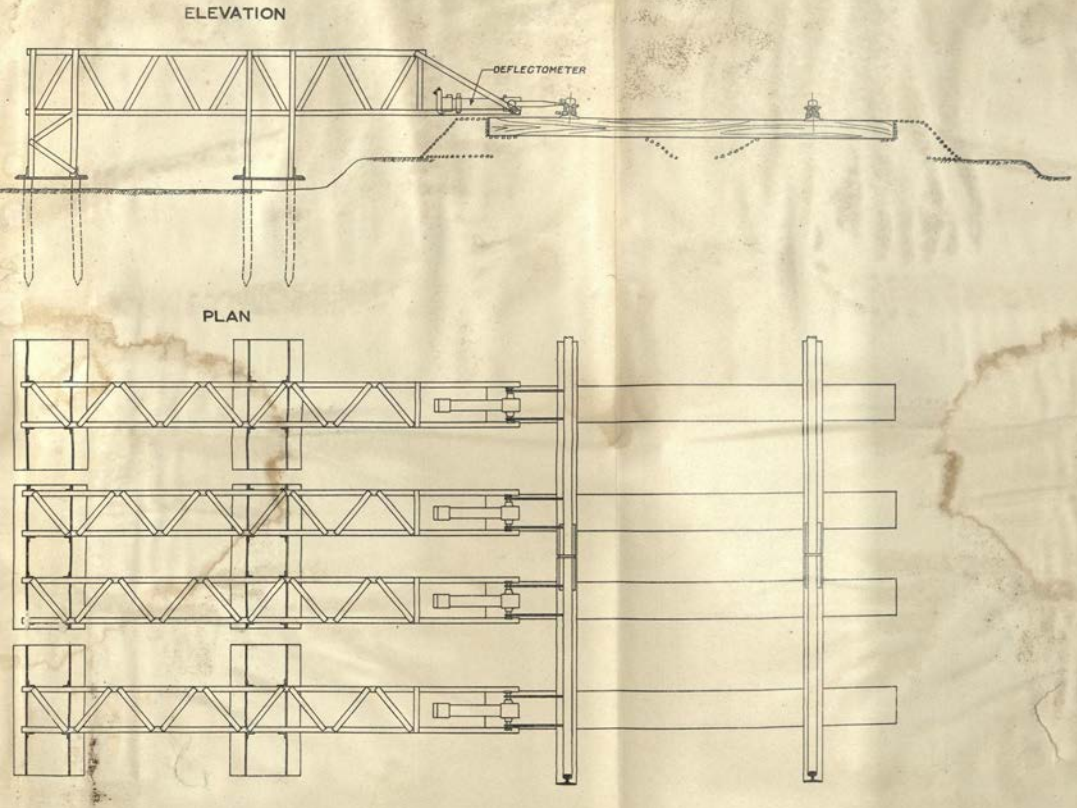

FIG. 39

10. Field Testing Equipment for Use in Connexion with Item

Optical Deflectometers.—One of these instruments is illustrated Figure 38. It consists of the camera portion of a Fereday-Palmer st recorder fitted with a special head H. Spindles D, E and F are carried in ball bearings housed in this head and each carries a spherical mirror (M_1, M_2 and M_3) rigidly attached to it inside the head. A fourth mirror (M_4) pivoted the tubular portion strument is tilted to fr by a small electro ect contre ma d break used to mar p ions of the whe e records. The speed was usually determin ti narkings o ponding stress records. Spindles D and F or ted to lig al D and D which are in turn connected to or other pa ck by short lengths of piano wire G_1 and indl is connected to d of a light metal arm, to the other end hich a heavy ight is ched. This arm is kept in equilibrium an approximate horiz tion by means of a specail spring suspens on the principle of a torsion bar made from a six feet length of piano wire (see Figure 38). This spension, having little intrinsic inertia, ensures that the system will be simple per nic. Each deflectometer is mounted on a steel restle, four of which are shown assembled at a test site for rail joint experiments (see Figure 39). Any ground tremors, which are transmitted to the trestles and deflectometers due to the passage of a load at speed, are recorded by M_3 due to the tendency of W to remain stationary. The working of the arms which are connected to the rail is self-explanatory. Specimen records from these instruments are shown in Figure 40.

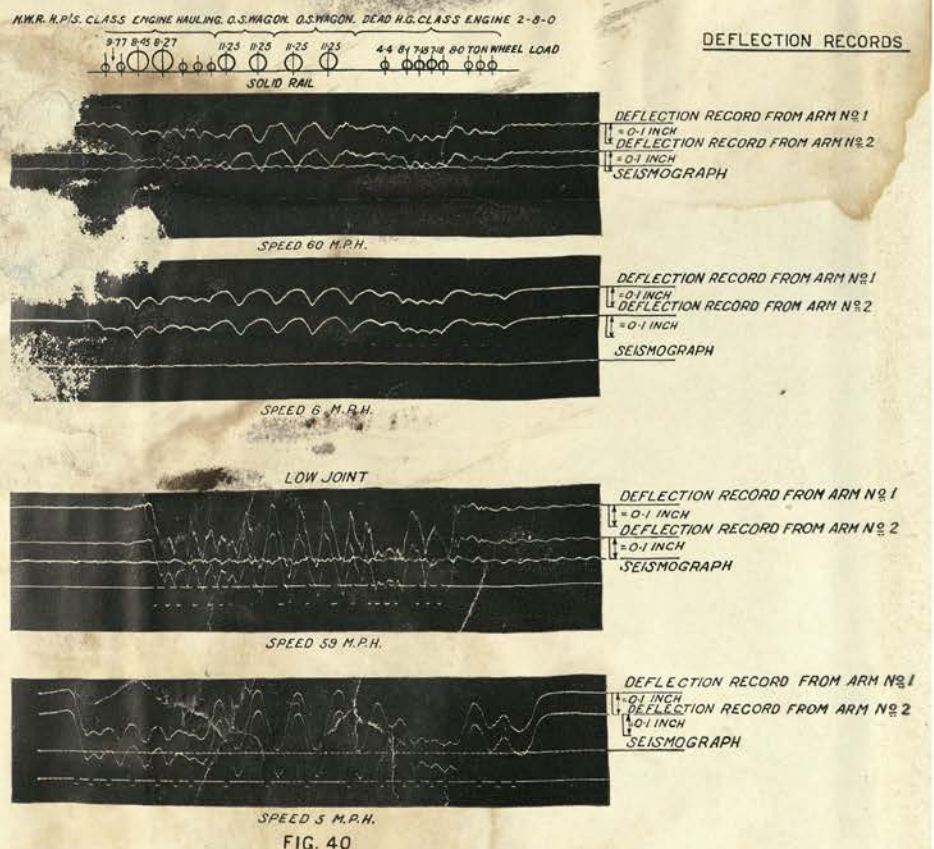

FIG. 40

ers for Rail and Fish-plate Stress Measurements.

nsisting of three telemeter strain gauges wa[illegible] com-
mencement of the field work from Messrs. Baldwin[illegible]
, Philadelphia, U. S. A. Before the commencement of the
nts which are described in this Report, an investigation was
the nsitivity of the oscillographs and their ability to follow
in ss.

iency of the vibrators was about 70 c.p.s. and the fre-
ing current which was supplied by a motor generato
stress records taken at dead slow speed under
gine were analysed up to the 20th harmonic. "T
es" were then construc[illegible] for each oscillogr
litude of swing when th[illegible] rgiser voltage was
nc[illegible] nd running at various spe[illegible]s.

for calibration curves to be applied to the r
[illegible] applied during the first six months' testing. In
[illegible] of 1936, ew oscillographs were received from Messrs. Baldw
[illegible]k having a considerably higher sensitivity for which fresh calibrat[illegible]s
were then constructed to suit. The tele-meter equipment was use[illegible]ns
condition for the first five hundred tests or up to December 1936 after which
the energising frequency was increased to 6,000 c.p.s. and the circuit arranged
as for the "weighbars" described on page 70. The undamped natural fre-
quency of the oscillographs was increased to 600 c.p.s. and the sensitivity of
the apparatus as finally modified was sufficiently high to render speed corrections
unnecessary. Specimen stress records are shown in Figure 41. Photographs
Figures 42 and 43 show the deflecto-meters and the electric telemeter strain
gauges assembled at a test site ready for use.

TEST LOAD: On [illegible] G.E.P. Electric Passenger Loco. Hauling one 45 ton [illegible] owed by one 2-[illegible] dead HG Engine and tender and one Bo[illegible]

DIRECTION OF MOTION ——————>

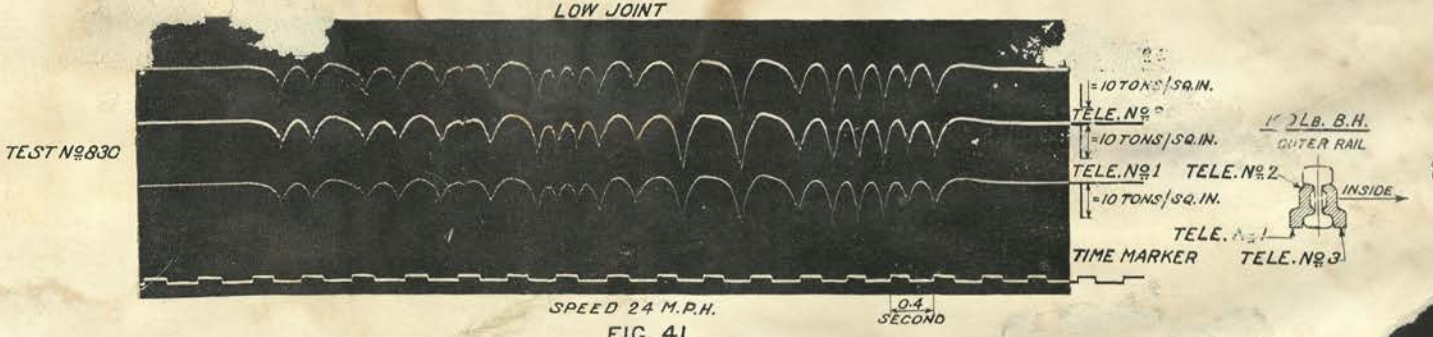

FIG. 41

FIG. 42

FIG. 43

11. Experiments to Determine the Lateral Strength and Stiffness of Permanent Way and the Lateral Loads Applied to it.

(Item 5 of the terms of reference)

Very little work had been done in connection with Item 5 up to the end of December 1936 when the Interim Report was completed. It was evident, however, that no reliable conclusions could be drawn unless due account was taken of the lateral forces which are imposed on the track.

The experimental investigation of Item 5 presented a problem of some difficulty and complexity but by the summer of 1937, apparatus had been designed and manufactured to be fitted between the axle-boxes of locomotive axles by means of which flange pressures imposed on the rails could be electrically recorded whilst the locomotives were travelling at speed. In addition and in connection with a separate investigation, arrangements were made to record the lateral movements of the front and rear of engines by means of electric telemeters, these being the same as used on the rails in the previous investigations but adapted for the purpose in view. Experiments to determine the lateral strength and stiffnesses of various types of Broad gauge tracks were carried out concurrently with these locomotive experiments.

Description of Apparatus and Experimental Methods (Item 5).

1. *Measurement of flange forces.*—The general character of the apparatus used on the locomotives has already been indicated. The flange pressures were recorded by electro-magnetic strain gauges incorporated in weighbars in the form of tubular struts (Figure 44) fixed in pairs between the axle-boxes, the channel liners of which are planed down at X Figure 44 to give sufficient clearance to ensure proper functioning of the weighbars,which requires that the path of the lateral forces between the flanges and the locomotive frame shall be via the weighbars or struts. The thickness of metal of the tubular struts is reduced to 0·19″ over the length GG and strain on this length is detected by an electro-magnetic strain detector assembly (See Fig. 44). In the assembly are three wound laminated cores of Rhometal separated by air gaps of ·020″. The central core, on which is wound the energising coil, is rigidly connected to one end of the gauge length by means of a duralumin forked plug. The two outer cores, with their windings connected in opposed series to give the difference of the voltages induced in them, are rigidly connected together and to the other end of the gauge length by means of the duralumin frame plates and plug. When a load is applied to the weighbar, the strain on the gauge length closes the air gap on one side of the central core and opens it on the other thus increasing and reducing the induced voltages in the respective outer core windings. As arranged for use, the number of coils on each of the outer cores is different so that under no load the difference of the induced voltages is 5 volts decreasing with load. Up to the maximum load the variation of voltage is very closely linear. The wieghbars are made in matched pairs and are retained between the axle-boxes by means of hemispherical sockets. The nett induced voltages from each of a pair of weighbars is added so that the total of the two nett induced voltages varies linearly with the total load on the pair of weighbars and is independent of the actual distribution of the load between weighbars.

The energising power is obtained from an oscillator-amplifier delivering about 6-7 watts at 6000 c.p.s. The whole group of the electro-magnetic strain detector assemblies are connected in parallel with each other. This parallel group is connected in series to a condenser to form a series resonant circuit which presents a load of pure resistance to the amplifier. The impedance of each assembly is practically constant for the working variations of the air gaps.

From each pair of weighbars and each deflexion-meter the nett induced voltage is applied to the grids of a pair of valves arranged for rectification. The anode current from each pair valves is filtered and passed through an adjustable resistance to a Duddell type oscillograph tube. The filters are designed to cut off about 60 c. p. s. in the case of the weighbars and 20 c. p. s. in the case of movement or deflexion-meters.

The battery of oscillograph tubes with their electro-magnetic D. C. field coils are arranged at one end of a light tight box which forms the "bellows" of a camera. The film box is located at the other end of but not touching the "bellows" box, the connection being made by means of a labyrinth light trap. Images of a straight filament are thrown on to a cylindrical lens in front of the film by the oscillograph mirrors. The cylindrical lens reduces this line image to a point image on the film. A slit 0·010" wide is placed across the film to protect it from stray images and dispersion. The film is wound past the slit at any required speed by a small motor. The "bellows" box is mounted on a sponge rubber mat one inch thick to protect the oscillograph tubes from possible vibration from this motor.

The whole group consisting of oscillator-amplifier, rectifying valves and camera oscillograph is mounted on a board and slug from the roof of a bogie vehicle by rubber ropes. In practice, the suspension is satisfactory and no influence of train motion can be detected on the records.

THE
BOMBAY
BRANCH OF THE
ROYAL ASIATIC

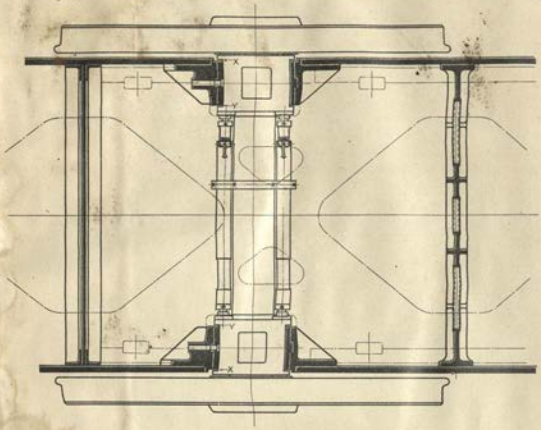

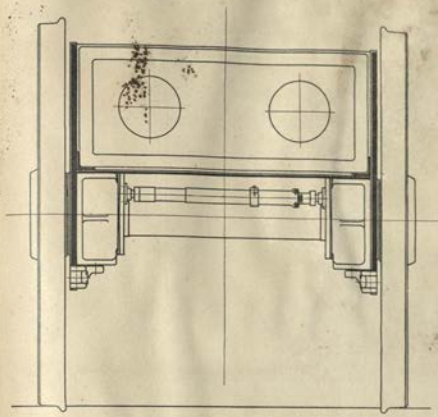

ELECTROMAGNETIC DETECTOR FOR WEIGHBARS

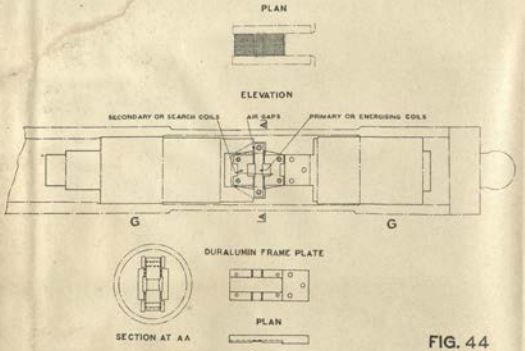

ELETROMAGNETIC STRAIN DETECTOR ASSEMBLY

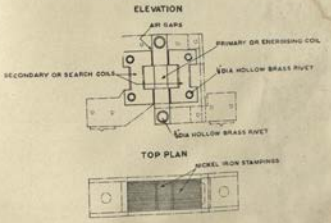

FIG. 44

WEIGH BAR CALIBRATOR

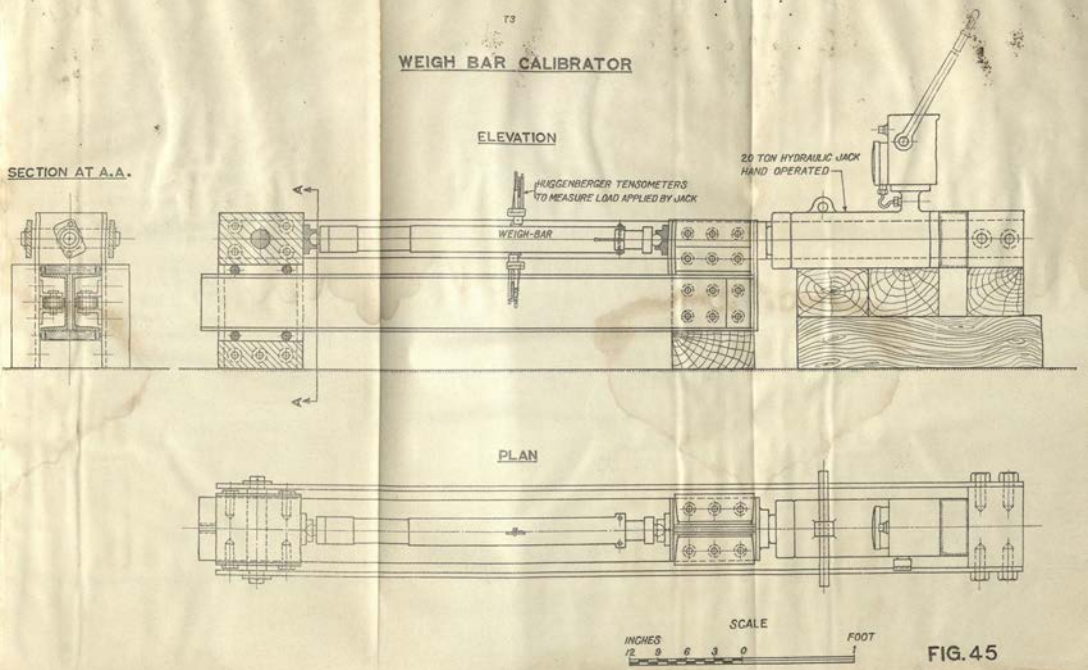

FIG. 45

Calibration of Weighbars.

A direct calibration is obtained by applying known loads to the weighbars in a calibration assembly Figure 45 and adjusting the weighbar oscillographs to a convenient scale. The scale usually adopted is 1 cm = 5 tons. The calibration can vary about 5 per cent due to heating up of the oscillograph tubes by the field current. To minimise errors due to such variations, calibrations were taken before and after each day's tests.

Apparatus to Determine the Lateral Strength and stiffness of Railway Tracks by Static Methods.

Apparatus known as "track pulling gear" was designed and constructed for applying measured horizontal static loads up to 30 tons to the rail or to the wheel of the vehicle with provision in the form of dial indicators for measuring the deflection at intervals during the progress of tests. A drawing of this apparatus is given in Figure 46 and photographs (four) Figures 47 to 50 show it in operation. Measurements of the elastic curves assumed by the rail have also in certain cases been made in addition to the deflection at the point of application of the load.

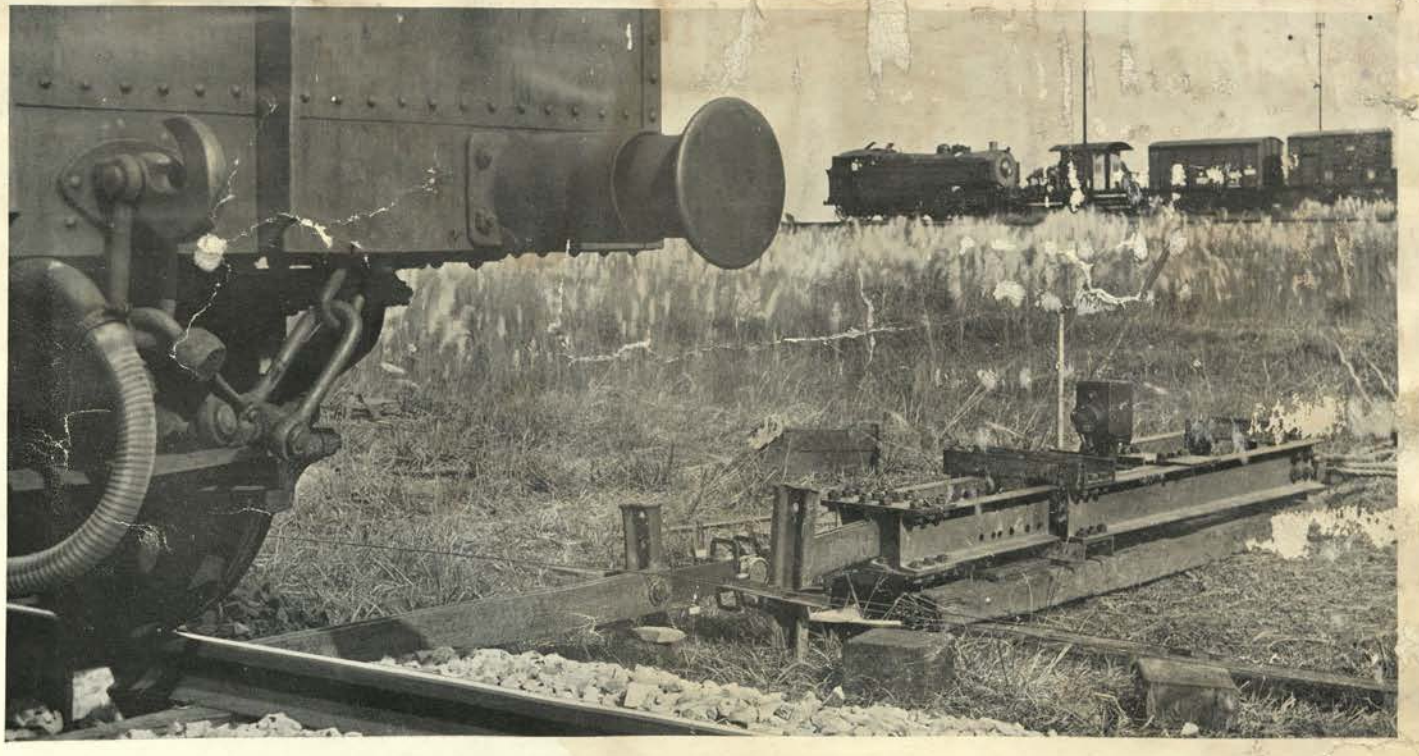

FIG. 47

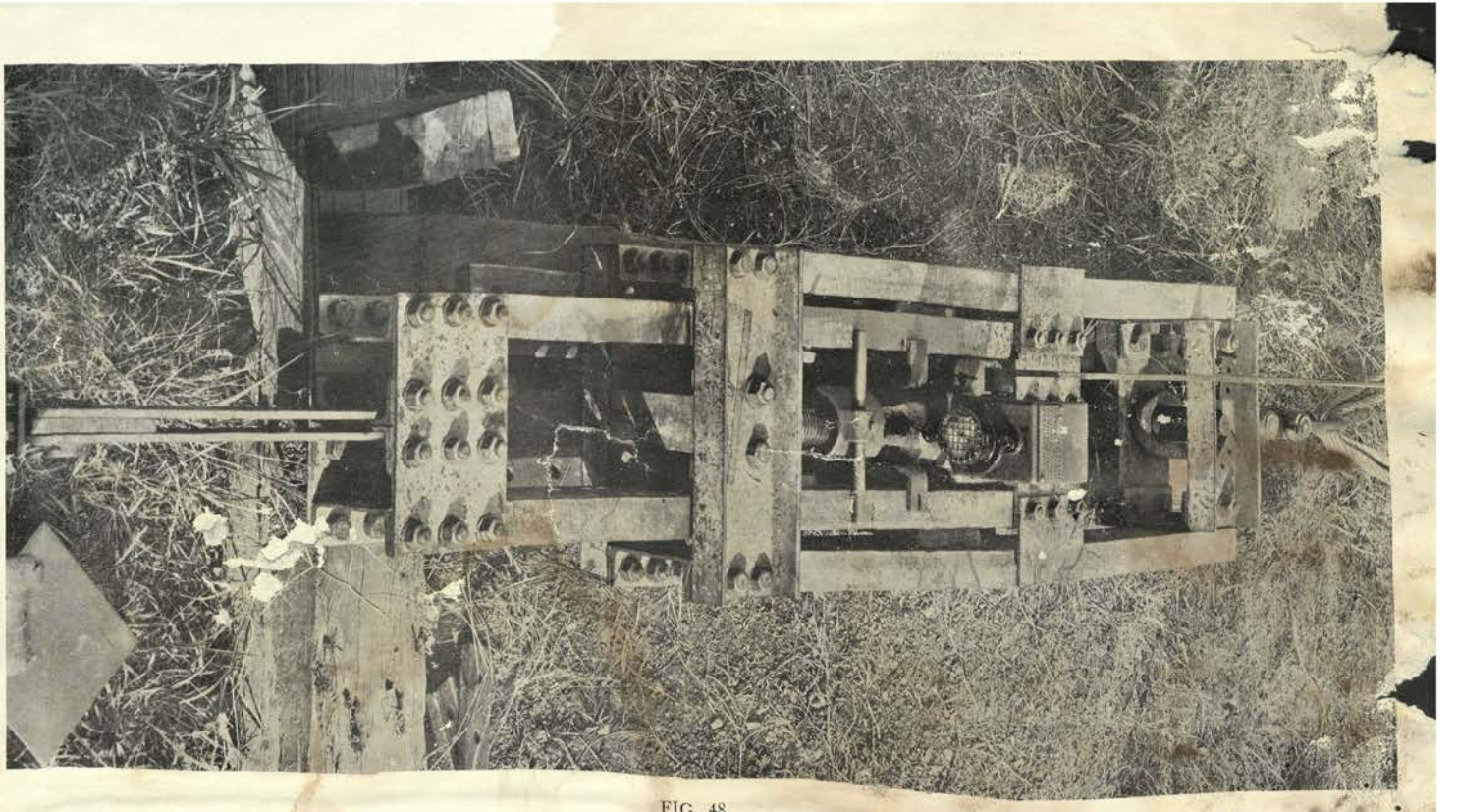

FIG. 48

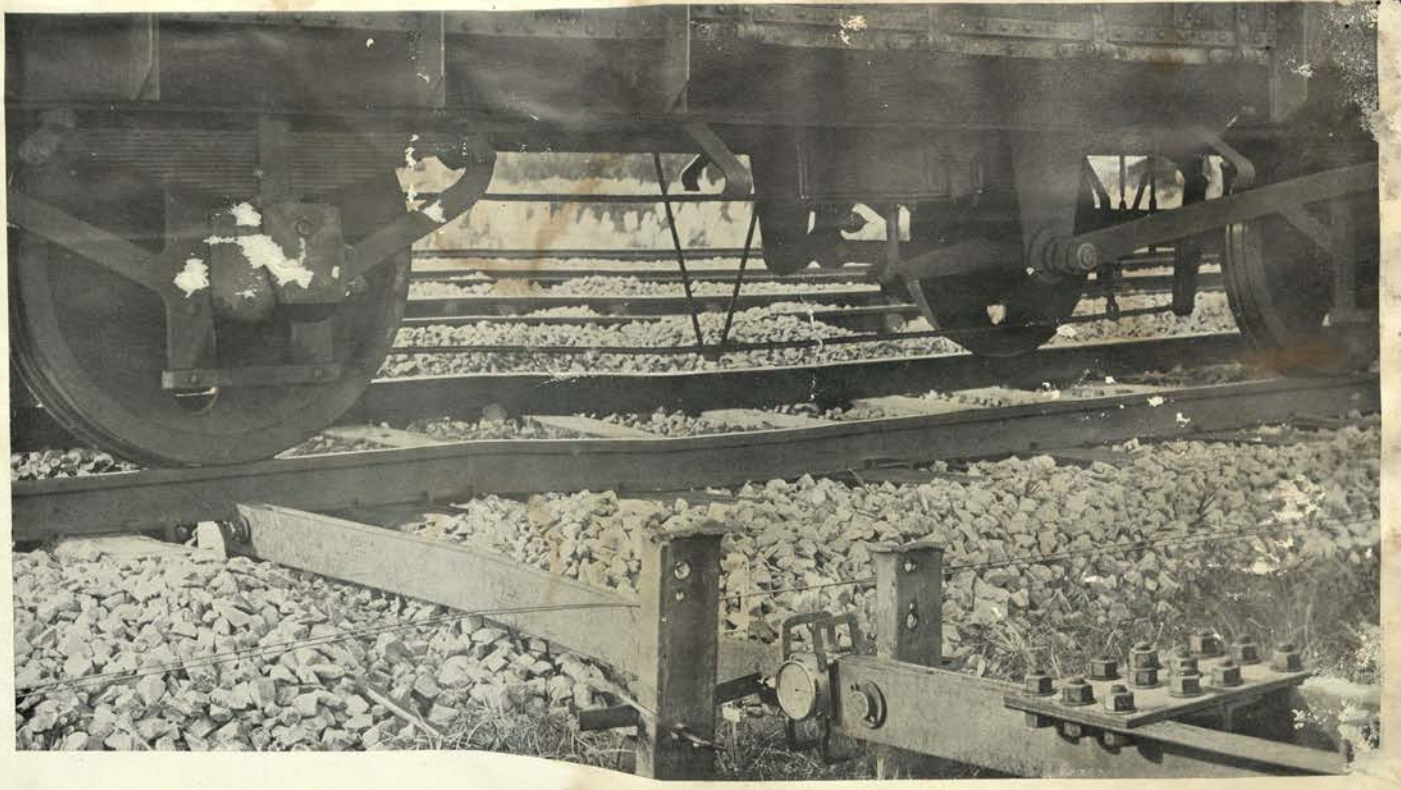

FIG. 49

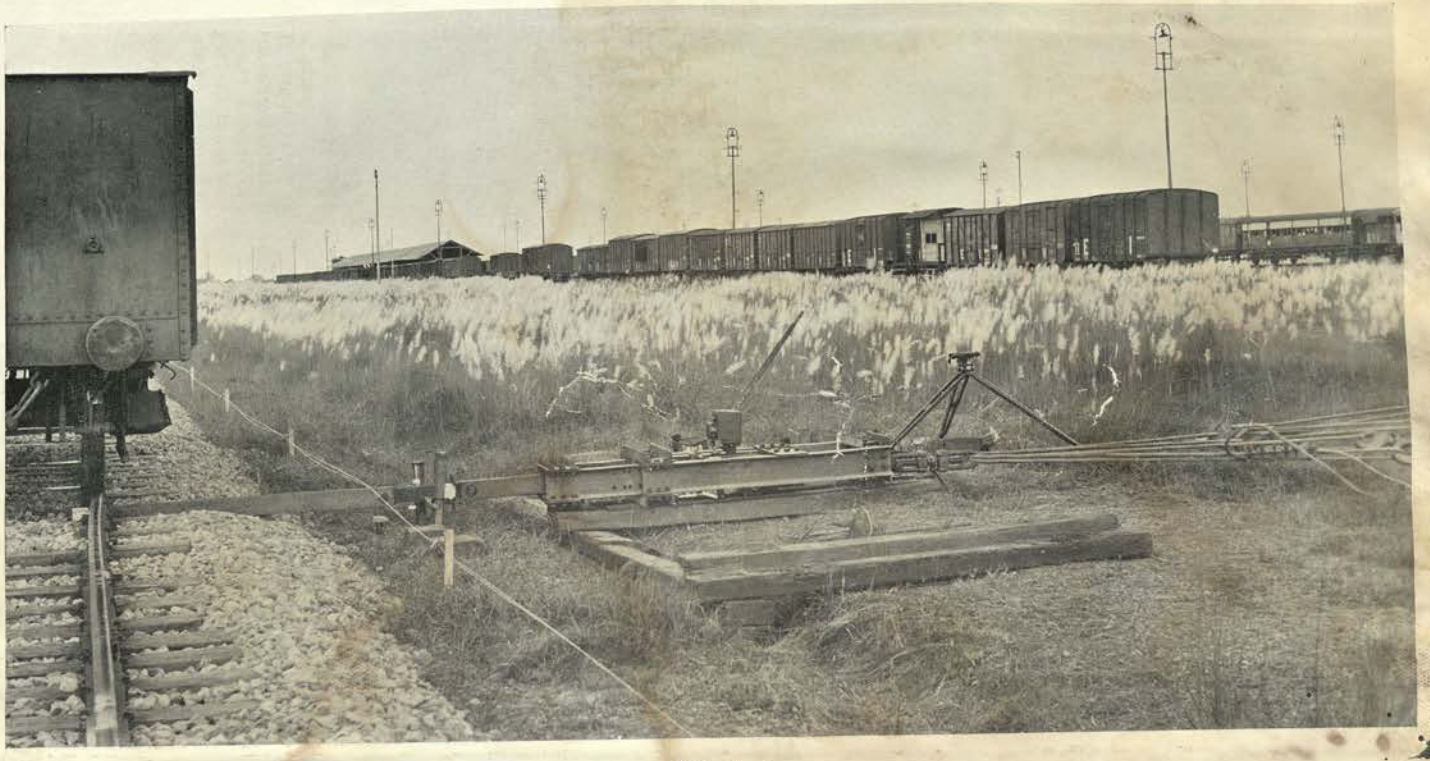

FIG. 50

Apparatus for Measuring Rail Web and Fillet Stresses due to Vertical Eccentric and Lateral Loads.

Web stresses in a vertical direction in 90 lb. flat footed rails under vertical concentric and vertical eccentric static loads have been measured by means of Huggenberger Strain Gauges.

The stresses at the junction of the rail head and the rail foot with the web were measured by apparatus specially designed for the purpose, and the work was performed partly in the track and partly in the laboratory.

First the lateral and angular deflexions of the rail head in relation to the foot on the application of vertical eccentric loads and lateral loads in combination with vertical loads were measured by dial indicators and micrometers operating from a datum consisting of a rigid frame lightly clamped to the foot of the rail. The vertical eccentric loads were produced by providing a shim ramp of high carbon steel ¾" wide lying on the rail table to one side of the centre-line, and the lateral loads were provided by the track pulling gear described above.

Having measured the distortions, a full size transparent model in xylonite of the cross section of the rail was prepared and a jig was constructed to hold the model in a circular polariscope for analysis with monochromatic light. The jig is arranged so that a combination of lateral and angular distortions can be applied to the rail head by forcing it against adjustable stops by jack screws. This operation can be performed with sufficient rapidity to eliminate errors due to mechanical and optical creep. Young's modulus was determined for a rectangular tension test specimen which had been cut from the same slab of xylonite as the rail specimen. This rectangular specimen was then placed in the circular polariscope and was subjected to cycles of simple bending, observations being made of extreme fibre stresses (measured by Huggenberger Strain Gauges) and the number of dark fringes, which is proportional to the extreme fibre or boundary stresses. This enabled the boundary stresses at points along the fillets of the rail to be determined by counting the number of dark fringes which passed from the boundary as the load was gradually applied.

This part of the investigation was inspired by the work of Timoshenko and Langer described in their paper entitled "Stresses in Railroad Track," Transactions of the American Society of Mechanical Engineers, APM 54—26 pages 278 to 302, 1931—32. The authors give a method of analysis incorporating photo-elasticity for determining stresses due to lateral and eccentric loading. The method described in the present report is, however, entirely different from the method described in the above paper.

Apparatus for Measuring the Lateral Strength and Stiffness of Railway Tracks under Moving Loads.

Arrangements were made to apply combined vertical and lateral loads to the track by pairs of similar vehicles running abreast on parallel tracks with gear inserted between the vehicles tending to spread the tracks apart. The gear is illustrated in Figure 51. The telescopic spring shafts were inserted between the axle centres in the case of tests with wagons and between the axle centres of the leading coupled wheels and between the centres of the bogie spring pins midway between the bogie axles in the case of locomotive tests.

The gear assembled between vehicles ready for test is illustrated in photographs, Figures 52 to 55. It is designed for working lateral loads up to 15 tons per spring and the stiffness of each assembly is 2·16 tons per inch. It is, therefore, necessary that the two tracks should be sensibly parallel over the test lengths in order to ensure constancy of lateral load. The speed of the moving loads in these tests was kept as nearly uniform as possible at about 5 miles per hour.

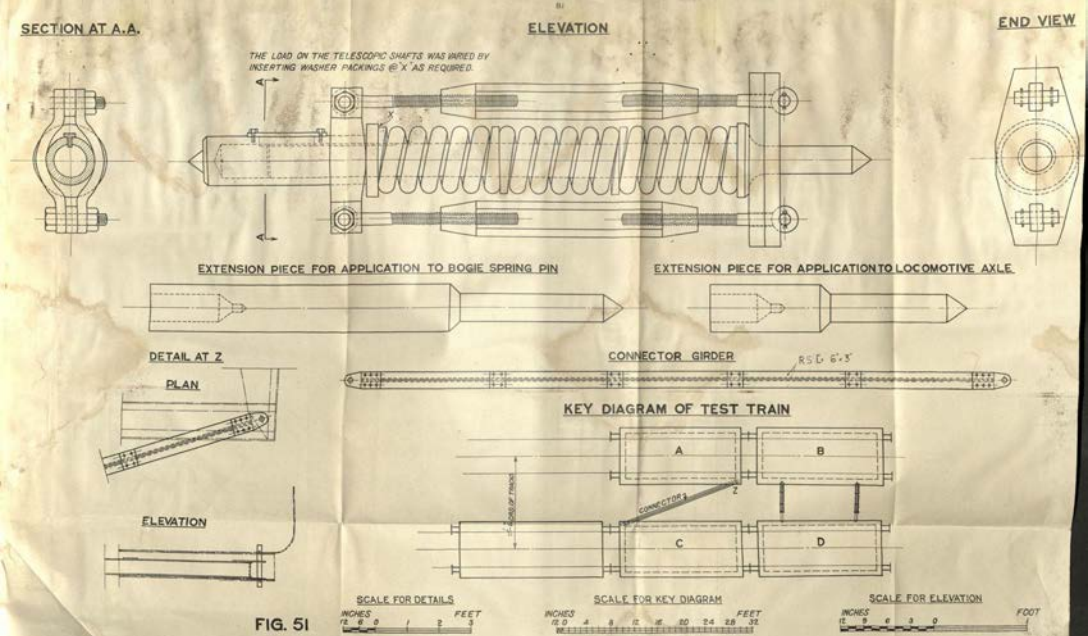
SECTION AT A.A.
ELEVATION
END VIEW
THE LOAD ON THE TELESCOPIC SHAFTS WAS VARIED BY INSERTING WASHER PACKINGS @ 'X' AS REQUIRED.
EXTENSION PIECE FOR APPLICATION TO BOGIE SPRING PIN
EXTENSION PIECE FOR APPLICATION TO LOCOMOTIVE AXLE
DETAIL AT Z
PLAN
ELEVATION
CONNECTOR GIRDER
R.S.D. 6'-3"
KEY DIAGRAM OF TEST TRAIN
A
B
C
D
CONNECTOR
Z
CENTRE OF TRACK
SCALE FOR DETAILS
INCHES
FEET
SCALE FOR KEY DIAGRAM
INCHES
FEET
SCALE FOR ELEVATION
INCHES
FOOT

FIG. 51

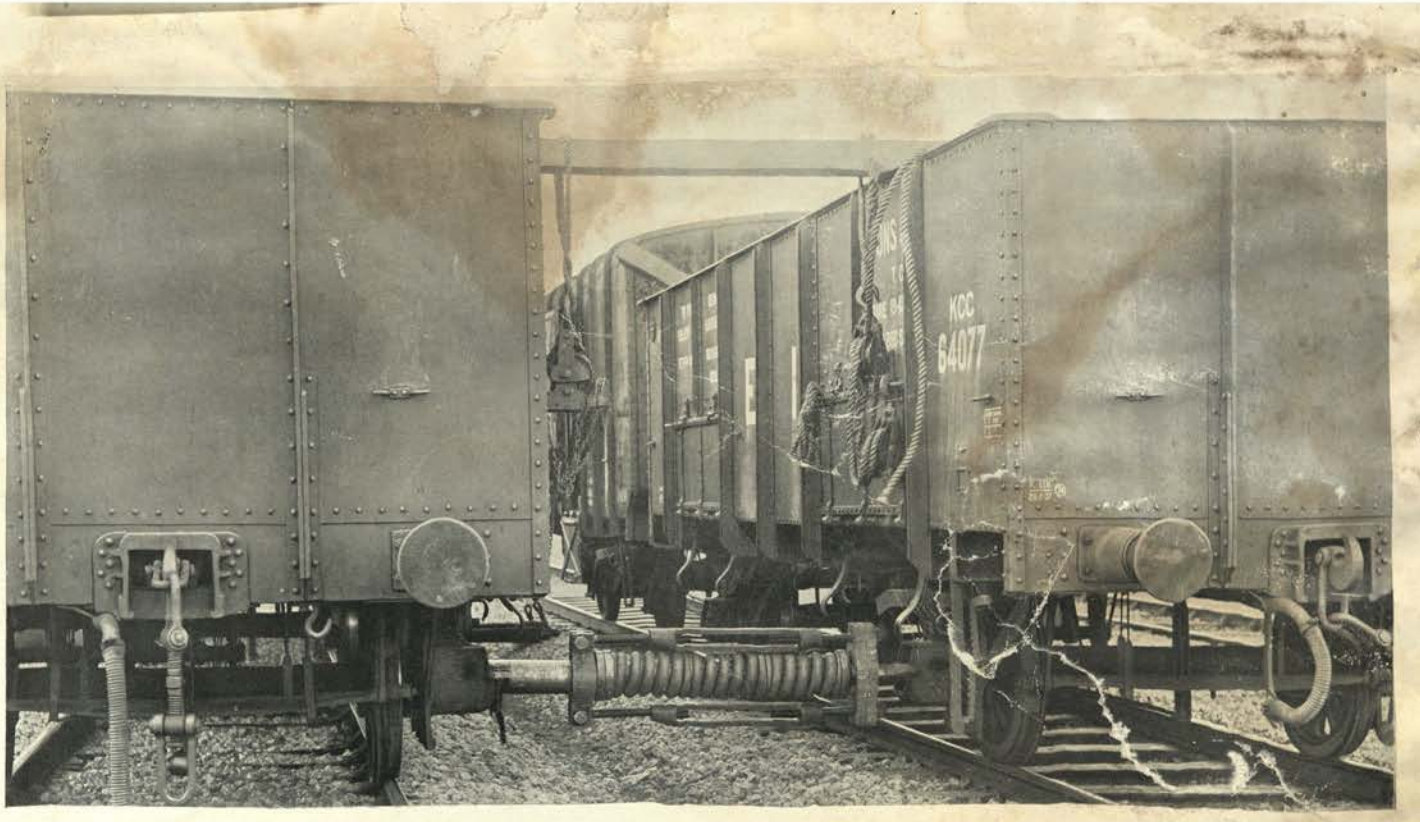

FIG. 52

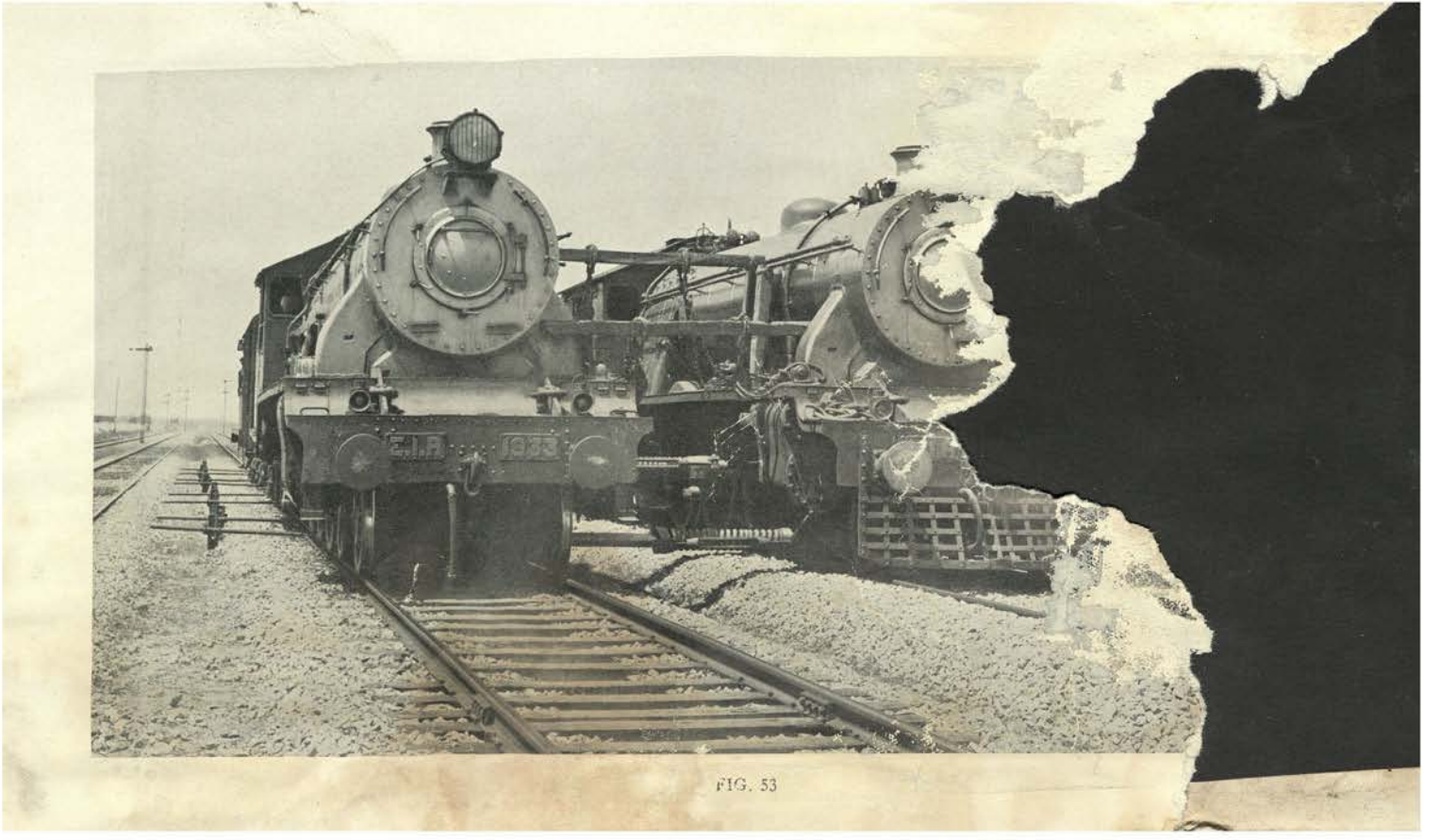

FIG. 53

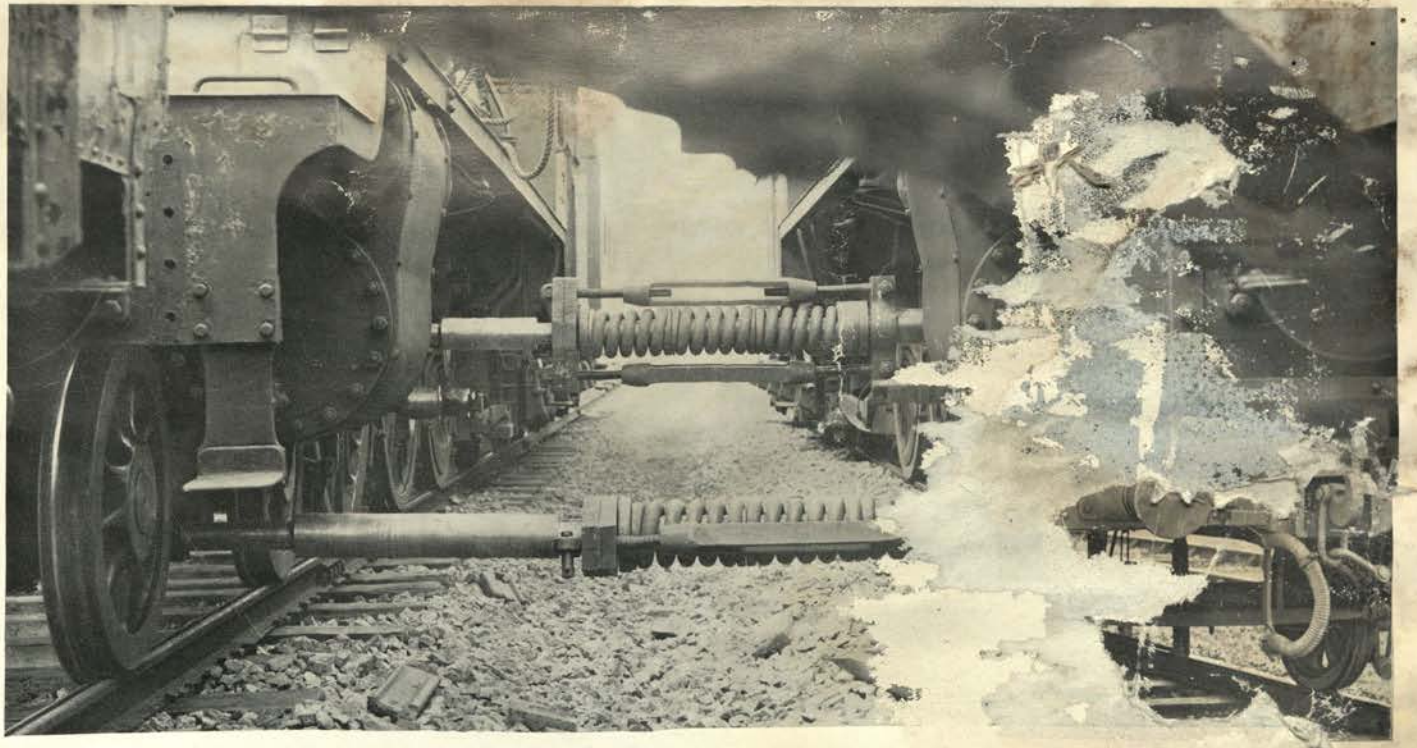

FIG. 54

FIG. 55

The elastic and permanent distortions of the track during moving load tests are measured with the help of telescopic detector gauges, Figure 56, forty-four of which were used. Prior to the tests, the gauge points are brought up against the rail head. When the detector gauges are located against the rail which takes the lateral thrust, the total rail distortion is given by the gap remaining between the rail and the detector after the test. When the detector gauges are located against the other rail, the gap between the gauge and the rail after a test indicates only the permanent shift of the track. It is, therefore, more advantageous to locate the telescopic gauges at the laterally loaded rail and this has been the usual practice.

In addition to the moving load tests of lateral effects on straight parallel tracks, a number of measurements have been made of track distortion and rail stress on curved track at speed up to 65 miles per hour using the telescopic gauges Figure 56 and the electric telemeters attached to the rails.

TELESCOPIC DETECTOR GAUGE

END VIEW

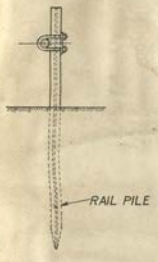

GENERAL ARRANGEMENT

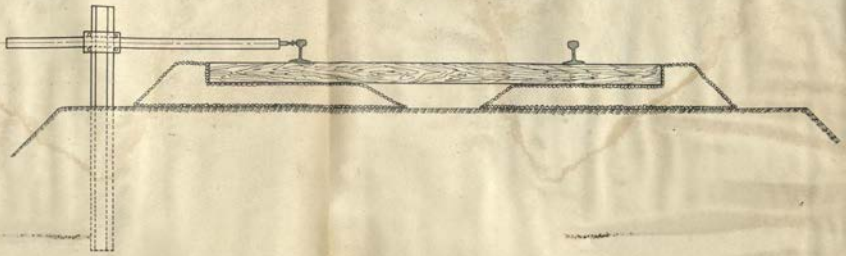

SECTION

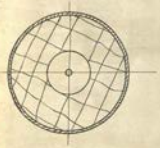

DETAIL

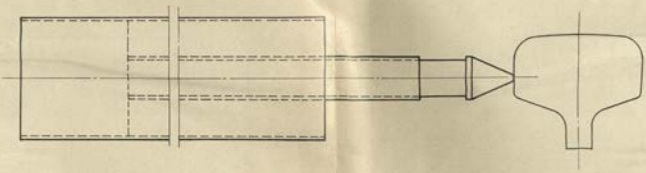

SCALE FOR DETAIL

INCHES

0 ¼ ½ ¾ 1 2 3 4 5 6

SCALE FOR GENERAL ARRANGEMENT

INCHES FEET

12 9 6 3 0 1 2 3 4

FIG. 56

TABLE 10.

Rail lb.	Sleepering	Track, boxed or unboxed	Vertical load tons axle	Solid rail or joint	No. of tests	Soil	Weather conditions	Section of line	Railway	Remarks
75 D. H.	D. & O. N+2 ..	..	22.5	Solid rail	2	Hard loam.	Monsoon	Sahibganj Loop.	E. I. ..	Load applied close to sleepers.
75 D. H.	D. & O. N+2 ..	..	22.5	Do. ..	1	Do. ..	Do. ..	Do. ..	E. I. ..	Load applied midway between sleepers.
75 D. H.	D. & O. N+2 ..	..	No load	Do. ..	2	Do. ..	Do. ..	Do. ..	E. I. ..	Load applied close to sleepers.
82 B. H.	C. I. Pot N+2 ..	..	9	Do. ..	1	Black cotton.	Dry ..	KNW-ET	G. I. P.	Load applied midway between sleepers.
88½ B. H.	D. & O. N+2 ..	..	22½	Do. ..	1	Sandy clay	Do. ..	MGS Yard.	E. I. ..	Ditto.
88½ B. H.	D. & O. N+2 ..	..	No load	Do. ..	1	Do. ..	Do. ..	Do. ..	E. I. ..	Ditto.
88½ B. H.	Existing hard-wood laid in 1926 N+2.	..	22½	Do. ..	1	Do. ..	Do. ..	Do. ..	E. I. ..	Ditto.
88½ B. H.	Do. ..	..	No load	Do. ..	1	Do. ..	Do. ..	Do. ..	E. I. ..	Ditto
88½ B. H.	Hardwood laid on 12th November 1937.	..	22½	Do. ..	1	Do. ..	Do. ..	Do. ..	E. I. ..	Ditto.
88½ B. H.	Do. ..	..	No load	Do. ..	1	Do. ..	Do. ..	Do. ..	E. I. ..	Ditto.
88½ B. H.	N+1 1926 Hard-wood.	..	22½	Do. ..	2	Do. ..	Do. ..	Do. ..	E. I. ..	Ditto.
88½ B. H.	N+1 new Hard-wood.	..	22½	Do. ..	4	Do. ..	Do. ..	Do. ..	E. I. ..	Ditto.
88½ B. H.	D. & O. N+1 ..	..	22½	Do. ..	4	Do. ..	Do. ..	Do. ..	E. I. ..	Ditto.
88½ B. H.	D. & O. N+2 ..	..	22½	Do. ..	7	Do. ..	Do. ..	Do. ..	E. I. ..	Ditto.
88½ B. H.	D. & O. N+2 ..	..	12	Do. ..	7	Do. ..	Do. ..	Do. ..	E. I. ..	Ditto.
88½ B. H.	D. & O. N+2 ..	..	12	Joint ..	4	Sandy clay	Do. ..	MGS Yard.	E. I. ..	Ditto
88½ B. H.	D. & O. N+3+D.	..	22½	Solid rail	3	Do. ..	Do. ..	Do. ..	E. I. ..	Ditto.
88½ B. H.	D. & O. N+3+D.	..	12	Do. ..	3	Do. ..	Do. ..	Do. ..	E. I. ..	Ditto.
88½ B. H.	D. & O. N+3+D.	..	12	Joint ..	2	Do. ..	Do. ..	Do. ..	E. I. ..	Ditto.
88½ B. H.	D. & O. N+4+D.	..	22½	Solid rail	7	Do. ..	Do. ..	Do. ..	E. I. ..	Ditto.
88½ B. H.	D. & O. N+4+D.	..	12	Do. ..	7	Do. ..	Do. ..	Do. ..	E. I. ..	Ditto.
88½ B. H.	D. & O. N+4+D.	..	12	Joint ..	4	Do. ..	Do. ..	Do. ..	E. I. ..	Ditto.
88½ B. H.	D. & O. N+2 ..	..	22½	Solid rail	2	Do. ..	Monsoon	Do. ..	E. I. ..	Ditto.
88½ B. H.	D. & O. N+2 ..	..	12	Do. ..	2	Do. ..	Do. ..	Do. ..	E. I. ..	Ditto.
88½ B. H.	D. & O. N+3+D.	..	22½	Do. ..	2	Do. ..	Do. ..	Do. ..	E. I. ..	Ditto.

Rail lb.	Sleepering	Track boxed or unboxed	Vertical load tons axle	Solid rail or joint	No. of tests	Soil	Weather conditions	Section of line	Railway	Remarks
88½ B. H.	D. & O. N+3+D.	..	12	Solid rail	2	Sandy clay	Monsoon	MGS Yard.	E. I. ..	Load applied midway between sleepers.
90 BSS ..	Hardwood N+2	..	22½	Do. ..	1	Soft clay	Do. ..	GYA-MGS	E. I. ..	Ditto.
90 BSS ..	Hardwood N+2	..	No load	Do. ..	1	Do. ..	Do. ..	Do. ..	E. I. ..	Ditto.
90 R ..	CST 9 N+2 ..	..	22½	Do. ..	1	Sandy clay	Dry ..	LHR-LDH	N. W.	Ditto.
90 R ..	CST 9 N+2 ..	..	No load	Do. ..	1	Do. ..	Do. ..	Do. ..	N. W.	Ditto.
90 R ..	CST 9 N+2 ..	..	22½	Joint ..	1	Do. ..	Do. ..	Do. ..	N. W.	Ditto.
90 R ..	CST 9 N+2 ..	..	No load	Do. ..	1	Do. ..	Do. ..	Do. ..	N. W.	Ditto.
90 R ..	Steel loose jaws N+3.	..	22½	Solid rail	1	Do. ..	Dry ..	LHR-LDH	N. W.	Ditto.
90 R ..	Do. ..	..	No load	Do. ..	1	Do. ..	Do ..	Do. ..	N. W.	Ditto.
90 R ..	Do. ..	..	22½	Joint ..	1	Do. ..	Do. ..	Do. ..	N. W.	Ditto.
90 R ..	Do. ..	..	No load	Do. ..	1	Do. ..	Do. ..	Do. ..	N. W.	Ditto.
90 R ..	Steel pressed jaws N+2.	..	22½	Solid rail	2	Black cotton.	Do. ..	KNW-ET	G. I. P.	"
90 R ..	Do. ..	..	22½	Joint ..	1	Do. ..	Do. ..	Do. ..	G. I. P.	Ditto.
90 R ..	Deodar N+3 ..	..	22½	Solid rail	1	Sandy clay	Do. ..	LHR-LDH	N. W.	Ditto.
90 R ..	Do. ..	..	No load	Do. ..	1	Do. ..	Do. ..	Do. ..	N. W.	Ditto.
90 R ..	Do. ..	..	22½	Joint ..	1	Do. ..	Do. ..	Do. ..	N. W	Ditto.
90 R ..	Do. ..	..	No load	Do. ..	1	Do. ..	Do. ..	Do. ..	N. W.	Ditto.
90 R ..	CST 9 N+1+D ..	..	22½	Solid rail	3	Do. ..	Do. ..	MGS Yard.	E. I. ..	Ditto.
90 R ..	CST 9 N+1+D ..	..	12	Do. ..	3	Do. ..	Do. ..	Do. ..	E. I. ..	Ditto.
90 R ..	CST 9 N+1+D ..	..	12	Joint ..	2	Do. ..	Do. ..	Do. ..	E. I. ..	Ditto.
90 R ..	Hardwood N+3 ..	..	22½	Solid rail	5	Do. ..	Do. ..	Do. ..	E. I. ..	Ditto.
90 R ..	Hardwood N+3 ..	..	12	Do. ..	5	Do. ..	Do. ..	Do. ..	E. I. ..	Ditto.
90 R ..	Hardwood N+3 ..	..	12	Joint ..	4	Do. ..	Do. ..	Do. ..	E. I. ..	Ditto.
90 R ..	Steel trough N+3 ..	..	22½	Solid rail	7	Sandy clay	Do. ..	MGS Yard.	E. I. ..	Ditto.
90 R ..	Steel trough N+3 ..	..	12	Do. ..	7	Do. ..	Do. ..	Do. ..	E. I. ..	Ditto.
90 R ..	Steel trough N+3 ..	..	12	Joint ..	4	Do. ..	Do. ..	Do. ..	E. I. ..	Ditto.
90 R ..	Steel trough N+6 ..	..	22½	Solid rail	5	Do. ..	Do. ..	Do. ..	E. I. ..	Ditto.
90 R ..	Steel trough N+6 ..	..	12	Do. ..	5	Do. ..	Do. ..	Do. ..	E. I. ..	Ditto.
90 R ..	Steel trough N+6 ..	..	12	Joint ..	4	Do. ..	Do. ..	Do. ..	E. I. ..	Ditto.
90 R ..	Hardwood N+3 ..	..	22½	Solid rail	2	Do. ..	Monsoon	Do. ..	E. I. ..	Ditto.
90 R ..	Hardwood N+3 ..	..	12	Do. ..	2	Do. ..	Do. ..	Do. ..	E. I. ..	Ditto.
90 R ..	Steel trough N+3 ..	..	22½	Do. ..	2	Do. ..	Do. ..	Do. ..	E. I. ..	Ditto.
90 R ..	Steel trough N+3 ..	..	12	Do. ..	2	Do. ..	Do. ..	Do. ..	E. I. ..	Ditto.

LATERAL DISTORTION OF RAIL FOOT
UNDER LATERAL LOAD APPLIED AT ISOLATED AXLE

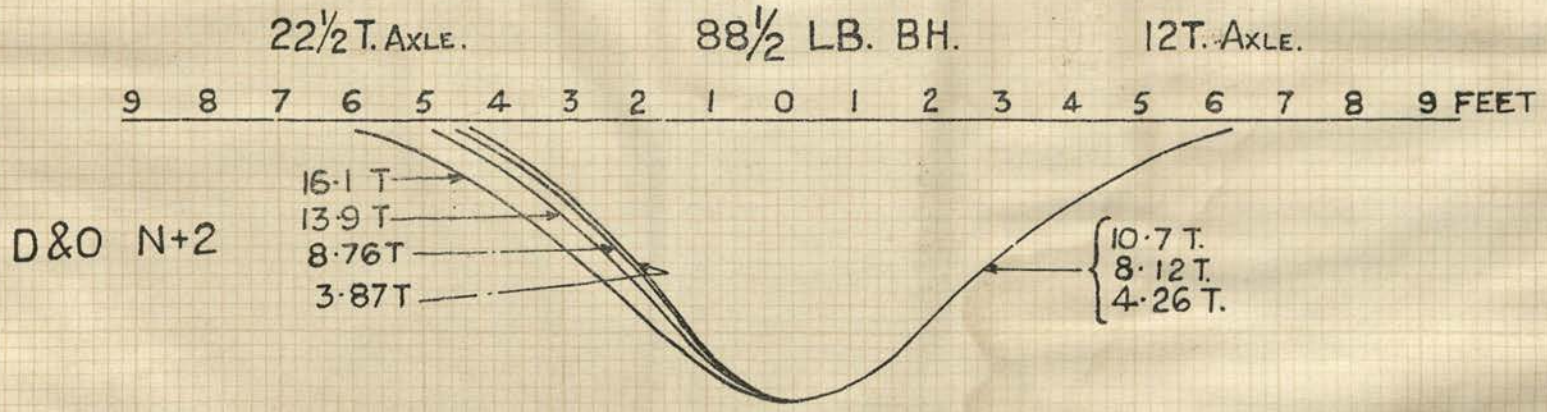

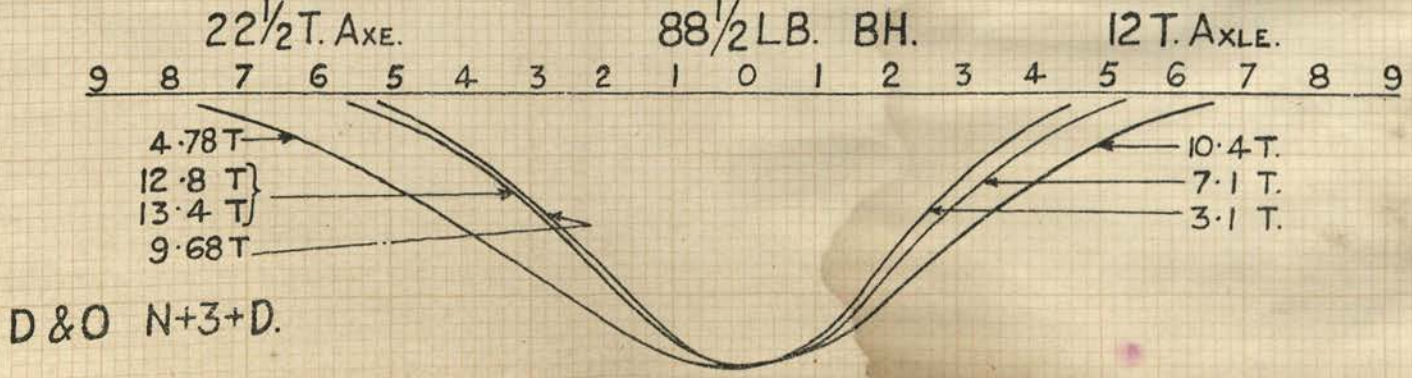

FIG. 57

LATERAL DISTORTION OF RAIL FOOT

UNDER LATERAL LOAD APPLIED AT ISOLATED AXLE

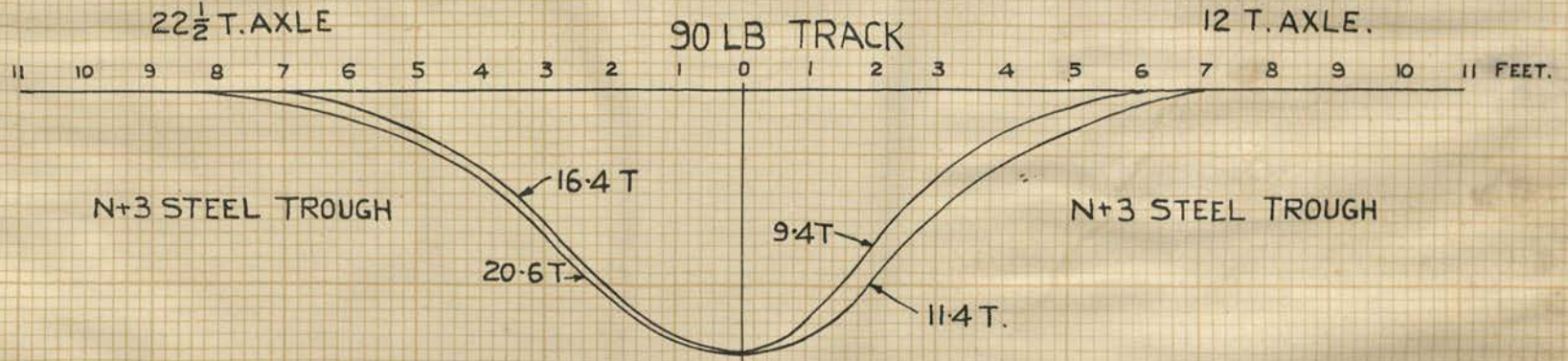

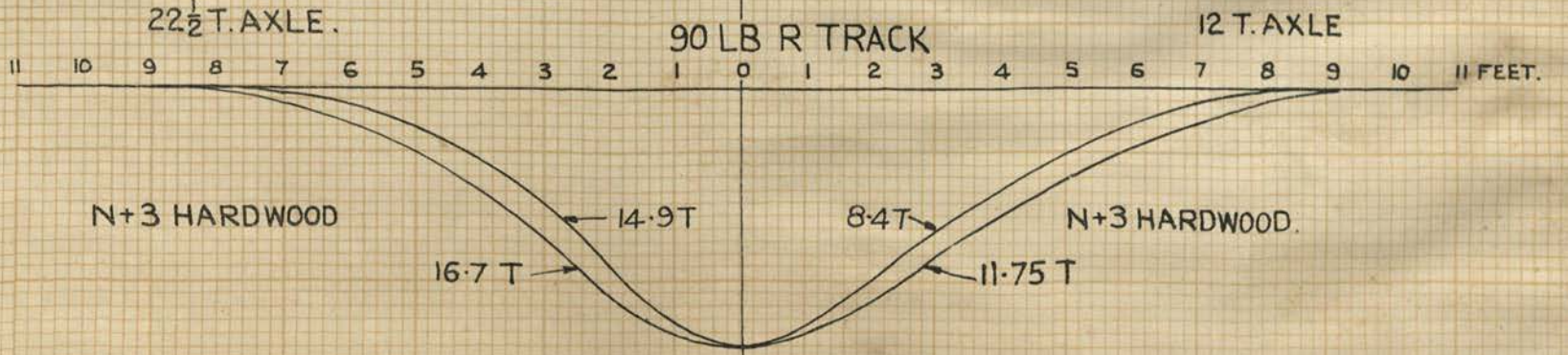

FIG. 58.

Results of Tests in connexion with Item 5.

1. *Static side-pulling tests.*—The types of track which have been tested with the chief particulars are tabulated in Table 10.

It will be seen that the majority of the tests were made at Moghal Sarai. The remainder (See graphs Dry Weather Figures E3 to E6 and E10 to E15 and Monsoon E1 to E2 and E7 to E9), Appendix III were earlier tests confined to one or two sites only for each class of track. In the case of the Moghal Sarai tests, however, several experiments were made for each class of track, and this series may, therefore, be considered to be of the most value. Graphs (Dry Weather), Figures A1 to A10 (Monsoon), Figures A11 to A14 Appendix III show applied load plotted against maximum deflexion for one complete cycle and each curve is an average of all the experiments made on that particular class of track. The number of experiments is written against the corresponding curve. The point of application of the lateral load was close to one sleeper in Test No. 1, Figure E1 and it was mid-way between sleepers for the same track conditions in Test No. 2, Figure E1. As the track stiffness is least when the load is applied mid-way between sleepers, this position was adopted in all the other experiments recorded. Variations up to about 25% in lateral stiffness were recorded at different sites for particular classes of track. Graphs B1 to B14, Appendix III show applied load plotted against maximum deflexion in special tests in which the lateral load was entirely removed when half the maximum load had been reached and re-applied immediately afterwards and the cycle completed as in the series Figures A1 to A14 above.

From the residual deflexions on removal of all lateral load shown in graphs series Figures A1 to A14 and B1 to B14 comparison can be made between various classes of 90 R and certain 88½ lb. tracks at Moghal Sarai as regards their ability to resist permanent distortion.

For the 88½ lb. tracks comparison is more difficult than for the 90R as it was only in test Figures A7 to A9 and B7 to B9 that the loading procedure was standardized, the loading being stopped after approximately twenty tons or alternatively one inch deflexion had been reached.

No very definite conclusions on a quantitative basis can be reached from consideration of graphs Figures E1 to E15, because only one test of each class of track was made.

Typical curves showing the deflected shape of the rail under isolated wagon axles in a horizontal plane are given in Figures 57 and 58, in which the ordinates represent the ratios borne to the central deflexion. These curves are generally similar to those for vertical deflexion and the wave lengths are within the limits usual for vertical rail deflexion on broad gauge tracks. It will be observed that there is a small but definite tendency for the wave length to increase with increase of deflection.

Figures 59 and 60 show actual lateral deflections in the case of a four-wheeled wagon and an XB locomotive respectively.

There appears to be no relation between the values of lateral and vertical track stiffnesses.

The time required to complete one cycle of loading with the "track pulling gear" from zero up to 20 tons and back to zero is usually about 40 minutes. As the amount of permanent lateral deflection of track under given vertical loads depends upon the number of applications of the loads and the time required for one application, and as the time required for a cycle of loading is long compared with the speed of load application under ordinary traffic conditions, the constants obtained from the static track pulling experiments do not give actual quantitative figures for the lateral resistance of track to nosing of vehicles. It is, however, considered that the results afford a useful means for comparing the characteristics of one class of track with another.

Effect of End Boxing on the Lateral Strength of Track.

A definite increase in lateral resistance on account of end boxing can be detected in the "no load" tests but, as might be expected, it is small. The advantage of boxing lies in its providing a surcharge which protects the "packing ballast" from disturbance.

Effect of Rainfall on Lateral Strength of Track.

As regards the tracks at Moghalsarai, which were tested both in dry and monsoon seasons, there was not on the average any noticeable reduction or gain in lateral strength due to rain. The rainfall at Moghalsarai from 1st May to 15th September 1938, the period of the monsoon tests, was 34·28 inches which is 12 per cent less than for the same period for 1937.

Web Stresses in 90R Flat Footed Rails.

Curves showing the intensity of maximum compressive web stress in horizontal planes due to a vertical concentric load of 11·25 tons as measured by Huggenberger Strain Gauge at sections of the rail both over a sleeper and midway between sleepers are given in Figure 61.. It will be observed that there is considerably more dispersion of stress at the point midway between sleepers than for over a sleeper.

Fillet Stresses in 90R Flat Footed Rails.

Four types of loading have been examined, i.e.—

(1) Vertical eccentric load on head for a point over the sleeper.

(2) Vertical eccentric load on head for a point midway between sleepers.

(3) Lateral load combined with vertical eccentric load for a point over the sleeper.

(4) Lateral load combined with vertical eccentric load for a point midway between sleepers.

LATERAL DEFLECTION OF RAIL LOADED WITH 15 TON AXLES
AND 8·2 T LATERAL FORCE ON EACH AXLE

SCALE OF ORDINATES TEN TIMES FULL SIZE

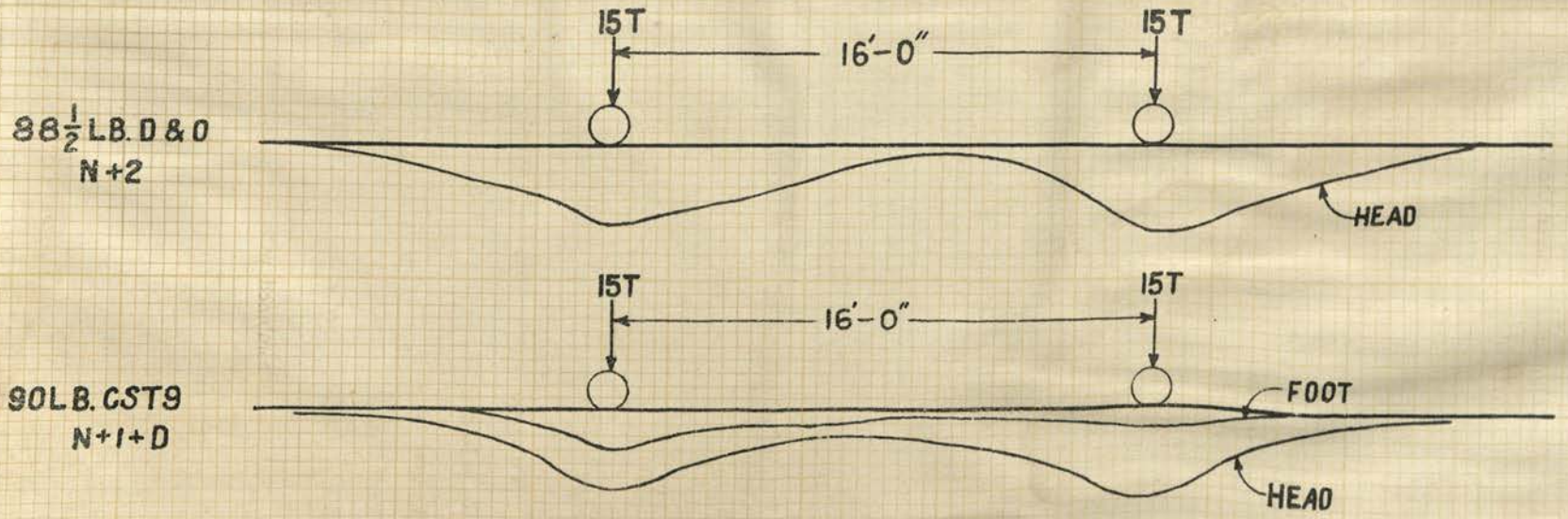

FIG. 59

LATERAL DEFLECTION UNDER AN X B. ENGINE
13 TONS LATERAL LOAD ON LEADING COUPLED AXLE
AND 6·4 TONS AT 'A'.

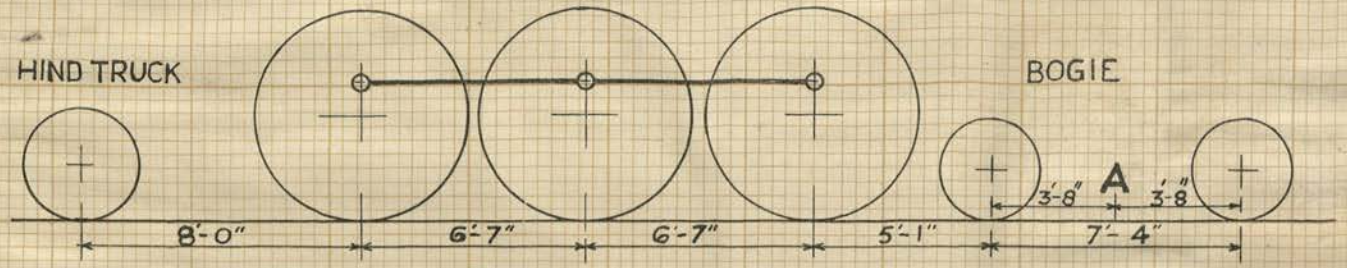

88½ LB, BH.
D&O. N+2.

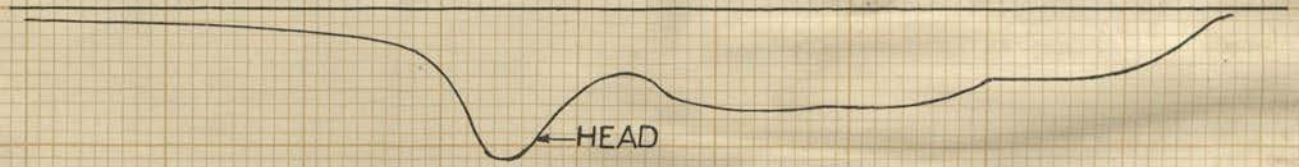

90 LB, R.
CST/9 N+1+D.

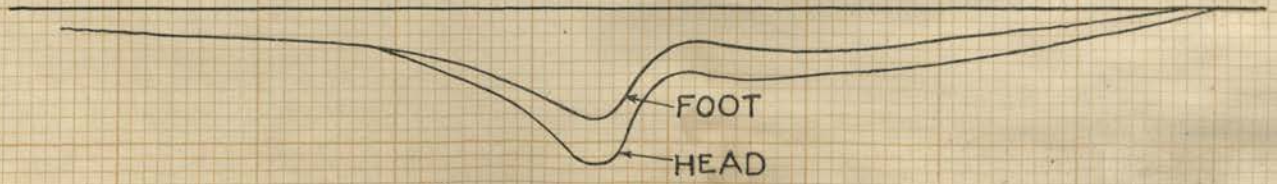

SCALE OF ORDINATES 10 TIMES FULL SIZE

FIG. 60

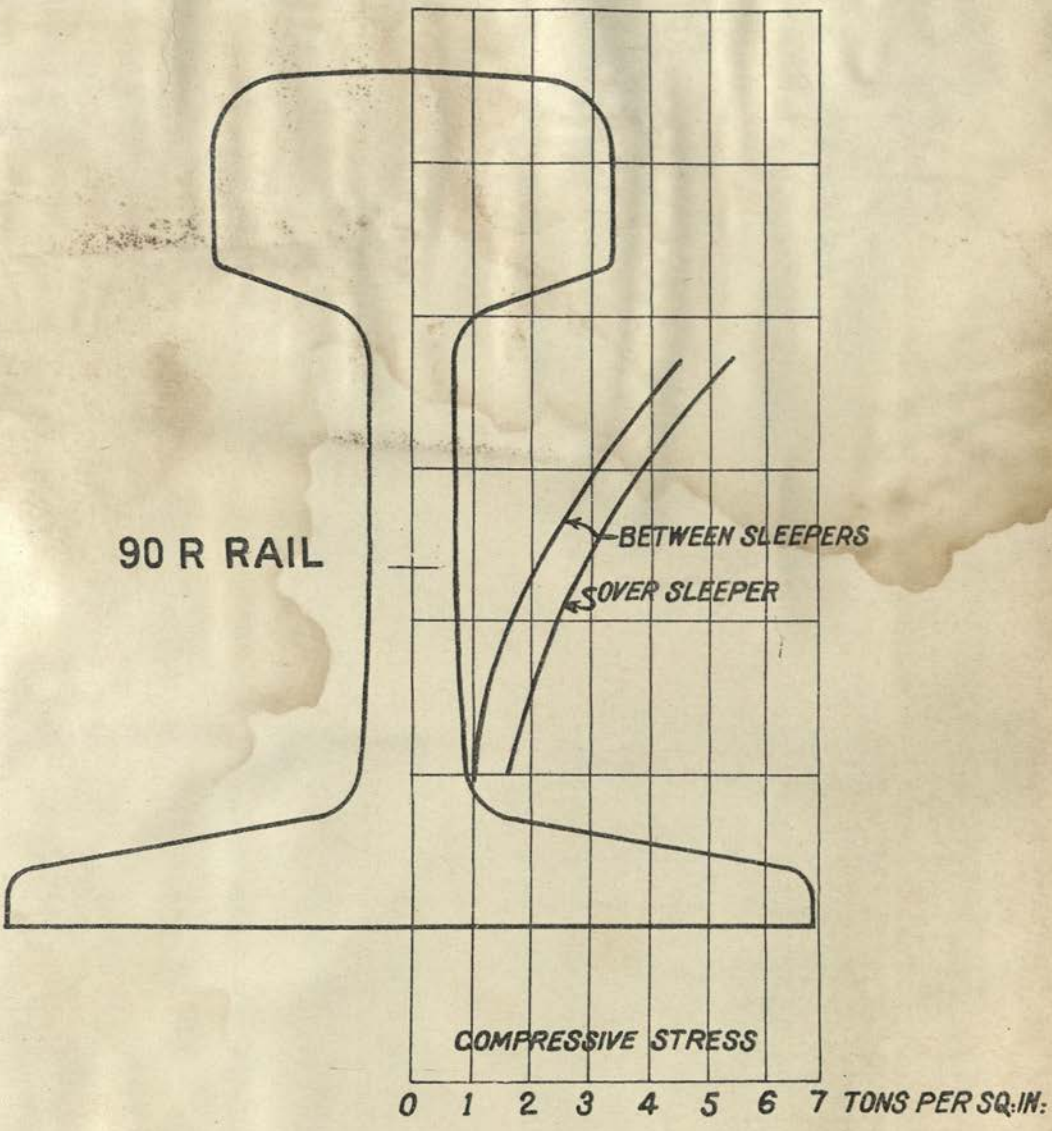
90 R RAIL
BETWEEN SLEEPERS
OVER SLEEPER
COMPRESSIVE STRESS
0 1 2 3 4 5 6 7 TONS PER SQ.IN.

FIG.61

Photographs showing the character of the stress-optical effects in each of the above cases are given in Figures 62, 63, 64 and 65 for types 1, 2, 3,and 4 respectively.

Maximum fillet stresses determined by the photo-elastic method are tabulated in Taple 11.

FIG. 62

FIG. 63

FIG. 64

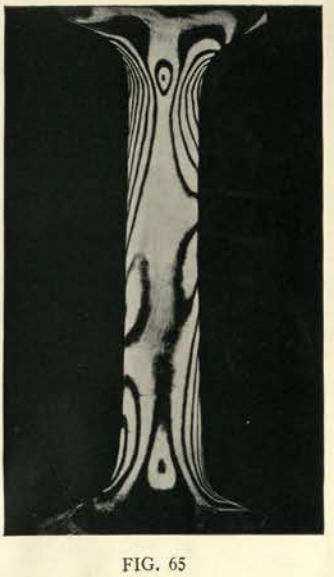

FIG. 65

TABLE II.

A	B		C	D		E	F	
LOADING	ELASTIC TRACK MODULUS	POSITION OF GAUGES	SLEEPER SPACING	FILLET	RESULTS OF POLARISCOPE ANALYSIS TONS PER SQ.IN.		DIRECT COMPRESSION (HUGGENBERGER) TONS PER SQ.IN.	RESULTANT STRESS TONS PER SQ.IN.	
11·25 T ECCENTRICITY 0·6" APPROX. 90R RAIL	lbs/inch sq.	OVER CENTRE LINE OF SLEEPER	2' - 8"	A	12.10	Tension	5.4	6.7	Tension
				B	13.70	Compression	5.4	19.1	Compression
	u = 1530			C	8.86	Tension	1.6	7.3	Tension
				D	8.06	Compression	1.6	9.7	Compression
11·25 T ECCENTRICITY 0·6 APPROX. 90R RAIL		MIDWAY BETWEEN SLEEPERS	2' - 8"	A	7.53	Tension	4.55	3.0	Tension
				B	8.06	Compression	4.55	12.6	Compression
	u = 1530			C	3.66	Tension	1.10	2.6	Tension
				D	4.02	Compression	1.10	5.1	Compression
11.25T 10·0T ECCENTRICITY 1·0 APPROX. 90R RAIL		OVER CENTRE LINE OF SLEEPER	2' - 8"	A	5.76	Compression	5.40	11.2	Compression
				B	16.20	Tension	5.40	10.8	Tension
	u = 1150			C	16.20	Compression	1.63	17.8	Compression
				D	17.0	Tension	1.63	15.4	Tension
11.25T 10·0T ECCENTRICITY 1·0 APPROX. 90R RAIL		MIDWAY BETWEEN SLEEPERS	2' - 8"	A	22.60	Tension	4.55	18.1	Tension
				B	19.55	Compression	4.55	24.1	Compression
	u = 1150			C	14.50	Tension	1.10	13.4	Tension
				D	9.26	Compression	1.10	10.36	Compression

In all cases the resultant stresses are below the yield point of rail steel. The most serious stress condition is 24·1 tons per square inch compression at a section midway between sleepers under a vertical eccentric load of 11·25T combined with a lateral load of 10·0T. Cases of rail failure due to excessive stresses in the web or fillets are not common on Indian Railways but these stresses can be very high under unfavourable conditions and are no doubt responsible for local rail distortions such as tippling of the head where capacity loads are run under conditions of poor maintenance. **A reduction in fillet stresses is secured by closer spacing of sleepers.**

A xylonite model was prepared of a 90 lb. Rail section similar to the 90R but with the fillet radii increased to 0·5 inch and a complete series of photo-elastic experiments were carried out with the same loads as in the experiments described above. The reduction in the intensity of fillet stress was less than 5 per cent and this is insufficient to justify a change in this standard dimension.

Tests with Moving Loads on Parallel Tracks.

The results of these tests are plotted in sheets Figures 66 to 71 & 73.

Six of these sheets relate to the tests with XB engines. An outline drawing giving main dimensions and weights of the XB class engine is given in Figure 72.

Figures 66 to 68 show lateral load at leading coupled axle plotted to basis of permanent, elastic and total mean distortions respectively for seven applications of the load for the following types of track.

88½ D and O N+2.
88½ D and O N+4+D.
90 R Steel Trough N+3.
90 R Hardwood N+3.

Figure 69 shows permanent distortion plotted against number of load applications for the above tracks.

Figure 70 shows the amount of gauge spreading for seven applications of the lateral load for

88½ D and O N+2.
88½ D and O N+4+D.
88½ Hardwood N+2.
90 R Steel Trough N+3.
90 R Hardwood N+3.

Figure 71 shows the effect on the lateral strength due to a trench dug transversely in 88½ lb. D and O track.

Axle loads of 15 and 22½ tons were used in the moving load tests with four-wheeled O.S. type wagons. In the case of these wagons, their wheel base is 16 feet and the virtual axle load for determining the deflexions and sleeper pressures calculated by formulae obtained by the Elastic Theory is nearly equal to the actual axle load. In the case of the XB locomotives, however, owing to the proximity of adjacent axles, the virtual load at the leading coupled axle, where the lateral loads were applied, is considerably greater than the nominal axleload. For the test sites (at Moghalsarai), the Elastic Track Modulus was on the average 1640 and it did not vary more than 7 per cent above or below this figure. Under these conditions, the virtual load at the leading coupled axle (17·0 tons weighbridge load) is calculated equal to 21·0 tons approximately for both the 90 R and 88½ lb. tracks at Moghalsarai.

—MOVING LOAD TESTS—

XB LOCOS

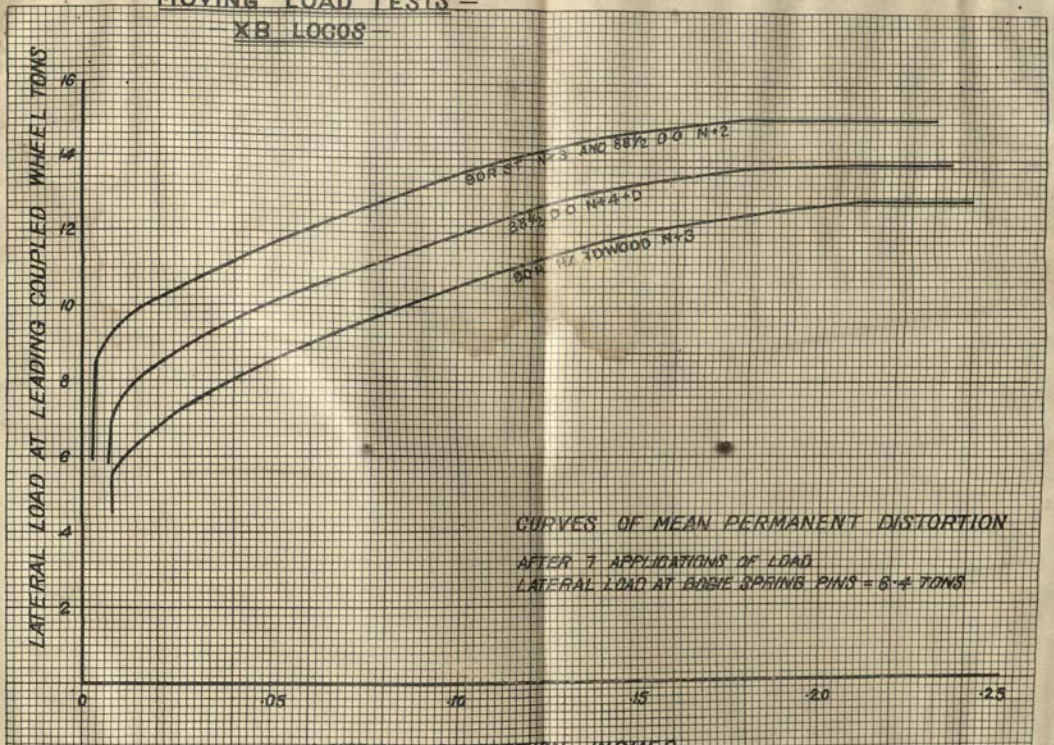

FIG. 55

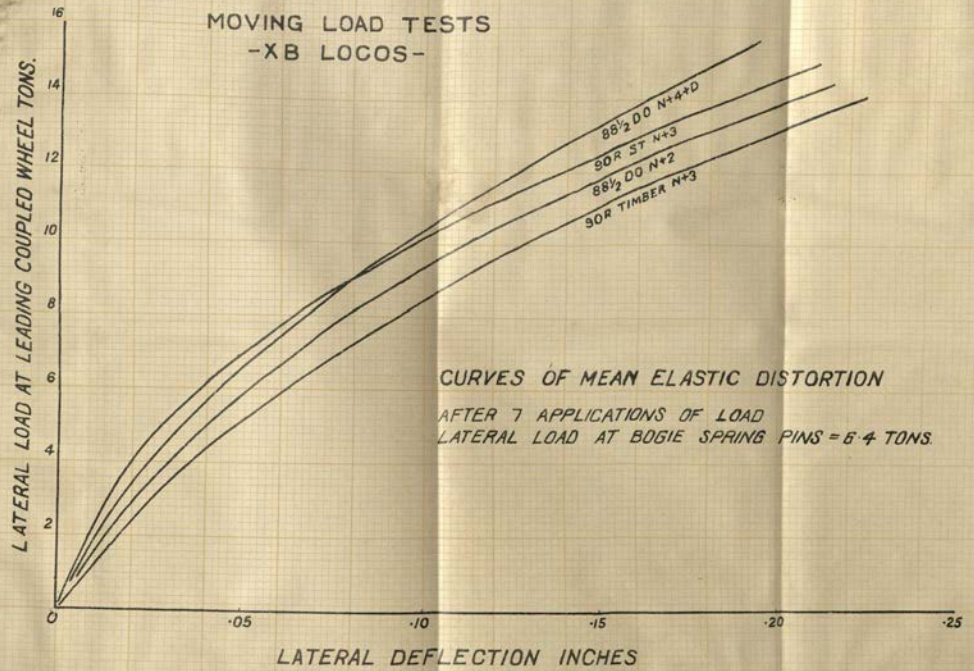
MOVING LOAD TESTS
-XB LOCOS-
88½ DO N+4+D
90R ST N+3
88½ DO N+2
90R TIMBER N+3
CURVES OF MEAN ELASTIC DISTORTION
AFTER 7 APPLICATIONS OF LOAD
LATERAL LOAD AT BOGIE SPRING PINS = 6·4 TONS.
LATERAL LOAD AT LEADING COUPLED WHEEL TONS.
16
14
12
10
8
6
4
2
0
·05
·10
·15
·20
·25
LATERAL DEFLECTION INCHES

FIG. 67

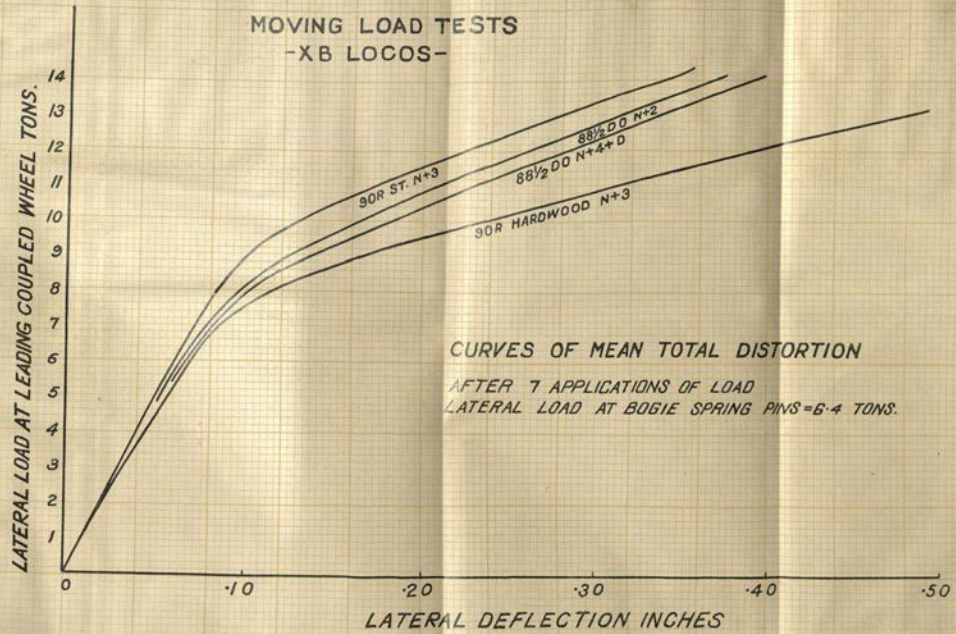
MOVING LOAD TESTS
-XB LOCOS-
LATERAL LOAD AT LEADING COUPLED WHEEL TONS.
14
13
12
11
10
9
8
7
6
5
4
3
2
1
0
·10
·20
·30
·40
·50
LATERAL DEFLECTION INCHES
90R ST. N+3
88½ DD N+2
88½ DD N+4+D
90R HARDWOOD N+3
CURVES OF MEAN TOTAL DISTORTION
AFTER 7 APPLICATIONS OF LOAD
LATERAL LOAD AT BOGIE SPRING PINS=6·4 TONS.

FIG. 68

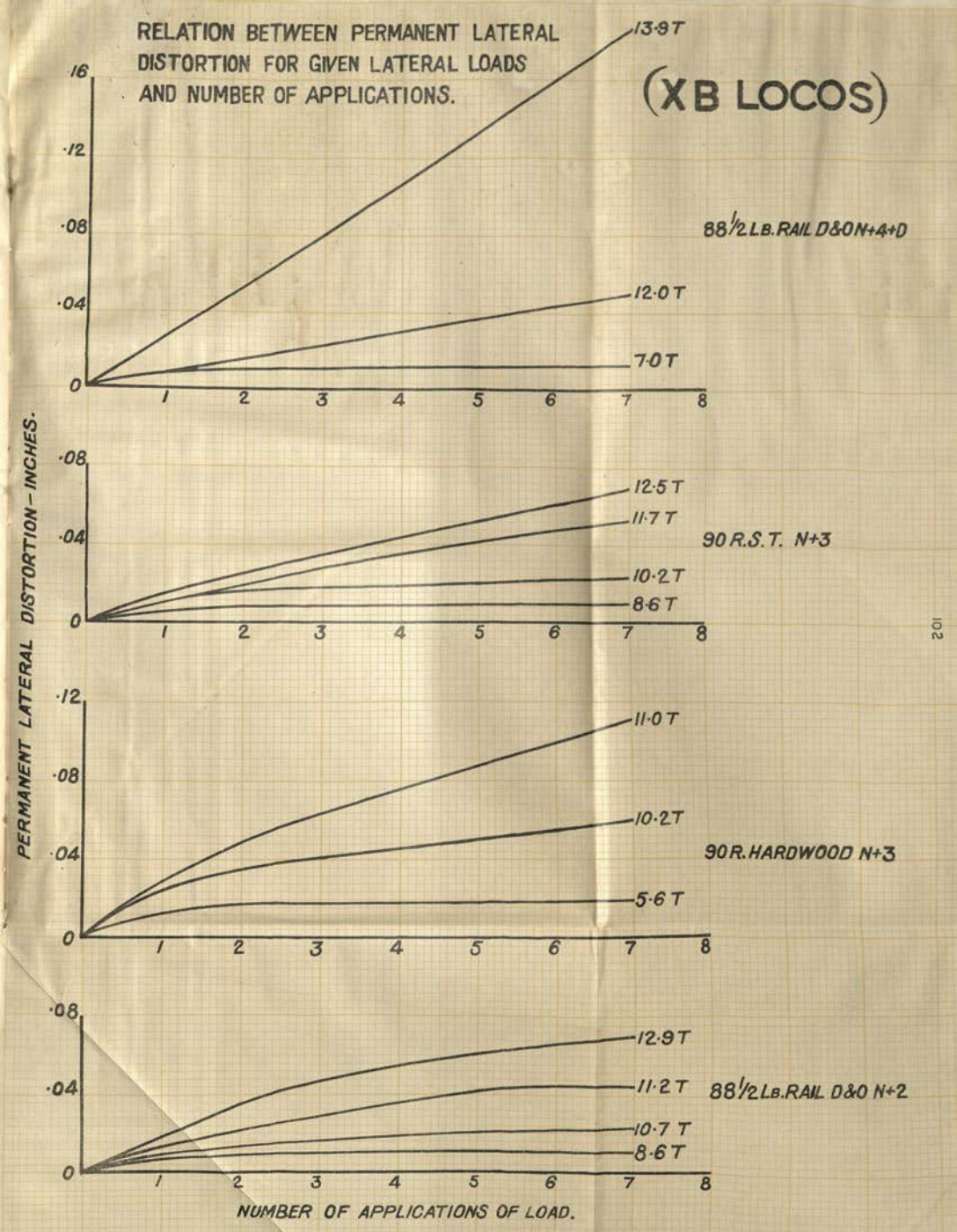
RELATION BETWEEN PERMANENT LATERAL DISTORTION FOR GIVEN LATERAL LOADS AND NUMBER OF APPLICATIONS.
(XB LOCOS)
88½ LB. RAIL D&O N+4+D
13·9 T
12·0 T
7·0 T
90 R.S.T. N+3
12·5 T
11·7 T
10·2 T
8·6 T
90 R. HARDWOOD N+3
11·0 T
10·2 T
5·6 T
88½ LB. RAIL D&O N+2
12·9 T
11·2 T
10·7 T
8·6 T
PERMANENT LATERAL DISTORTION – INCHES.
NUMBER OF APPLICATIONS OF LOAD.
·16
·12
·08
·04
0
1
2
3
4
5
6
7
8

FIG. 69

MOVING LOAD TESTS
(X. B. LOCOS)

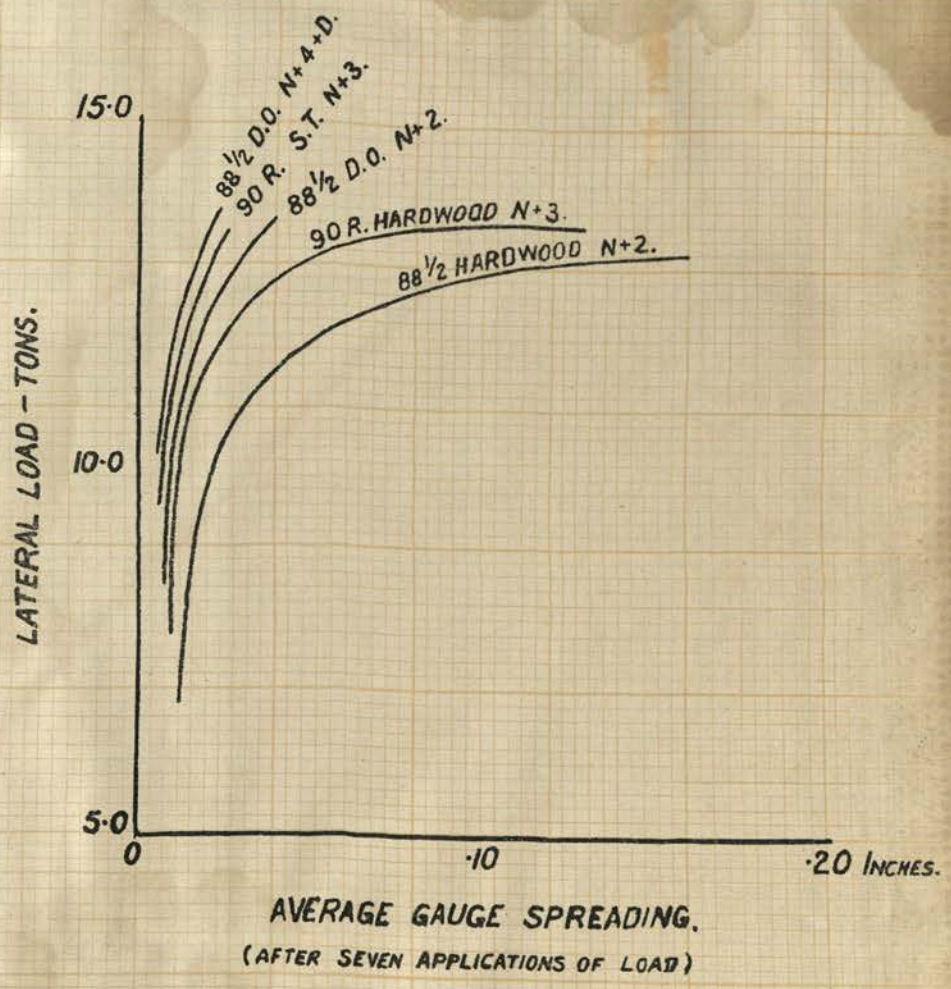

FIG. 70

MOVING LOAD TESTS
(XB LOCOS)
EFFECT OF CROSS DRAINS

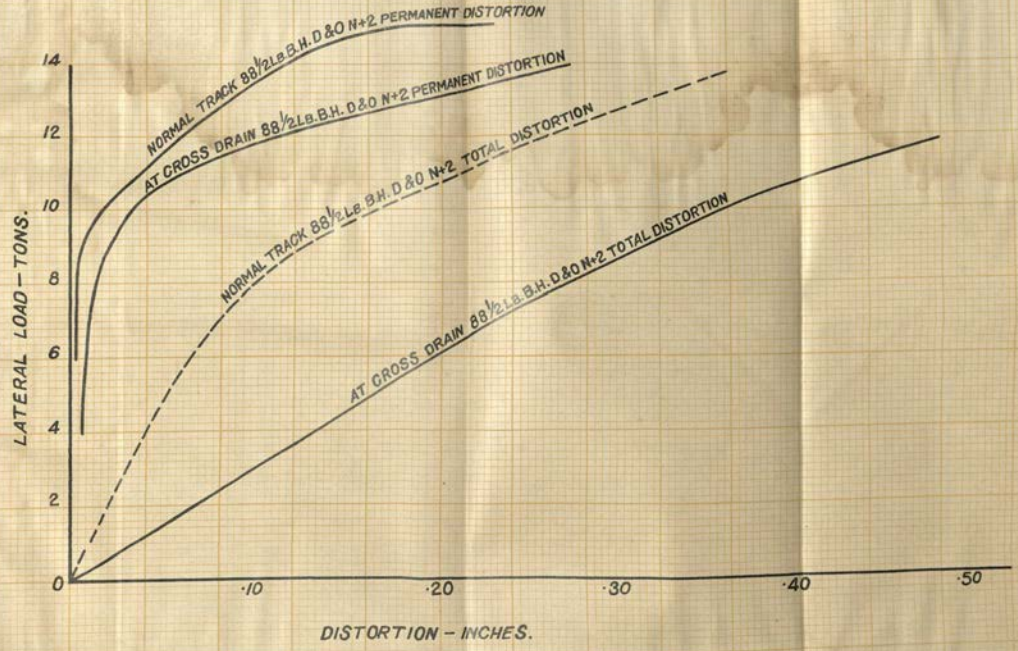

AFTER SEVEN APPLICATIONS OF LOAD

FIG 71

4-6-2 XB ENGINE

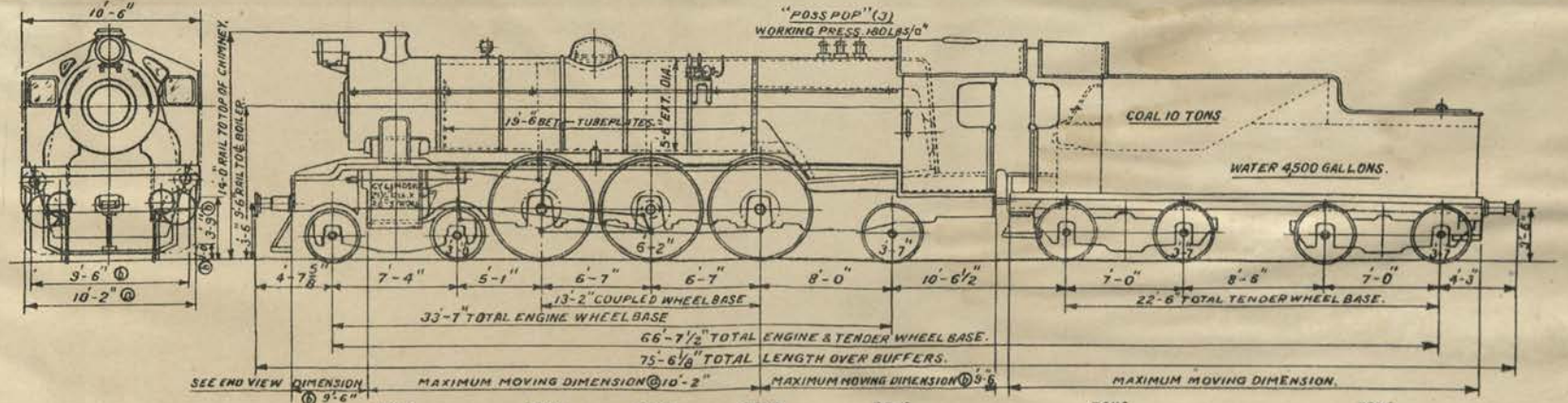

	TONS	TONS	TONS	TONS	TONS	TONS	TONS
WEIGHT IN WORKING ORDER	20·125	17·0	17·0	17·0	16·0	32·2	32·3
WEIGHT EMPTY	18·85	15·125	16·2	14·925	14·3	17·2	17·25

FIG. 72

MOVING LOAD TESTS

AVERAGE RESULT FOR ONE APPLICATION OF THE LATERAL LOAD

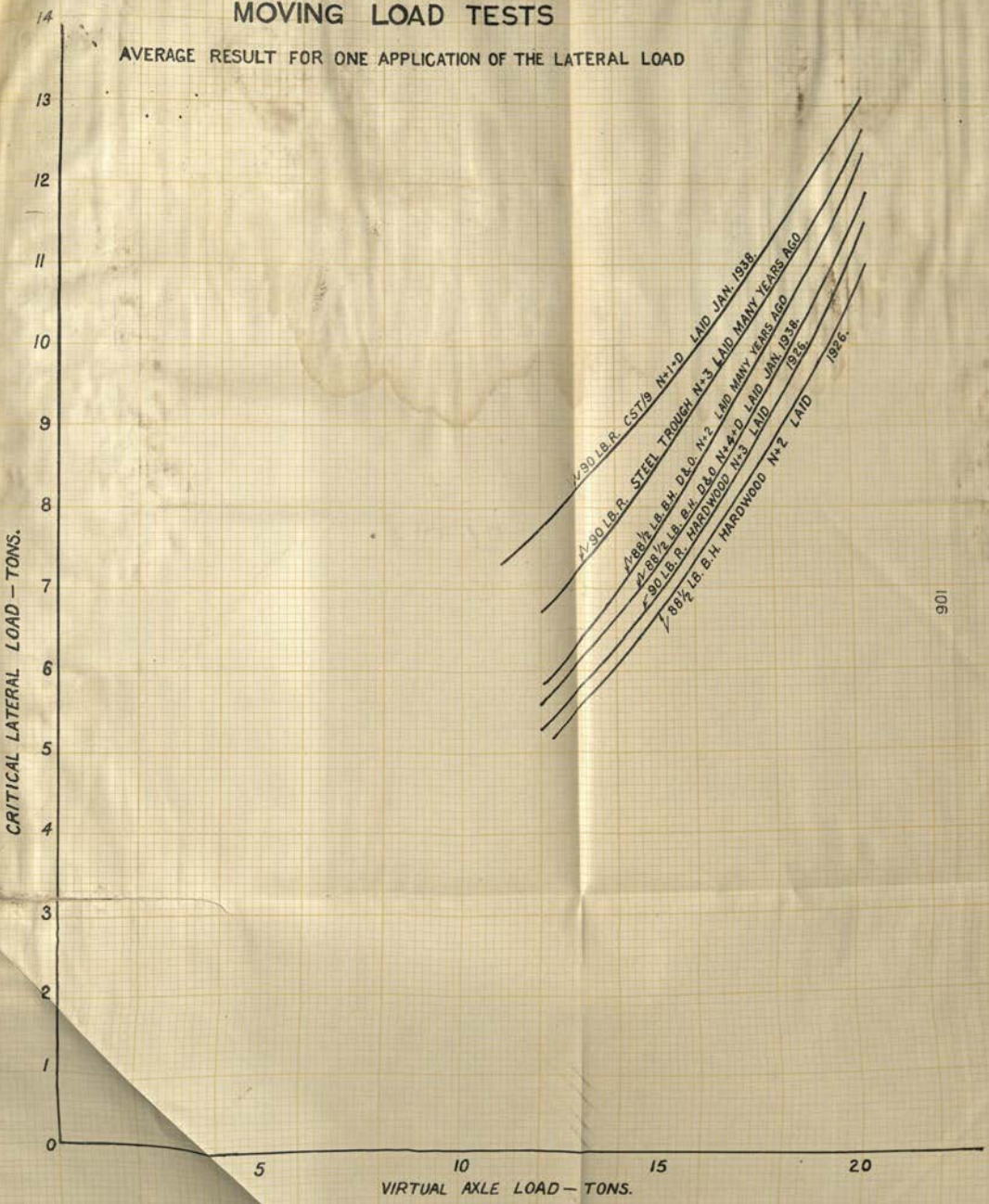

FIG. 73

The control of flange guiding forces on curves is within the powers of the locomotive designer. If it were required to run such locomotives as the North Western Railway H.G. 2-8-0 type at speeds beyond 45 miles per hour, further guiding assistance from the pony truck would be very desirable.

Track Distortions.—Track distortions were recorded on a stretch of curved line on the Bhusaval-Nagpur section, Great Indian Peninsula Railway, where the severest flange forces had been recorded. A survey of the particular length was made on 1st August 1938 by the local engineers and it was noticed that an increase of 300 per cent in curvature existed at the particular spot over a length of 15 feet.

This stretch of track was surveyed again 5 weeks afterwards and it was found that this kink had moved forward twenty feet and was of the same magnitude as that previously measured on 1st August 1938.

Telescopic gauges were installed in the line at the kink and observations were made of elastic and permanent shift under two runs with XB locomotive No. 1920 and test train travelling at 60 miles per hour. The maximum total recorded movement due to the first run was 0·191 inch and the maximum permanent shift was 0·025 inch and in the second run the total recorded movement was 0·233 inch and the maximum permanent shift was 0·027 inch, both maxima occurring at the same telescopic gauge.

Exhaustive tests of XB class engines with friction damping at the bogie and hind truck slides at express speeds on straight track under dry and monsoon weather conditions on tracks in average conditions and on other tracks laid on black cotton soil have shown that the maximum flange forces do not exceed seven tons.

On badly aligned curves (2,640 feet radius), however, flange forces of 12 to 13 tons have been recorded. While spreading of the gauge in pot or metal trough sleepered track would not occur under loads up to thirteen tons, the maintenance of line would certainly be a serious problem.

As regards the 90 R and 88½ lb. B. H. tracks on hardwood sleepers, gauge spreading appears to become serious after about 11 and 10 tons lateral forces respectively have been reached but maintenance would be likely to become troublesome at somewhat smaller lateral loads than these.

12. Safe Working Loads and Speeds.

The calculated safe loads and speeds determined from the experiments for the various vehicles which have been examined are given in Table 12. The only exterpolations which have been made in calculations are for u, I, Z_c and Z_t when these are different from those in the actual tests. No attempt has been made to estimate the effect of BL broad gauge axles. It is regrettable that more data could not have been collected regarding the various types of hauling engines which were used in the tests before the sensitivity of the recording strain gauges was increased so as to eliminate the necessity for a specially calibrated test load.

TABLE 12

SAFE LOADS AND SPEEDS

LOCOMOTIVES

Load	Rail	Condition	Tensile strength tons/□"	Sleepers	Gauge	Maximum speed M. P. H.		u	
Electric 4-6-0 Passenger Metrovik.	100 B. H.	Worn ..	52	N+3	B. G.	75		1,000	Straight and curved tracks.
Do. ..	90 R. ..	Worn ..	52	N+3	B. G.	75		1,000	Ditto.
4-6-0 BESA, G. I. P. D/5 class Passenger.	82 B. H.	As tested	40	N+3	B. G.	70	*	1,000	Ditto.
Do. ..	82 B. H.	As tested	40	N+3	B. G.	40		1,000	Ditto.
2-8-0 BESA, N. W. R. HG class freight Zero HB Zero steam.	100 B. H.	Worn ..	52	N+3	B. G.	75		1,000	Straight track.
Do. ..	100 B. H.	Worn ..	52	N+3	B. G.	50		1,000	Curved track.
Do. ..	82 B. H.	As tested	40	N+2	B. G.	70		1,000	Straight track.
Do. ..	82 B. H.	As tested	40	N+2	B. G.	40		1,000	Curved track.
Do. ..	73 B. H.	As tested	40	N+2	B. G.	70		1,000	Straight track.
Do. ..	73 B. H.	As tested	40	N+2	B. G.	40		1,000	Curved track.
YB 4-6-2 Passenger.	50 F. F.	Worn ..	52	N+1	M. G.	55		600	Straight track.
Do. ..	50 F. F.	Worn ..	40	N+1	M. G.	40		600	Ditto.

WAGON AXLES

Load	Rail	Condition	Tensile strength tons/□"	Sleepers	Gauge	Maximum speed M. P. H.		u	
22½ T. Axles at 16'-0" crs.	100 lb. B. H.	Worn ..	52	N+3	B. G.	70		1,000	Straight and curved tracks.
Do. ..	90 R. ..	Do. ..	52	N+2	B. G.	70		1,000	Ditto.
Do. ..	90 B. S. S. F. F.	Do. ..	52	N+2	B. G.	70		1,000	Ditto.
Do. ..	88½ B. H.	As tested	40	N+3	B. G.	60	*	1,000	Ditto.
Do. ..	88½ B. H.	Do. ..	40	N+3	B. G.	45		1,000	Ditto.
Do. ..	85 F. F. B.N.R.	Do. ..	40	N+3	B. G.	40		1,000	Ditto.
Do. ..	82 F. F.	Do. ..	40	N+2	B. G.	30		1,000	Ditto.
Do. ..	75 F. F.	Do. ..	40	N+2	B. G.	10	*	850	Ditto.
Do. ..	75 F. F.	Do. ..	40	N+2	B. G.	10	*	1,000	Ditto.
Do. ..	75 D. H.	Do. ..	40	N+2	B. G.	10		1,000	Ditto.
Do. ..	73 B. H.	Do. ..	40	N+2	B. G.	10		1,000	Ditto.
12 T. Axles 12'-0" crs.	50 F. F.	Do. ..	52	N+2	M. G.	55		600	Straight tracks.
Do. ..	50 F. F.	Worn ..	40	N+2	M. G.	30	*	600	Ditto.
10 T. Axles 12'-0" crs.	50 F. F.	Do. ..	52	N+2	M. G.	55		600	Ditto.
Do. ..	50 F. F.	As tested	40	N+2	M. G.	45		600	Ditto.

Note.—"Worn" means head wear of proportionally equivalent amounts to those given in Technical Paper No. 303.

* are cases where the maximum stress is greater than 0·45 multiplied by the ultimate tensile strength but does not exceed this amount by more than 20 per cent.

13. Summary of Conclusions.

Items 1, 2 and 3 of the terms of reference.

Stresses in Rails.—In order to ensure that there shall be no permanent distortion of the rail with consequent increase in the work of track maintenance, the maximum compressive and tensile stresses should not exceed 18 tons per square inch and 23·4 tons per square inch for rails of 40 and 52 tons per square inch ultimate tensile strength respectively. Assuming however that the maximum reversal stress is never greater than —0·30 times the maximum positive stress, the figures of 18 and 23·4 tons per square inch can be increased to 22·8 and 29·6 tons per square inch without exceeding the limiting safe range of stress. This is an increase of about 27 per cent.

In preparing the tables of safe loads and speeds, the maximum stresses have been fixed at 18 and 23·4 tons per square inch for the two qualities of rail steel except for those items which are starred. In those cases an increase of not more than twenty per cent has been allowed. The use of high working stresses such as these calls for comment.

The alternative would be to separate the secondary effects such as those of cross bending and contact stresses from those due to vertical bending moment and to adopt a working stress for calculating vertical bending moment stresses sufficiently low to allow for the secondary stresses. The secondary stresses form a large proportion of the total rail stress.

The existence of high secondary effects is not by any means a new discovery; the Bridge Sub-Committee on Track Stresses (Technical Paper No. 245, page 5. Government of India Central Publication Branch, Calcutta) in referring to certain experiments made in America, reported that maximum stresses in the rail-foot did sometimes exceed the mean stress there by as much as 5 or 6 tons per square inch and they recommended that a low working stress should be adopted to provide for maximum effects.

The elastic theory formulae give good approximations for the static deflection and primary static stress in the rail and a closer approximation is obtained by application of factors R Table 4. Dynamic rail deflections and sleeper loads may be determined by multiplying the static deflection or sleeper load by $(1{\cdot}10+0{\cdot}0037V)$ where V is the speed in miles per hour.

Dynamic rail stresses may be calculated by multiplying the static stress by the appropriate factor in Table on page 31.

Rail Joints.—Considerable attention has been given to rail-joint action and formulae are given from which sleeper spacing, deflection and fishplate stress may be derived. It has been shown that an urgent need exists for stronger fishplates in practically all cases to facilitate the work of maintenance. Rail joint problems could be studied expeditiously and cheaply, using existing equipment by fitting a recording accelerometer direct to the axlebox of the vehicle. Little mention has been made in the report of the free oscillations of the track. Rail-joint and other irregularities set up free oscillations whch are usually heavily damped but which should be taken into account. Experiments with an accelerometer fitted to axleboxes would enable these oscillations to be recorded and analysed.

It is considered that designs of rail-joints which are of inadequate strength for the loads for which the track is intended are responsible for much of the impact effect. There is need for higher strength fishplates and it is recommended that a new fishplate steel be adopted which after suitable heat treatment will be capable of withstanding stresses up to ± 25 tons per square inch indefinitely and have a satisfactory elongation when tested to destruction in a tensile test.

The Duplex joint sleeper provides an effective joint support and relieves the fishplate of considerable stress.

Track Maintenance.—Track maintenance has a most important bearing on the impact effect. The tests have shown that the lighter the rail for a given axle load, the heavier are the impact effects. It is considered that the number of sleepers per rail should be increased especially in the case of the lighter rails in order to reduce the impact effect. The economics in connexion with this proposal however needs careful investigation.

Item 4 of the Terms of Reference.

Experiments so far made indicate that the shape of the sleeper has no noticeable influence on its vertical deflexion under a given load but nothing has yet been established regarding the effect of shape upon safe load capacity. The whole question of the mechanics of the stress distribution between the base of the sleeper and the subsoil requires investigation.

Item 5 of the Terms of Reference.

Curved Tracks.—Further investigation is recommended in the case of curved tracks. It is considered probable that in the case of suitably designed rolling stock, the reduction in secondary stresses consequent on reduced nosing on the sharper main line curves may offset the increased stresses due to centrifugal effects.

Conclusions on Results of Experiments on Lateral Strength of Tracks.

1. The lateral strength of track depends upon the time it has had to consolidate after being laid or re-packed.

2. The type of rail has no appreciable effect on the ultimate lateral strength of the tracks within the limits of the experiments. This conclusion is based on comparison of tests on 88½ and 90 R tracks tested under similar conditions up to the point of failure.

3. D and O plate track shows superior strength to 90 R track with hardwood sleepers. This applies even to D and O track freshly laid or re-packed.

4. CST 9 type and steel trough sleeper (90 R rail) tracks show higher lateral strength even after re-packing than either D and O (88½ lb.) or timber sleeper (90 R) tracks under ordinary conditions of maintenance.

5. The D and O plate track shows a rate of growth of lateral strength due to consolidation inferior to both steel trough and CST 9 type sleeper track but superior to hardwood sleeper track.

6. 88½ lb. D and O track with only N+2 sleepers is superior to timber sleeper track in its ability to hold gauge and is almost as efficient as CST 9 and steel trough tracks in this respect.

7. The tests have shown that the lateral strength of track depends chiefly upon the sleeper spacing and the value of the grip they take in the ballast. The lateral strength and stiffness of track follows similar laws to the vertical strength and stiffness of the sleeper support. It may be taken to vary inversely as $\sqrt[4]{l^3}$ where l equals the sleeper spacing, with a substantial margin of safety.

8. Sheet 65 shows that there is a fairly well defined value of the lateral load where permanent distortion appears after 7 load applications i.e.—

Table A.

for	90 R Hardwood N+3	5·6 tons.
	88½ D and O N+4+D	7·0 „
	90 R ST N+3	8·6 „
	88½ D and O N+2	8·6 „

The small permanent distortions indicated for loads below the value for definite breakdown are neglected, as they do not appear to increase with the number of load applications. Some criterion of failure is looked for. M. Blondel in his article " The Resistance of Track to the Nosing Oscillation of Vehicles " appearing in the " Revue Generale de chemins de fer " for December 1932 takes the criterion of failure to be a permanent displacement of 4 mm. (0·16 inch). On this basis, the critical loads are:—

Table B.

for	90 R Hardwood N+3	12·2 Tons.
	88½ D and O N+4+D	13·5 „
	90 R ST N+3	14·9 „
	88½ D and O N+2	14·9 „

Flange forces at any point on well maintained straight tracks are just as likely to occur on one side of the track as on the other during a given period. In view of this and the very small distortions produced by the loads in Table A, it is considered that lateral loads up to 10 tons combined with 21 tons virtual axle load on metal sleepered broad gauge straight tracks can be safely tolerated.

Further track tests at high speeds on curves would be necessary to ascertain how much load in excess of those given in Table A can be tolerated in cases where a large number of load applications can occur between inspections.

9. The ability of track to retain good surface and alignment is an important feature. If one type of track due to features of the sleeper, ballast or sub-soil is prone to run down more quickly than another, it will have to resist greater disturbing forces even though it may have the greater lateral resistance. Advantage may also be taken of the fact that the oscillations of succeeding vehicles in a train are usually antiphased with each other and any **slight** permanent distortion set up by the leading vehicle is neutralized by the next one. In view of this fact, few permanentway engineers would, it is thought, object to small lateral movements of the permanent way which are, in many cases, of daily occurrence.

14. Personnel.

The following staff were selected for work in connexion with the Track Research.

B. Abdul Rahim ..
- Designation—Assistant Technical Inspector.
- Served—From November 1934 to December 1938.
- Duties—In-charge of field-work, photography, and assisting in analysis of the results.

B. Abdur Rafi ..
- Designation—Draughtsman.
- Served—From November 1936 to December 1936.
- Designation—Assistant Technical Inspector.
- Served—From February 1938 to December 1938.
- Duties—In-charge of field-work, photography and preparation of diagrams in connexion with the Report.

B. Shiv Dayal ..
- Designation—Research Clerk.
- Served—November 1937 to December 1938.
- Duties—Clerk In-charge of office records and stenotypist.

EI. 2007—1,000—29-6-39—EIR.

00109203

Digitized with financial assistance from
Government of Maharashtra
on 13 March, 2020